University of Dundee

MASTER OF SCIENCE

Investigating the role of the Nrf2-Keap1 pathway in mitophagy

Bento-Pereira, Claudia

Award date:
2020

University of Dundee

Investigating the role of the Nrf2-Keap1 pathway in mitophagy

Claudia Bento-Pereira

A thesis submitted for the degree of Masters of Science

University of Dundee

2020

Table of Contents

List of Figures

List of Tables

Abbreviations

AD	Alzheimer's disease
ADP	Adenosine diphosphate
ATP	Adenosine triphosphate
ARE	Antioxidant response element
AKR1B10	Aldo-keto reductase family 1, member B10
AKR1C1	Aldo-keto reductase family 1, member C1
Baf	Bafilomycin A1
BCL2	B-cell lymphoma 2
BCL2L13	BCL2 like 13
BNIP3	BCL2 interacting protein 3
CDK2	Cyclin-dependent kinase 2
cDNA	Complementary deoxyribonucleic acid
DFP	Deferiprone
FCCP	Carbonyl cyanide 4-(trifluoromethoxy)phenylhydrazone
FUNDC1	FUN14 domain containing 1
GCL	γ-Glutamyl-cysteine ligase
GFP	Green fluorescent protein
HD	Huntington's disease
HMOX1	Heme-oxygenase 1
LC3	Microtubule-associated protein 1A/1B-light chain 3
LIR	LC3 interaction motif
Keap1	Kelch-Like-ECH Associated Protein 1

MEFs	Mouse embryonic fibroblasts
mRNA	Messenger ribonucleic acid
NIX	NIP (Nodulin 26-like intrinsic protein) -like protein X
NQO1	NAD(P) H:quinone acceptor oxidoreductase 1
Nrf2	Nuclear factor-erythroid 2-related factor 2
OXPHOS	Oxidative phosphorylation
PARL	Presenilins-associated rhomboid-like protein
PCR	Polymerase chain reaction
PD	Parkinson’s disease
PINK1	PTEN-induced kinase 1
PMI	p62-mediated mitophagy inducer
ROS	Reactive oxygen species
SFN	Sulforaphane
Src	Proto-oncogene tyrosine-protein kinase Src
TBE-31	[(±)-(4bS,8aR,10aS)-10a-ethynyl-4b,8,8-trimethyl-3,7-dioxo-3,4b,7,8,8a,9,10,10a-octahydrophenanthrene-2,6-dicarbonitrile

Acknowledgments

Firstly, this project and my growth as a researcher would be impossible without my supervisor, Albena. I would like to thank her for all the time and effort she has invested in me. More importantly for giving me the strength and motivation when projects didn't work out. To my second supervisor, Miratul, thank you for your support, both intellectually and through various resources you have provided me.

My appreciation also goes to the ADK and JDH lab members with whom I have shared many laughs and happy moments. Thank you for sharing your wisdom and knowledge in both scientific matters and general life. Particularly to Dina, Ritu and Dot who welcomed me into the labs and made me feel so comfortable, creating the best work environment anyone could ask for. Also, to Kevin, who shared with me the highs and lows of this journey. And lastly, to Daniela, my Portuguese buddy who allowed me to exercise my mother tongue daily and filled my day with hilarity.

In addition, a great thank you to the MeDen group. We were forced to come together but I think we made a winning team and I hope you continue to succeed in my absence. More specifically to Richard, Lisa and Marilia, for all the positivity and support.

To all the individuals in the Jacqui Wood Cancer Centre, the School of Life Sciences and the members of my thesis committee, thank you for providing me with the experiences that made be grow. Especially, the MRC and Wellcome Trust funded PhDs who embarked on this journey with me since the 4th September 2016. Despite a PhD not being for me, I wish you all the success for the remaining two years.

Most importantly, a big thank you to my parents who have been there from day one, right up to the last day, cheering me on to the finish line. Despite me choosing to finish earlier, I can't thank them enough for being such an empathetic, patient and supportive pillar in my life.

Finally, a big thank you to my boyfriend, Tom, for his infallible support throughout the last couple of years. Despite only moving to Dundee for the last 9 months, I have appreciated every sacrifice he has made for this project. Whether it was driving me to and from the lab, listening to my ideas or reading my work.

Declaration

I hereby declare that the candidate below is the author of this thesis, that all the references cited have been consulted by the candidate, that the work of which the thesis is a record, has been carried out by the candidate, except where clearly stated, and has not previously been submitted for the award of any degree.

Signed: [redacted]

Date: 28th Oct 2019 (28/10/19)

Claudia Bento Pereira

(Student)

I hereby declare that Claudia Bento Pereira has carried out her research under my supervision and has fulfilled the relevant Regulations of the University of Dundee, so she is qualified to submit the following thesis in application for the degree of Master of Science.

Signed: [redacted]

Date: 29th Oct 2019

Professor Albena Dinkova-Kostova

(Supervisor)

ABSTRACT

Mitophagy prevents damaged mitochondria from compromising cell survival and homeostasis. Various mitophagy pathways have been discovered with the PINK1-Parkin pathway being most investigated. PINK1-Parkin mediated mitophagy occurs in stress-induced conditions. Interestingly, another pathway, the Nrf2-Keap1 pathway, which acts as sensor for stress within the cell, is also activated and mediates several cytoprotective functions, including redox and intermediary metabolism homeostasis, and autophagy. Studies have also indicated crossover between Nrf2 and mitophagy but there is limited knowledge of the underlying mechanisms. The aim of this research was to gain a deeper understanding of the relationship between the Nrf2-Keap1 pathway and mitophagy.

Previous studies have shown PINK1 to be regulated by Nrf2 in conditions of stress. To elucidate the underlying mechanisms, experiments were carried out in wild-type and PINK1 knockout S-HeLa cells under basal and stress conditions induced by treatment with carbonyl cyanide 4-(trifluoromethoxy)phenylhydrazone (FCCP), an uncoupler of oxidative phosphorylation. PINK1 did not influence Nrf2 transcript, protein levels, half-life, subcellular localisation or transcriptional activity. However, FCCP induced Nrf2 at the transcript and protein levels, and upregulated the expression of Nrf2-target genes, regardless of the presence of absence of PINK1.

A sub-population of the Nrf2-Keap1 protein complex is tethered to mitochondria due to a Keap1-PGAM5 interaction, and it has been shown that Keap1 mediates the ubiquitination and proteasomal degradation of PGAM5. PGAM5, a mitochondrial serine/threonine phosphatase, stabilises PINK1 for mitophagy. Thus, it was hypothesised that Keap1 knockdown would lead to PGAM5 and PINK1 stabilisation and increase mitophagy. However, our studies showed that this was not the case, despite an over two-fold increase in PINK1 transcript levels. Instead, PINK1 protein levels decreased.

Overall, it was found that reduction in the Keap1 levels (consequent to FCCP treatment, Keap1 knockdown or high dose of the electrophilic cyanoenone, TBE-31, which modifies cysteine sensors in Keap1) correlated with a reduction in the levels of PINK1. The implications of these findings are not fully understood and further investigation is necessary.

CHAPTER 1: INTRODUCTION

Chapter 1: Introduction

1.1 Nrf2/Keap1 Pathway

The nuclear factor-erythroid 2 p45-related factor 2 (Nrf2) – Kelch-like ECH-associated protein 1 (Keap1) pathway is essential for the maintenance of redox homeostasis and regulation of cellular stress responses (Motohashi and Yamamoto, 2004). It is typically regarded as the main defence mechanism against environmental insults where Keap1 is a biosensor for electrophiles and reactive oxygen species (ROS) and Nrf2, the coordinator of downstream responses (Kobayashi and Yamamoto, 2006).

1.1.1 Nrf2

Nrf2 belongs to the cap'n'collar (CNC) subfamily of basic leucine zipper (bZip) transcription factors (Moi et al., 1994). It was initially discovered in 1994 and identified due to its ability to bind to the nuclear factor erythroid 2 (NFE2)-motif found in the β-globin locus control region; a region which is required for erythropoiesis and platelet development (Moi et al., 1994). Despite its discovery in haemopoietic tissue, Nrf2 is ubiquitously expressed and highly conserved across species (Moi et al., 1994, Maher and Yamamoto, 2010).

Structurally, there are seven highly conserved regions known as Nrf2-ECH homology domains 1-7 (Neh1-7) (Figure 1.1). Of these domains, Neh1 contains a basic leucine zipper domain (bZip) required for DNA binding and dimer formation (Itoh et al., 1997). The Neh3, 4 and 5 regions are transactivation domains (Nioi et al., 2005, Katoh et al., 2001). The Neh5 region also contains a redox-sensitive nuclear-export signal (NES) which is involved in the regulation of Nrf2's intracellular localization (Li et al., 2006). Alternatively, the presence of several destruction motifs in the Neh2 and Neh6 domains are involved in Nrf2 repression (Itoh et al., 1999, McMahon et al., 2004). For example, within the Neh2 domain there are two motifs, the lower affinity DLG and the higher affinity ETGE

motifs (Tong et al., 2006) (Figure 1.1). These are recognised by Keap1, the main negative regulator of Nrf2 which keeps it in low abundance in the cell (Tong et al., 2006). The Neh7 domain is also involved in the repression of Nrf2 via an interaction with the DNA-binding domain of retinoic acid X receptor α (Wang et al., 2013). Additionally, the expression of Nrf2 can be also regulated, for example by epigenetic inactivation of its gene promoter. This occurs during mouse cortical neuronal development and has a critical role in creating a supportive redox environment (Bell et al., 2015).

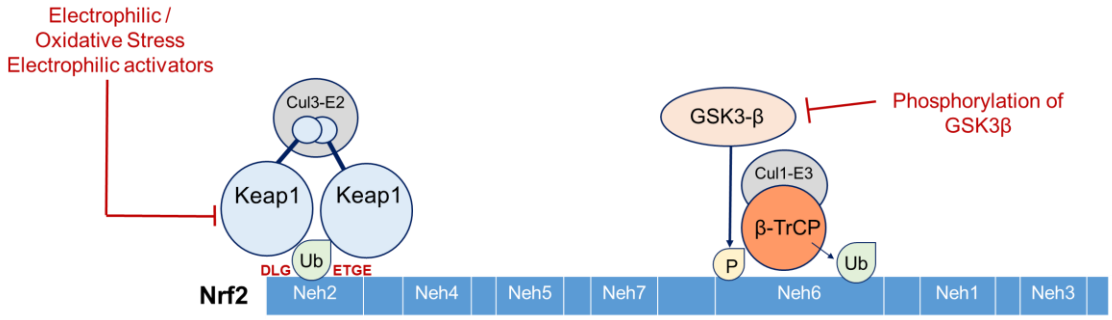

Figure 1.1. **Nrf2 structure and regulation**. Nrf2 is targeted for proteasome degradation through GSK3/β-TrCP/Cul1 and Keap1/Cul3 via the Neh6 and Neh2 domains, respectively. The Keap1/Cul3 pathway is the main pathway involved in Nrf2 degradation. In this pathway, Keap1 is able to bind to the DLG and ETGE motifs in the Neh2 domain of Nrf2. This then recruits the Cullin 3 (Cul3-E2) complex which ubiquitinates seven lysine residues found between the two motifs. During electrophilic/oxidative stress or exposure to electrophilic activators of Nrf2, Keap1 is modified and unable to target Nrf2 for degradation. In addition to the Keap1/Cul3 pathway, Nrf2 can also be phosphorylated by GSK3β which recruits the β-TrCP/Cul1 complex. This complex can also ubiquitinate Nrf2 for proteasomal degradation. Phosphorylation of GSK3β, for example by Akt, causes it to become inactive. Here it is unable to phosphorylate Nrf2 at the Neh6 domain and therefore prevents β-TrCP/Cullin 1 dependent degradation.

1.1.2 Keap1

Keap1 or KLHL19 is a member of the BTB-Kelch protein family discovered in a yeast two-hybrid screen as an Nrf2 binding partner (Itoh et al., 1999). It possesses three functional domains, a Broad complex, Tramtrack and Bric-a-Brac (BTB) domain, an intervening region (IVR) and a double glycine repeat (DGR)/ Kelch

domain (Itoh et al., 1999). Both the BTB and Kelch domains are protein-interacting domains. The BTB domain facilitates homodimerisation (Zipper and Mulcahy, 2002) and binding of Cullin 3, a scaffold for the required E3 ubiquitin ligase involved in Nrf2 ubiquitination (Chauhan et al., 2013). The Kelch domains mediate Nrf2 binding via the Neh2 domains, bringing the E3-Cullin 3 complex in proximity of Nrf2 (Lo et al., 2006) (Figure 1.2).

Aside from Nrf2, affinity purification and shotgun mass spectrometry has shown that Keap1 can interact with a variety of other proteins; all of which contain an ETGE motif or an ESGE motif (Hast et al., 2013). For example, PALB2 has an extended ETGE motif (LDEETGE) (Ma et al., 2012) and WTX tumour suppressor has an SPETGE motif (Camp et al., 2012). Other interactors include MCM3, TSC22D4, WDR1, DPP3, SLK, PGAM5 and p62 (SQSTM1) (Hast et al., 2013, Lo and Hannink, 2008, Lau et al., 2010).

A key property of Keap1 which enables its ability to act as an endogenous oxidative and electrophilic sensor, is its cysteine-rich nature. In total there are 27 cysteine residues in the human Keap1 protein, all of which are reactive to varying degrees (Holland et al., 2008). In the presence of Nrf2 inducers and/or conditions of electrophilic or oxidative stress, these cysteine residues can be alkylated or oxidised, leading to conformational changes in Keap1 which result in the dissociation of the Nrf2-Keap1 complex (Li et al., 2012) (Dinkova-Kostova et al., 2002). For example, oxidised cysteine residues in Keap1 can lead to the formation of disulphide bridges within the protein (Dinkova-Kostova et al. 2002). Another example of a chemical modification which can lead to conformational changes in Keap1 is treatment with inducers, such as dexamethasone 21-mesylate that cause irreversible alkylation of cysteine residues (Dinkova-Kostova et al., 2002).

Specific cysteines, such as cysteine 273 and 288 are shown to be vital for both Keap1-dependent basal Nrf2 repression and ubiquitination (Zhang and Hannink, 2003, Saito et al., 2016). However, the best-characterised cysteine, cysteine 151, present in the BTB domain, is one of the most critical for the dynamic stress

response of the Keap1/Nrf2 pathway (Zhang and Hannink, 2003, Dayalan Naidu et al., 2018, Ohnuma et al., 2010). Evidence suggests that this cysteine is one of the most reactive and is often modified in a range of conditions (Eggler et al., 2007, Hu et al., 2011, McMahon et al., 2010, Zhang and Hannink, 2003). Such heightened reactivity is thought be caused by its environment where it is surrounded by basic amino acids. This lowers its pKa under physiological conditions making it more likely for alkylation reactions to occur (Dinkova-Kostova et al., 2017). Such conditions are also present in close proximity to cysteines 23, 38, 241, 273, 288, 297, 319 and 613, making them increasingly reactive too (Dinkova-Kostova et al., 2002) (Figure 1.2).

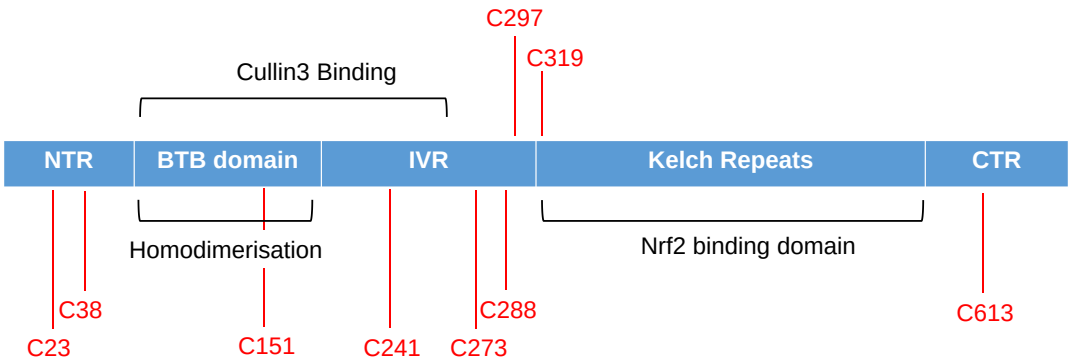

Figure 1.2. **Keap1 Structure.** Keap1 is made up of an amino terminal region (NTR), a Broad complex, Tramtrack and Bric-a-Brac (BTB) domain, an intervening region (IVR), a Kelch repeat domain and a carboxyl terminal region (CTR). The BTB domains are involved in the homo-dimerisation of Keap1 and in the association with the Cullin3 ubiquitin ligase required for Nrf2 ubiquitination. The Kelch repeats recognise Nrf2 and are fundamental for Nrf2 binding. Labelled in red are examples of the reactive cysteine residues present in Keap1.

As Keap1 is susceptible to inactivation by electrophilic activity, it is expected that Keap1 must be turned over to maintain a stable population to keep Nrf2 continuously supressed in homeostasis. In contrast to Nrf2, evidence suggests that Keap1 is not degraded via an ubiquitin-dependent mechanism for 26S proteasome-dependent degradation, despite being ubiquitinated by the same Cul3-dependent complex which it serves as a substrate for (Zhang et al., 2005).

Alternatively, it was considered that Keap1 turnover occurs through the process of autophagy, the bulk removal of excess or damaged cellular components (Taguchi et al., 2012). Taguchi et al. showed that in *Sqstm1*-deficient mouse livers, Keap1 protein accumulated and was unaffected by pharmacological inhibition of the proteasome. Similar observations were made in *Atg7*-deficient mouse livers. The *Atg7* gene encodes autophagy-related protein 7 and like p62, functions in the process of autophagy. Despite these observations, treatment with a variety of autophagy inhibitors including bafilomycin A, did not show an increase in Keap1 protein levels suggesting autophagy may not be the main mechanism involved in Keap1 turnover (Taguchi et al., 2012). Additionally, Nrf2 was shown to bind to an ARE in the Keap1 promoter suggesting that continuous induction of Nrf2 causes Nrf2-dependent transcription of Keap1 required for its repression (Jain et al., 2010). Overall, the underlying mechanisms by which Keap1 is turned over remains enigmatic and requires further investigation.

1.1.3 Nrf2 regulation

In unstressed conditions, Keap1 is continuously binding to Nrf2 via its double glycine repeat (DGR)/Kelch domain and C terminal region, collectively known as the Keap1-DC domain (Itoh et al., 1999). More specifically, it forms a homodimer where each molecule binds to either the DLG or ETGE motif on Nrf2 (Tong et al., 2006). Between these motifs, lie seven lysine residues which are correctly positioned, via Keap1 binding, for Cullin3-dependent ubiquitination (Tong et al., 2007). Consequently, ubiquitinated Nrf2 is then targeted for degradation by the 26S proteasome, keeping cellular levels of Nrf2 low (Stewart et al., 2003) (Figure 1.3).

In environments of oxidative and electrophilic stress, such as those observed in Parkinson’s disease or cancer, Nrf2 protein levels are stabilised (Beal, 2003, Liou and Storz, 2010, Sajadimajd and Khazaei, 2018, Ramsey et al., 2007). In such environments key cysteine residues within Keap1 are modified and therefore may consequently alter its Cullin-3 substrate adaptor function (Dinkova-Kostova et al.,

2017). These alterations allow Nrf2 to bind, but prevent the crucial alignment of the lysine residues required for ubiquitination and hence ubiquitin-dependent degradation of Nrf2 (Taguchi et al., 2011). This saturates the Keap1 and allows newly synthesised Nrf2 to translocate to the nucleus to dimerise with small MAF (musculo-aponeurotic fibrosarcoma) proteins for gene transcription of Nrf2 downstream targets (Li et al., 2008) (Figure 1.3).

In addition to the described canonical pathway above, Nrf2 can also be regulated by Keap1's other interactors. One hypothesis suggests that p62 can regulate Nrf2 activity by outcompeting it for Keap1 binding (Dodson and Zhang, 2017). p62 has an STGE motif which can be phosphorylated to increase its binding affinity for Keap1 at the same position Nrf2 binds (Ichimura et al., 2013). This reduces the amount of Nrf2 bound to Keap1 and therefore reduces its systematic ubiquitin-dependent degradation (Lau et al., 2010, Komatsu et al., 2010). Instead, unbound Nrf2 stabilises in the cell and can mediate ARE-dependent transcription (Lau et al., 2010, Komatsu et al., 2010). Interestingly, this includes the induction of p62 as it is a recognised Nrf2 downstream target, establishing a positive feedback loop of Nrf2 induction (Jain et al., 2010). Conditions which lead to this phosphorylation event are poorly studied, however one study has shown it to occur in mouse embryonic fibroblasts in response to *Salmonella* infection (Ishimura et al., 2014). Other phosphorylation events in p62 have also been reported. For example, serine 403 is phosphorylated in response to mitochondrial depolarisation in cultured mouse neuroblastoma Neuro2a cells (Matsumoto et al., 2015) and serine 293 (294, in humans) to insulin withdrawal in rat hippocampal neurones (Ha et al., 2017). Despite these findings showing effects on p62 activity and location, the potential knock on effects on Nrf2 were not explored.

More recent findings show that Nrf2 can also be regulated by another ubiquitin dependent pathway, independently of Keap1, via the formation of a phosphor-degron, DpSGIpS, in its Neh6 domain (McMahon et al., 2004). This is via the GSK3/β-TrCP/Cul1 (glycogen synthase kinase 3/ beta-transducin repeat-containing protein/ Cullin1) complex. In this pathway, following priming by an

unidentified kinase, active GSK3 phosphorylates serine 335 and 338 within the DSGIS motif, causing the E3 ligase substrate adaptor, β-TrCP, to bind (Chowdhry et al., 2013, Rada et al., 2012). This leads to the formation of the complex causing ubiquitination and redox-independent proteasome degradation of Nrf2 (Rada et al., 2012) (Figure 1.3).

Collectively, it is proposed that a ‘dual degradation’ model can explain why these two regulatory ubiquitin-dependent Nrf2 pathways are present (Rada et al., 2011). In normoxia, Nrf2 is predominantly targeted for degradation via the Keap1-depenedent pathway due lack of modifications to the cysteine residues. In these same conditions, active kinases like Akt phosphorylate GSK3 making it inactive. However, in conditions of extreme oxidative or electrophilic stress, both pathways are altered. Firstly, cysteine residues become modified and lead to Keap1 inactivation and ultimately Nrf2-dependent gene transcription. After, to shut down the Nrf2 activation loop, GSK3 is likely to become activated due to the inhibition of Akt by ceramide-activated phosphatases. This will then lead to Nrf2 proteasomal degradation via the βTrCP/Cul1 complex reducing Nrf2 stabilisation and hence ARE-gene expression. The coordination of both pathways is essential as shutting down Nrf2-dependent transcription before homeostasis is achieved can result in cell death. Thirdly, in conditions of slight alterations to redox homeostasis and deprivation of growth or trophic support or signalling, Keap1 is unlikely to be modified but GSK3 is likely to be active. This causes Nrf2 to be targeted by both pathways simultaneously. Upon ROS accumulation, Keap1 is inactivated to initiate Nrf2-dependent gene transcription (Rada et al., 2011).

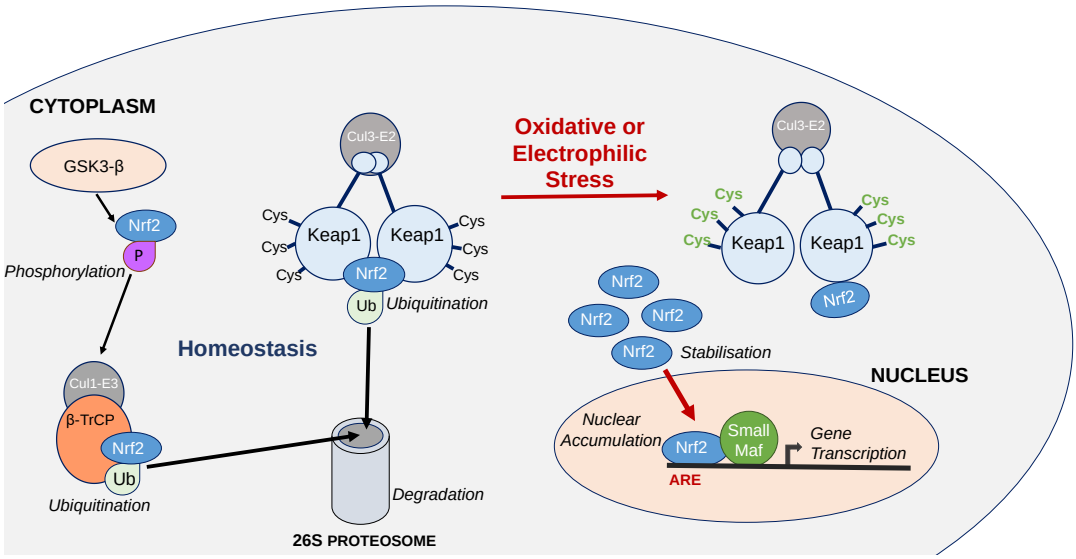

Figure 1.3. **Nrf2 regulation in homeostasis and in electrophilic/oxidative stress.** In oxidative/ electrophilic stress or exposure to electrophilic Nrf2 activators, Keap1 is unable to target Nrf2 for degradation. This is due to modifications in important cysteine residues of Keap1, causing it to change conformation. Nrf2 remains bound but is not ubiquitinated, saturating Keap1. Newly synthesised Nrf2 is able to stabilise in the cytoplasm and translocate to the nucleus. In the nucleus, Nrf2 binds to small Maf proteins and together they bind to antioxidant response elements (ARE) found in the promoters of Nrf2 target genes to initiate gene transcription.

1.1.4 Nrf2-dependent transcription

Nrf2 regulates approximately 200 cytoprotective genes, all of which contain a cis-acting element upstream of their promoters called an antioxidant response element (ARE) (Hayes and Dinkova-Kostova, 2014, Friling et al., 1990, Nguyen et al., 2009). Here, Nrf2-small MAF dimers bind to initiate gene transcription of an array of Nrf2-dependent genes. Interestingly, the ARE was discovered before Nrf2 in the late 1980s due to research focusing on the 5'-flanking sequences of the rat inducible glutathione *S*-transferase Ya subunit (*GSTYa)* (Telakowski-Hopkins et al., 1988). In this study, it was discovered that there were two cis-acting regulatory elements upstream of *GSTYa*, one of which was involved in basal level expression and the second involved in inducible expression of the gene. A few years later, the ARE core sequence *GSTYa* was found to be 5'-puGTGAC---GC-3', which was confirmed with a series of deletion and mutational

experiments (Raghunath et al., 2018). The study showed that both ROS and oxidants could induce the ARE-dependent transcription of *GSTYa*, providing the first insight into the ARE being necessary to induce antioxidant genes in conditions of oxidative stress. It was later revealed that Nrf2 was the primary transcription factor which activated ARE-dependent gene transcription which conferred this protective response (Venugopal and Jaiswal, 1996, Itoh et al., 1997).

The discovery of the ARE sequence and the association to Nrf2 led to the identification of potential Nrf2 downstream targets, particularly those involved in detoxification processes within the cell. A well-established Nrf2 target is NQO1 (NAD(P)H dehydrogenase [quinone] 1, a phase I detoxification enzyme which protects cells from quinone-mediated redox cycling, oxidative stress, and sulfhydryl depletion (Dinkova-Kostova and Talalay, 2000). Another Nrf2 target is the family of aldo-keto reductases, including enzymes AKR1B10 and AKR1C1, which are also involved in the detoxification pathways of the cell, reducing aldehydes and ketones (Lou et al., 2006). Nrf2 also plays a significant role in the maintenance of redox homeostasis through the replenishment of glutathione in the cell (Harvey et al., 2009). It does this through glutamate-cysteine ligase (GCL), the enzyme catalysing the rate-limiting step in glutathione biosynthesis, by regulating both its catalytic (GCLC) and modifier subunit (GCLM) (Erickson et al., 2002, Xiong et al., 2015).

Besides detoxification and defending against electrophilic and oxidative stress, Nrf2 also regulates genes involved in a range of other biological processes. For example, it regulates heme-oxygenase 1 (HMOX1) and glucose-6-phosphate dehydrogenase (G6PD) which are involved in heme metabolism and the production of NADPH via the pentose phosphate pathway, respectively (Reichard et al., 2007, Thimmulappa et al., 2002). Nrf2 has also been reported to transcriptionally regulate proteasomal protein degradation by regulating subunits which make up the 26S proteasome (Kwak et al., 2003). Amongst these processes Nrf2 has also been described to regulate autophagy (Jain et al., 2010),

apoptosis (Niture and Jaiswal, 2012) and cell proliferation (Murakami and Motohashi, 2015).

1.1.5. Small-molecule activators of Nrf2 (Nrf2 inducers)

As previously mentioned, modified cysteine residues in Keap1 occur in environments of oxidative and electrophilic stress. Such modifications induce Nrf2's elaborate cytoprotective transcription program to overcome the stress encountered. Based on this dogma, it is considered that many Nrf2 activating compounds work by targeting these cysteines on Keap1 to stabilise Nrf2 (He and Ma, 2009). Indeed, many Nrf2 inducers, both natural and synthetic, are electrophilic and react with sulfhydryl groups of Keap1 despite their structural differences (Prestera et al., 1993).

Nrf2 inducers have previously been distributed across ten broad classes; including diphenols, phenylenediamines and quinones, Michael acceptors, isothiocynates and thiocarbamates (Tkachev et al., 2011). Aside from these types of compounds, Nrf2 can also be induced by cellular species or environments like heme complexes, oxidized lipoproteins and hypoxia (Lyakhovich et al., 2006). A well-studied Nrf2 inducer is sulforaphane (*R,S*-1-isothiocyanato-4-methylsulfinylbutane) (Figure 1.4), an isothiocynate present in a variety of cruciferous vegetables (Zhang et al., 1992). Sulforaphane forms thiocarbamate products with Keap1's reactive cysteine residues due to the high electrophilic carbon within the isothiocyanate group (Itoh et al., 1999, Mi et al., 2011, Zhang, 2012). More specifically, it has been reported to react with cysteine 151 (Hu et al., 2011) and a cysteine to serine mutation at this site repressed Nrf2 despite being in the presence of sulforaphane (Zhang and Hannink, 2003).

Acetylenic tricyclic bis (cyano enone), TBE-31, is another potent Nrf2 inducer which contains a 3-ring system with two highly reactive Michael acceptor groups, ready to react with Keap1 (Figure 1.4) (Dinkova-Kostova et al., 2010). Like sulforaphane, TBE-31 primarily modifies cysteine 151, more specifically at lower

concentrations of up to 10nM (Dayalan Naidu et al., 2018). Interestingly, at higher concentrations (>30nM), Nrf2 induction occurs in the absence of cysteine 151 suggesting an element of redundancy among the cysteines of Keap1 (Dayalan Naidu et al., 2018).

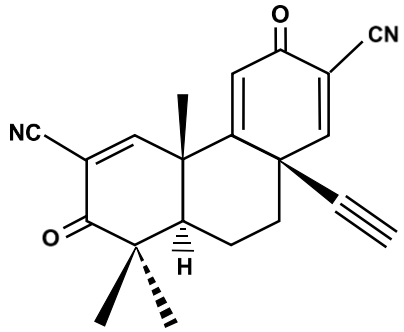

TBE-31

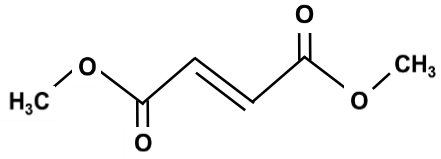

Dimethyl fumarate

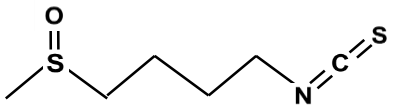

Sulforaphane

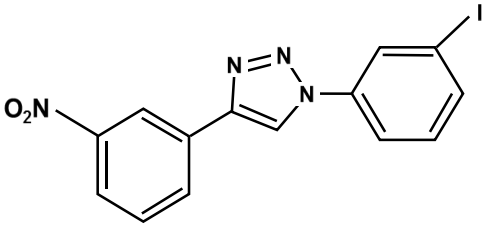

PMI

Figure 1.4**. Examples of small-molecule Nrf2 activators**. Chemical structures of 10a-ethynyl-4b,8,8-trimethyl-3,7-dioxo-3,4b,7,8,8a,9,10,10a-octahydrophenanthrene-2,6-dicarbonitrile (TBE-31), 1-isothiocyanato-(4R)-(methylsulfinyl)butane (sulforaphane), 1-(3-iodophenyl)-4-(3-nitrophenyl)-1,2,3-triazole (PMI) and dimethyl fumarate (Tecdifera).

More recently, various peptides and small molecules have been developed which stabilise Nrf2 without covalently modifying Keap1's cysteine residues (Zhuang et al., 2017). For example, reversible protein-protein interaction inhibitors which inhibit the Nrf2 and Keap1 interaction. An example of such compound is HB229, also identified as p62-mediated mitophagy inducer (PMI) (East et al., 2014). PMI was shown to upregulate Nrf2 and Nrf2-downstream target genes, NQO1 and HO-1 to a similar extent as sulforaphane (East et al., 2014). More interestingly,

PMI upregulated p62 and induced mitophagy, the select removal of mitochondria via autophagy (East et al., 2014). Despite the induction of p62, mitophagy was not observed with sulforaphane treatments (Georgakopoulos et al., 2017). Actually, sulforaphane was shown to prevent p62 recruitment, restricting mitochondrial ubiquitination, an essential process required for mitophagy (Georgakopoulos et al., 2017). Interestingly, it was recently shown that p62 recruits Keap1 to mitochondria to promote mitochondrial ubiquitination and mitophagy independently of PINK1 and Parkin (Yamada et al., 2018, Yamada et al., 2019). A similar lack of mitophagy induction to that by sulforaphane was observed with other electrophilic Nrf2 inducers, *tert*-butylhydroquinone (TBHQ), dimethyl fumarate and curcumin (Georgakopoulos et al., 2017). Further investigation is essential to determine the mechanisms in which different types of Keap1 inhibitors can lead to different biological outcomes (Georgakopoulos et al., 2017).

1.1.6 Nrf2 and Keap1 sub-cellular localisation

Although few studies have been carried out, it is considered that the majority of endogenous Keap1 is localised in the perinuclear region of the cytoplasm with few molecules in the nucleus and endoplasmic reticulum (Watai et al., 2007). When cells were treated with electrophiles or Leptomycin B, a nuclear export inhibitor, Keap1's cytoplasmic localisation did not change whilst nuclear accumulation of Nrf2 occurred (Watai et al., 2007).

Interestingly, it has also been shown that both Keap1 and Nrf2 are present on the mitochondria in a complex with phosphoglycerate mutase family member 5 (PGAM5), a mitochondrial serine/threonine phosphatase (Lo and Hannink, 2008, Lu et al., 2014), suggesting a potential regulation of mitochondrial functions by the pathway. Indeed, it was shown that PGAM5 or Nrf2 depletion caused aberrant degradation of the mitochondrial Rho GTPase, Miro2, which is involved in linking mitochondria to microtubules (O'Mealey et al., 2017). This was carried out under proteasome inhibition where Keap1 was acting in a dominant negative manner

due to absence of its binding partners. This caused Keap1-dependent degradation of Miro2, ultimately, inhibiting mitochondrial retrograde trafficking in conditions of proteasome inhibition (O'Mealey et al., 2017). Still, it was not explained how Keap1 was still able to target Miro2 despite losing its mitochondrial anchor PGAM5.

1.2 PGAM5

PGAM5 is a 32kDa phosphatase due to its proposed existence on the mitochondria (Lu et al., 2014). However, its precise location on the mitochondria is still highly debated. On the one hand, it has been shown to be targeted to the outer mitochondrial membrane via its N-terminal transmembrane domain (Lo and Hannick, 2008). Identification of cytoplasmic binding partners like Keap1 and CK2 support this hypothesis (Panda et al., 2016, Chen et al., 2014). Alternatively, PGAM5 has also been shown to be cleaved by inner mitochondrial membrane resident proteases such as rhomboid protease, PARL (Sekine et al., 2012). .

PGAM5 is nuclear encoded and belongs to the wider histidine acid phosphatase superfamily, more specifically as the fifth member of the phosphoglycerate mutase branch (Lo and Hannink, 2008, Chaikuad et al., 2017). Despite sharing homology of its catalytic domain with various metabolic enzymes, it lacks characteristic phosphotransferase and/or phosphohydrolase activity for small metabolites. Instead, PGAM5 contains a serine/threonine (and potential histidine) phosphatase activity (Panda et al., 2016, Takeda et al., 2009).

Two isoforms of PGAM5 have been reported (Panda et al., 2016). These are denoted as PGAM5-L and PGAM5-S, where PGAM5-L is the longer and main isoform compromising by 289 amino acids. In PGAM5-S, the shorter isoform derived from an mRNA splicing variation, there is a swap of 50 amino acids for 16 amino acids at the C-terminal (Lo and Hannink, 2008). More importantly, overexpression of either isoforms caused opposing morphological changes in

mitochondria (Lo and Hannink, 2008). In both COS1 and HeLa cells, transfected PGAM5-S protein caused the typical reticular-tubular mitochondrial network to become detached and punctuate, dispersed throughout the cytoplasm (Lo and Hannink, 2008). However, when PGAM5-L protein was transfected, individual mitochondria formed perinuclear aggregates (Lo and Hannink, 2008). Despite these observations, the significance of these PGAM5 isoforms in mitochondrial function isn't known. It is postulated that they are involved in regulating mitochondrial dynamics which is essential for several mitochondrial functions such as mitochondrial quality control (Lo and Hannink, 2008).

Several studies have shown PGAM5 to bind to a variety of proteins to mediate various signalling processes (Moriwaki et al., 2016). Originally, PGAM5 was discovered as a binding partner to the antiapoptotic protein, BCL-XL (Hammond et al., 2001) and later as a substrate for Keap1. Via the ESGE motif present in the N-terminus, PGAM5 binds to Keap1 causing it to be ubiquitinated by the Keap1-Cullin3 complex for proteasomal degradation (Lo and Hannink, 2006). Similarly to Nrf2, this is prevented with oxidative stress and treatment with sulforaphane, allowing PGAM5 to stabilise (Lo and Hannink, 2006). The requirements of such stabilisation aren't well-studied suggest that PGAM5 is likely to play a decisive role in the cell fate in environments of oxidative stress.

Interestingly, it was also shown that this Keap1-PGAM5 interaction is actually part of a larger ternary complex present on mitochondria (Lo and Hannink, 2008). The Keap1 homodimer is considered to bind to Nrf2 and PGAM5 simultaneously via the ETGE and ESGE motifs present in each respective protein (Lo and Hannink, 2008). The function of this mitochondrial complex remains to be elucidated, however PGAM5 and Keap1 knockdown was shown to increase Nrf2-dependent gene expression using an ARE-dependent firefly luciferase reporter gene construct (Lo and Hannink, 2008). However, how this population of Nrf2 on the mitochondria can induce cytoprotective gene transcription raises many questions. Such stoichiometry does not conform into what is currently understood about

canonical Nrf2 regulation and therefore necessitates further exploration of the complex.

In addition to this complex, PGAM5 is also found to interact with apoptosis signal-regulating kinase 1 (ASK1), a mitogen-activated protein kinase (MAPK) kinase (Takeda et al., 2008). It is hypothesised that PGAM5 may indirectly activate ASK1 by direct dephosphorylation of unknown phosphorylation sites that contribute to the suppression of ASK1 kinase activity. This dephosphorylation event is considered to unleash phosphorylation of the residue threonine-838 in the kinase domain, leading to the activation ASK1 (Takeda et al., 2008).

Another PGAM5 interactor is the protein kinase, RIP3, where the significance of this interaction in necroptosis is disputed (Wang et al., 2012, Lu et al., 2016). Moreover, PGAM5 has also been associated with the proteins involved in mitophagy. For example, PTEN-induced kinase 1 (PINK1) (Lu et al., 2014), BCL2L (Wu et al., 2014) and FUNDC1 (Chen et al., 2014).

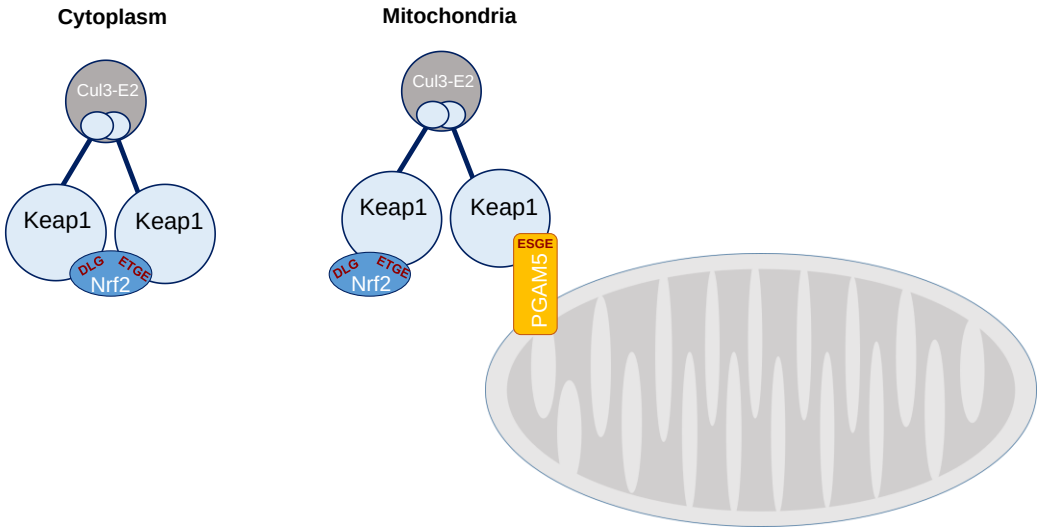

Figure 1.5. **The Keap1-Nrf2-PGAM5 complex present on the mitochondria**. The canonical Nrf2-Keap1 interaction is via the DLG and ETGE motifs present in the Neh2 domain of Nrf2. However, on the mitochondria, Nrf2 and Keap1 are found in a ternary complex with PGAM5. PGAM5 anchors the complex to the mitochondria and binds to Keap1 via an ESGE motif, a variant of the ETGE motif present in Nrf2. Nrf2 is then bound unconventionally to Keap1 via the ETGE motif alone.

1.3 Mitochondria and Mitophagy

Autophagy is a catabolic, evolutionary conserved process where, under various cellular stress environments, cytoplasmic components are removed from the cell (Mizushima, 2007). These tend to be removed via autophagic vesicles which fuse with lysosomes for ultimate degradation. There are three types of autophagy: macroautophagy, microautophagy and chaperone-mediated autophagy, which are categorised according to how each substrate is delivered to the lysosomes (Mizushima, 2007). Macroautophagy relies on double-membraned autophagasomes to deliver cellular components to the lysosomes for bulk degradation. Macroautophagy (hereafter referred to as autophagy) can also be further divided into selective and non-selective autophagy. Non-selective autophagy is often a response to starvation and nutrient deprivation where amino acids and nutrients are made available from several cellular components for cell survival (Mizushima, 2007). However, selective autophagy occurs even in nutrient rich conditions and is often a way to remove dysfunctional organelles such as mitochondria (Mizushima, 2007).

Mitochondria are double membrane bound, 1-10μM sized organelles which contain their own circular genome, encoding for tRNAs, rRNAs and 13 proteins (Nunnari and Suomalainen, 2012). They are often described as cellular “powerhouses” due to their crucial function in synthesising adenosine triphosphate (ATP) through the process of oxidative phosphorylation (OXPHOS). In addition to ATP synthesis, they also have key roles in other cellular processes such as apoptosis, iron metabolism and calcium regulation and storage (Duchen, 2004, Paul et al., 2017, Jeong and Seol, 2008).

ATP production via OXPHOS requires five complexes (I, II, III, IV, V). Complex I (NADH:ubiquinone oxidoreductase) and II (succinate dehydrogenase) are involved in the oxidation of substrates NADH and succinate, respectively. This leads to the transfer of electrons onto an electron carrier, called ubiquinone.

Ubiquinol (reduced ubiquinone) delivers the electrons to complex III (Coenzyme Q– cytochrome C reductase). Complex III's iron ion is reduced and the electrons are passed onto another carrier called cytochrome C. Next, cytochrome C delivers the electrons to complex IV (Cytochrome C oxidase) to reduce oxygen and ultimately produce water. During this electron shuttling process, protons are being pumped across the inner mitochondrial membrane at complexes I, III and IV. This creates a proton electrochemical gradient. These protons travel down their electrochemical gradient via ATP synthase (complex V) and drives the phosphorylation of adenosine diphosphate to make ATP (Bergman and Ben-Shachar, 2016). Electron leakage at complex I (Kussmaul and Hirst, 2006), II (Quinlan et al., 2012) and III (Kussmaul and Hirst, 2006) can partially reduce oxygen and lead to the formation of superoxide ions, a form of ROS (Kussmaul and Hirst, 2006). Unmanaged ROS can be detrimental to mitochondria, causing them to become dysfunctional and inefficient (Guo et al., 2013). This in turn creates further ROS, perpetuating the damage and sabotaging the cells chances of survival. Thus, it is imperative that quality control mechanisms for the mitochondrial network are present in the cell in order to maintain crucial functions and homeostasis.

Autophagy of mitochondria or mitophagy, is the selective removal of mitochondria in the cell (Lemasters, 2005). Mitophagy was first observed by Ashford and Porter (Ashford and Porter, 1962) in glucagon- treated rat hepatocytes where greater numbers of lysosomes were present. Besides this, each of these lysosomes contained a mitochondrial fragment. Various observations were later reported but the first mechanistic study of mitophagy was studied in yeast (Kanki and Klionsky, 2008). It was revealed that the ATG11, ATG20 and ATG24 genes, essential to selective-autophagy, were also essential for mitophagy (Kanki and Klionsky, 2008). More interestingly, a switch to amino acid starvation supplemented with glucose after cells were cultured with lactate as the only carbon source caused mitophagy to occur. This is because the glucose in media made the mitochondria non-essential. However, in media where lactate was the only carbon source, mitochondrial metabolism was required and therefore mitophagy was blocked.

Despite the different media conditions, macro-autophagy was strongly activated in both (Kanki and Klionsky, 2008). Collectively, this study showed that mitophagy is an example of selective autophagy but is likely to be induced by a specific set of conditions which differ to macro-autophagy.

1.3.1 PINK1-Parkin dependent mitophagy

Parkinson's disease (PD), an incurable, neurodegenerative disorder, is pathologically characterised by dopaminergic neuronal death in the substantia nigra and the accumulation of proteinaceous aggregates in surviving neurones (Braak et al., 2003). Degeneration of these dopaminergic neurones leads to insufficient levels of dopamine, an essential neurotransmitter involved in the regulation of motor function. Despite this knowledge, the underlying molecular mechanisms leading to PD were marginally understood. However, seminal work in the past couple of decades has identified approximately 20 different genes linked to PD which have provided invaluable insights into the molecular pathways involved. Two examples are the genes encoding for PINK1 and Parkin, an E3 ubiquitin ligase. Autosomal recessive mutations were reported in both of these genes (Valente et al., 2004, Kitada et al., 1998) giving rise to early autosomal recessive Parkinsonism and later found to be crucial for mitochondrial function.

PINK1 is a ubiquitously expressed serine/threonine kinase encoded by the *PARK6* (*PINK1*) gene. It is a 581 residue protein with a highly conserved C-terminal kinase domain, a transmembrane helix and a unique sequence encoding for a mitochondrial targeting motif (Gandhi et al., 2006). In homeostatic conditions, PINK1 is rapidly turned over. More specifically, it has a half-life of approximately 30 minutes (Lin and Kang, 2008), making it difficult to detect in cells. This is due to mitochondrial-dependent processing which occurs following its translocation to the mitochondria. As it is imported to the inner mitochondrial membrane, the mitochondrial targeting motif in cleaved PINK1 is imported into the mitochondria via the translocase of the outer membrane (TOM) complex (Lazarou et al., 2012) and the inner mitochondrial membrane (IMM)-localized Tim

(translocase of the inner membrane) 23 complex (Neupert and Herrmann, 2007). Next, various proteases, such as the mitochondrial processing peptidase (MPP) and the presenilins-associated rhomboid-like (PARL) proteases, cleave PINK1, producing a final 52 kDa form of PINK1 (Jin et al., 2010). This 52kDa form is rapidly degraded, except in the presence of proteasome inhibitors where it is subsequently stabilised (Narendra et al., 2010b). This indicates that cleaved PINK1 was being retro-translocated to the cytosol followed by proteasome dependent-degradation. This was further supported by Yamano and Youle (2013), who decrypted the underlying mechanism of PINK1 re-translocation known as the N-end rule-dependent degradation. When PINK1 is cleaved by PARL, a phenylalanine at position 104 becomes the new N-terminal acid. This created an ‘N-degron’, more specifically a ‘type-2 N-degron’ which was previously shown to signal for ubiquitination (Tasaki et al., 2005). PINK1 is then degraded by E3 enzymes UBR1, UBR2, and UBR4, which recognize these type-2 degrons (Tasaki et al., 2005).

In homeostatic conditions, PINK1 is found in low abundance so that mitophagy of healthy mitochondria does not occur. However, in situations of damage or stress, the mitochondrial membrane can become depolarised leading to mitochondrial dysfunctions and potential cell death. The mitochondrial membrane potential ($\Delta\Psi m$) is crucial for healthy mitochondria to perform their vital functions for the cell. It is ultimately driven by several redox transformations which generate an electrical potential and a proton gradient (Mitchell, 1966). When the $\Delta\Psi m$ becomes unstable or worse, remains in a depolarised state, several imperative functions in the cell are lost (Dey and Moraes, 2000). Therefore, it is obvious that cells require mitochondrial quality control mechanisms like mitophagy to avoid such situations. Parkin was first linked to these quality control mechanisms through studies involving loss-of-function mutations in *Drosophila melanogaster* flies (Greene et al., 2003). It was then observed that the absence of PINK1 created similar mitochondrial defects to those observed in the absence of Parkin (Clark et al., 2006, Park et al., 2006). Rescue experiments in these flies showed that the PINK1-KO phenotype could be rescued by Parkin overexpression

whereas the opposite was not the case. This disclosed that PINK1 was acting upstream of Parkin and was fundamental to understanding the mitophagy pathway induced in response to loss of ΔΨm.

When mitochondria become depolarised, for example after treatment with uncouplers like carbonyl cyanide m-chlorophenylhydrazone (CCCP), full length PINK1 is stabilised on the mitochondria. This is due to lack of processing by MPP or PARL which allows PINK1 to span the outer mitochondrial membrane with its kinase domain exposed to the cytosol (Zhou et al., 2008). PINK1 undergoes auto-phosphorylation at serine 402 and serine 228 via trans-phosphorylation of their activation loops; a similar mechanism used by many other auto-phosphorylating kinases (Okatsu et al., 2012). Activated PINK1 is then able to phosphorylate ubiquitin at serine 65 (Koyano et al., 2014). Phosphorylated-serine 65 ubiquitin binds to Parkin, priming it for phosphorylation by PINK1 at its equivalent serine 65 residue within its ubiquitin-like domain (Kazlauskaite et al., 2014). This leads to full Parkin activity where various outer mitochondrial membrane proteins are ubiquitylated. For example, the voltage-dependent anion channel (VDAC), mitochondrial Rho GTPases (MIRO) 1 and 2 and components of the TOM complex (Chan et al., 2011, Yoshii et al., 2011). It isn't fully understood how Parkin promotes mitophagy, but one hypothesis suggests that its targeted ubiquitination of these outer mitochondrial membrane proteins are critical to the process. Kirkin and colleagues (Kirkin et al., 2009) showed that ubiquitination played an important role in the selective removal of other cellular components and pathogens by autophagy. Adaptor molecules, such as the Nrf2 target p62, are thought to directly interact with both the ubiquitin chains on these proteins and LC3, microtubule-associated proteins 1A/1B light chain 3B (Pankiv et al., 2007). LC3 can be found in two forms, in a cytosolic or lipidated form. The lipidated form is important in the formation of the autophagasome and is often used as a reliable marker for monitoring autophagy and autophagy-like processes (Tanida et al., 2004). Alternatively, other potential roles for Parkin in mitophagy have been described. For example, it has been shown to recruit proteasomes to depolarised mitochondria for selective removal of the outer mitochondrial membrane and

intermembrane space proteins (Chan et al., 2011, Yoshii et al., 2011). It also causes the outer mitochondrial membrane to rupture (Yoshii et al., 2011) and can interact with Ambra1, a protein involved in the activation of the class III phosphatidylinositol 3-kinase complex, involved in Beclin-1 dependent mitophagy (Van Humbeeck et al., 2011).

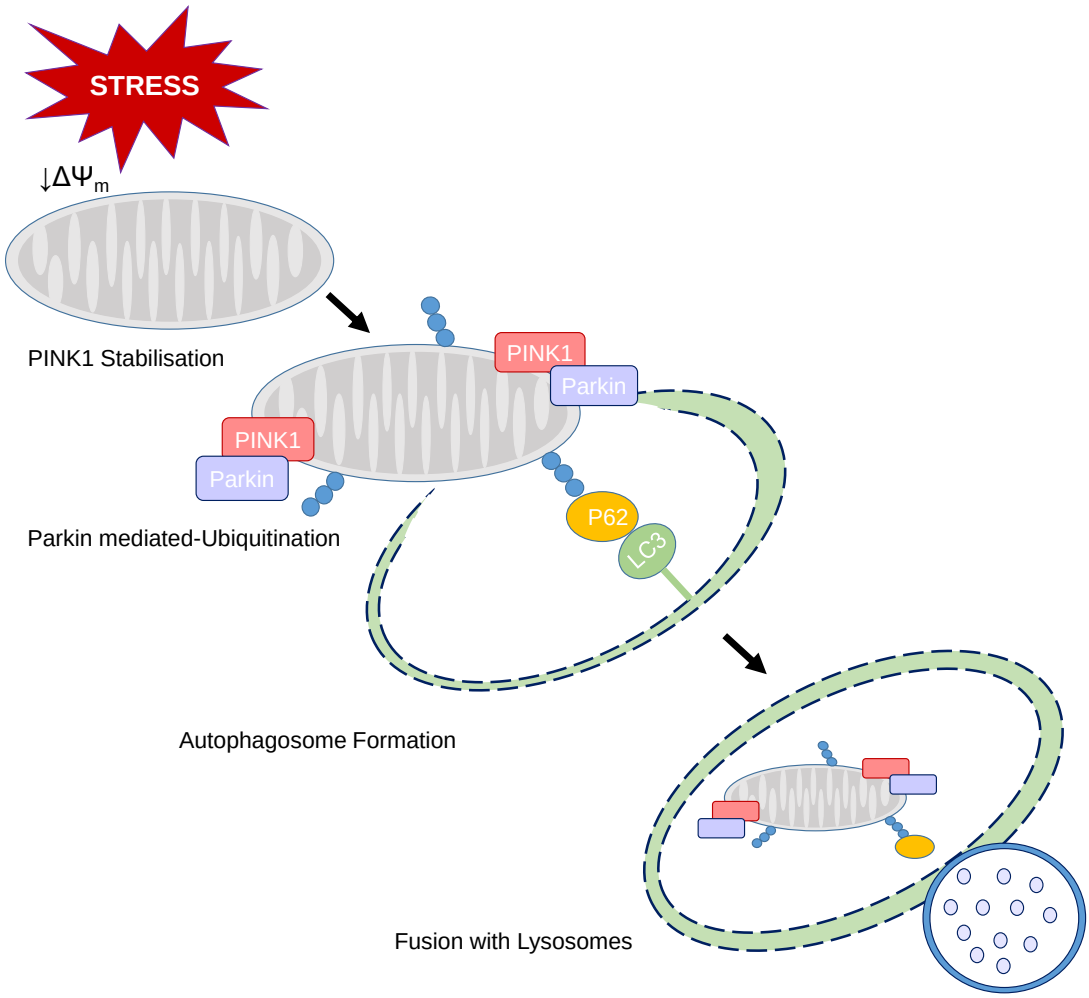

Figure 1.6 **Proposed mechanism of PINK1-Parkin mediated mitophagy**. When mitochondria are stressed or unhealthy, the mitochondrial membrane potential (ΔΨm) drops. This causes full length PINK1 to be stabilised on the mitochondrial membrane. The kinase activity of PINK1 causes it to autophosphorylate and phosphorylate ubiquitin. Parkin is then recruited to the outer mitochondrial membrane and ubiquitinates several outer mitochondrial membrane proteins. Such ubiquitin chains are then bound by mitophagic substrate adaptors like p62, which then bind to LC3-II to form an autophagosome. Here, damaged mitochondria are enclosed and fused with lysosomes for degradation.

Most knowledge linking PD to dysregulated PINK1-Parkin dependent mitophagy has been acquired *in vitro.* However, a recent study using Mito-QC reporter mouse *in vivo,* has shown the influence of knocking out PINK1 on basal mitophagy in various metabolically active organs (McWilliams et al., 2018). As expected, high levels of basal mitophagy were observed in neural cells but the absence of PINK1 didn't alter this. However, knockout of PINK1 did affect mitophagy in pancreatic islets, suggesting that different mitophagy pathways or mechanisms may be involved in different cellular conditions in various organs.

1.3.2 BNIP3 and Nix

Aside from the PINK1-Parkin pathway, mitophagy has been reported to occur through other mediators. For example, the outer mitochondrial transmembrane proteins, BNIP3 and its related protein NIX. Structurally, both share 50% homology, contain uncharacteristic BCL2-homology 3 (BH3) domains and form homodimers through glycine zippers present in their transmembrane domains (Ney, 2015). In addition, these proteins also contain an LIR (LC3 interaction motif) suggesting their potential as autophagy receptors, particularly in hypoxic environments (Zhang and Ney, 2009).

NIX was first associated with mitophagy when NIX-deficient mice displayed an atypical accumulation of mitochondria (Schweers et al., 2007). Moreover, NIX-deficient reticulocytes cultured *in vitro* were shown to have dysfunctional mitochondrial clearance (Zhang et al., 2008). To further elucidate the role of NIX, using both wild-type and NIX deficient reticulocytes, ultrastructural studies have shown the importance of NIX in the recruitment of membranes for immature autophagasome formation around individual mitochondria (Ney, 2015). Moreover, also in reticulocytes, mutations in NIX's LIR showed an effect on mitochondrial clearance (Novak et al., 2010).

BNIP3 has also been shown to be involved in hypoxia-mediated mitophagy (Zhang et al., 2008). In hypoxic conditions, high levels of ROS occur and HIF-1

(hypoxia inducible factor 1) increases BNIP3 expression. In turn, BNIP3 interferes with the BCL2-Beclin-1 interaction allowing Beclin-1-dependent mitophagy to occur. This leads to a decrease in ROS and increased cell survival (Zhang et al., 2008).

1.3.3. FUNDC1

The 155 amino acid protein, Fun14 domain-containing protein 1 (FUNDC1), is another important player in hypoxia-mediated mitophagy (Liu et al., 2012). Endogenously expressed FUNDC1 is exclusively found on the mitochondria. More specifically, it is thought to be an outer mitochondrial membrane protein with its amino acid terminus exposed to the cytosol and its carboxy terminus spanning across the intermembrane space (Liu et al., 2012). Within its N-terminal region, lies a motif of YxxL, a similar consensus sequence known as an LC3 interacting region (LIR), previously reported in autophagy receptors which bind to LC3 (Pankiv et al., 2007, Noda et al., 2010).

Overexpression of FUNDC1 in cell lines, such as HeLa and mouse embryonic fibroblasts, induced mitophagy (Liu et al., 2012). In the context of hypoxia, mitophagy was confirmed through western blot analysis of several mitochondrial markers, TOM20, TIM23 and VDAC1, all of which decreased. Treatment with bafilomycin A1, an inhibitor of the lysosomal ATPase responsible for lysosomal acidification, prevented this degradation (Liu et al., 2012). More importantly, FUNDC1-knockdown also prevented the degradation of these mitochondrial proteins and the loss of mitochondrial volume, suggesting FUNDC1 is an important regulator of hypoxia-mediated mitophagy. This was further established with rescue experiments in stably knocked down FUNDC1 cells transfected with wild-type but not mutant FUNDC1 (Liu et al., 2012).

Mechanistically, in normoxia, FUNDC1 is phosphorylated by Src and CDK2 kinases in the LIR motif at tyrosine 18 and serine 13, respectively (Liu et al., 2012, Chen et al., 2014). Phosphorylated FUNDC1 has a lower affinity for LC3 and

therefore downstream mitophagy does not occur. However, in hypoxic conditions, dephosphorylation of FUNDC1 occurs, allowing for a higher affinity for LC3 binding via the LIR motif (Liu et al., 2012). Interestingly, the binding of FUNDC1 to LC3 is unique, differing from other LC3-LIR binding structures found in other LC3 binding proteins like p62 (Kuang et al., 2016). It is also postulated that each phosphorylation event regulates FUNDC1 differently. Phosphorylation at tyrosine 18 was shown to be crucial for LC3 binding but serine 13 phosphorylation is thought to be involved in enhancing mitophagy via mediating interactions with various mitochondrial fission/fusion factors such as DNM1L/DRP1 and OPA1 (Chen et al., 2016, Kuang et al., 2016).

1.3.4 Bcl2L13

Previous studies in yeast have shown that Atg32 is vital for mitophagy. Atg32 localised to the mitochondria and is considered to be a receptor involved in mitophagy where it interacts with proteins involved in recognition of cargo receptors (Okamoto et al., 2009). In mammals, the same group discovered an Atg32 homologue called Bcl2-like protein 13 (Bcl2L13) (Murakawa et al., 2015).

Bcl2L13 belongs to the Bcl-2 family in an atypical fashion due to its lack of interaction with anti-apoptotic or pro-apoptotic Bcl-2 members despite containing four BH domains (Kataoka et al., 2001). Structurally, it has a C-terminal single transmembrane domain which embeds it into the outer mitochondrial membrane (Kataoka et al., 2001, Murakawa et al., 2015) and a LIR motif which binds to LC3. This interaction with LC3 is strengthened with CCCP treatment in HEK293 cells.

In cells, Bcl2L13 overexpression and small interfering RNA-mediated knockdown caused mitochondrial fragmentation and elongation, respectively (Murakawa et al., 2015). Fragmentation was shown to be dependent on Bcl2L13 having its four BH domains and its mitochondrial localisation. Moreover, this phenotype was shown to manifest independently of LC3 binding or activity of dynamin-1 like protein (Drp-1), a GTPase which regulates mitochondrial fission (Murakawa et al,

2015). This is particularly unique as most mitophagy pathways require Drp-1 activity (Chen et al., 2016, Park et al., 2018).

Using LC3-I/LC3-II conversion and the mtKeima model, as measurements for mitophagy, Bcl2L13 overexpression caused mitophagy. This occurred through LC3 interactions as mutants in the LIR domain failed to induce mitophagy. It was also shown that this Bcl2L13-mediated mitophagy was independent of Parkin as mitophagy occurred in HeLa cells, a cell line with a lack of functional *Parkin* gene (Murakawa et al., 2015). Mechanistically, CCCP-mediated depolarisation caused both an increase in Bcl2L13 protein levels and phosphorylation of the serine 272 (Murakawa et al., 2015). Despite this knowledge and observations of mitophagy, the underlying mechanisms involved in Bcl2L13-mediated mitophagy remain to be fully elucidated.

1.3.5 Atypical forms of mitophagy - Iron regulated mitophagy

Dysregulated iron metabolism is a common feature in neurodegenerative diseases (Matak et al., 2016). Interestingly, use of iron chelators like deferiprone (DFP) have been shown to induce mitophagy in a chemical screen (Allen et al., 2013). Moreover, immunofluorescence showed increased LC3 and COXIV (component of the complex IV subunit) co-localisation suggesting specific autophagy of mitochondria (Allen et al., 2013). At the protein level, decreases of 50% were observed in a variety of mitochondrial protein markers with a 24-hour DFP treatment (Allen et al., 2013). This decrease was prevented with autophagy inhibitor bafilomycin, further supporting the degradation of the mitochondria was dependent on lysosomal degradation (Allen et al., 2013). Most importantly, unlike many inducers of mitophagy, iron depletion-dependent mitophagy was shown to be independent of the Parkin-PINK1 machinery (Allen et al., 2013). How iron depletion induces mitophagy isn’t fully elucidated. The same study showed that a 4-hour treatment with the iron chelator reduced basal and maximal respiration despite not affecting the mitochondrial membrane potential (Allen et al., 2013). After 24 hours of treatment, oxygen consumption was obliterated. Interestingly,

ATP levels remained similar despite loss of oxidative phosphorylation, suggesting a potential metabolic switch to glycolysis (Allen et al., 2013). Regardless of these observations, mechanistically how this metabolic switch occurs and how it is related to mitophagy remains to be investigated.

1.4 Nrf2/Keap1 Pathway in Mitophagy

Research in the past few years has highlighted the significance of Nrf2 in mitochondrial integrity and function (Dinkova-Kostova and Abramov, 2015). As previously mentioned, Nrf2 has a plethora of downstream targets involved in several diverse functions in the cell, one of which includes selective autophagy (Pajares et al., 2016). Key influencers of selective mitophagy, for example p62 and autophagy-related gene 8 (ATG8), are downstream targets of Nrf2. More specifically to mitophagy, p62 is considered to be an important contributor to PINK1-Parkin mitophagy. Upon p62 knockdown in cells, some studies describe a decrease in mitophagy, suggesting p62 has an important role in the process (Geisler et al., 2010, Lee et al., 2010). However, another study found that p62 is important in aggregating damaged mitochondria but not for mitophagy (Narendra et al., 2010a).

PINK1 plays a prominent role in the quality control of mitochondria by initiating the process of mitophagy in unhealthy damaged mitochondria. Interestingly, PINK1 has also been shown to have four potential ARE sequences in its promoter, suggesting PINK1 is regulated by Nrf2 (Murata et al., 2015). Indeed, it was shown that pharmacological induction of Nrf2, for example by tBHQ, caused increased PINK1 protein expression and mRNA levels, which was then lost when validated Nrf2 siRNAs were used (Murata et al., 2015). These inducers increased hydrogen peroxide levels and co-treatment of them with the antioxidant *N*-acetylcysteine abolished the induction of PINK, suggesting the Nrf2-PINK1 axis is dependent on ROS (Murata et al., 2015). Further supporting the link between Nrf2 and PINK1, is the effect of tomatidine in the induction of mitophagy in *C.*

elegans, primary rat neurones and neuronal human cells via the SKN-1 (Nrf2 homologue) pathway (Fang et al., 2017). Tomatidine, abundantly found in unripen tomatoes, induced mitophagy through DCT-1 (PINK1 homologue) and similar to Murata et al. (2015) it was proposed that ROS are key to this process. Low levels of ROS induction by tomatidine are thought to activate Nrf2 signalling, which ultimately leads to mitophagy (Fang et al., 2017). However, in this study, the effect of Nrf2/SKN-1 KO or KD was not shown and therefore other pathways may be involved. Ultimately, emerging evidence suggests that Nrf2 may be an important mediator of PINK1-induced mitophagy through the management of ROS and therefore overall may be crucial for mitochondrial integrity.

Alternatively, a study also showed that PINK1 can influence Nrf2 activity and expression. In a model of ubiquitin proteasome system (UPS) dysfunction, mutant PINK1 (G309D) inhibited heme-oxygenase 1 (HO-1) expression, a Nrf2 target gene, in SH-SY5Y cells (Sheng et al., 2017). Moreover, in this MG132-induced model, nuclear translocation of Nrf2 was antagonised by G309D mutant PINK1 (Sheng et al., 2017). Moreover, both Nrf2 protein and mRNA levels of NQO1, a Nrf2 downstream target, were decreased in the presence of mutant PINK1 (Sheng et al., 2017). Firstly, this suggests that PINK1 has a role in regulating Nrf2 transcriptional activity. Secondly, the location of this mutation on PINK1 is responsible for Nrf2 suppression. This missense mutation is known to cause PD, possibly through impairment of PINK1 kinase activity, substrate recognition and more interestingly, defects in complex I. Together, these findings suggest that Nrf2 may potentially require PINK1 dependent signalling to mediate its cytoprotective effects through downstream targets on mitochondria independently of mitophagy.

Despite the consensus that Nrf2 can also be found tethered to the mitochondria in a quaternary complex with a Keap1 dimer and PGAM5, its actual function isn't fully understood. In fact, the actual role of the complex itself isn't clearly defined. Interestingly, knockdown of PGAM5 debilitated PINK1 induced mitophagy *in vitro*, led to degeneration of dopaminergic neurones and induced Parkinson-like

movement phenotype in mice (Lu et al., 2014). The same study showed that PGAM5, through an evolutionary conserved region (amino acids 98-110), directly binds and stabilises wild-type, but not PD-associated mutant PINK1 (Lu et al., 2014). The effect of Nrf2 within the PGAM5-Nrf2-Keap1 complex on mitophagy has yet to be studied. Collectively, based on the findings from the work of Murata et al. (2015) and Lu et al. (2014), it could be proposed that the PGAM5-Nrf2-Keap1 complex may function with Keap1 as an immediate mitochondrial ROS sensor which allows newly synthesised Nrf2 to accumulate and induce PINK1 expression. PINK1 is then stabilised by PGAM5 in the complex to initiate PINK1-dependent mitophagy.

Lastly, a non-electrophilic Nrf2 activator, PMI, was shown to drive mitophagy without dissipating the mitochondrial membrane potential or Parkin recruitment (East et al., 2014). PMI induces mitochondrial respiration, superoxide mediated mitophagy and expression of several autophagy-associated genes like p62/SQSTM1. Interestingly, other Nrf2 inducers such as sulforaphane and dimethylfumurate (DMF), which covalently modify Keap1, are unable to induce such a response. In fact, co-treatment of PMI with sulforaphane was shown to inhibit PMI-induced effects like the accumulation of p62 required for mitophagy (Georgakopoulos et al., 2017). However, both drugs induce similar alterations on mitochondrial morphology and bioenergetic profiles suggesting that the reversible inhibition of PMI is specifically important for mitophagy (Georgakopoulos et al., 2017). As this was dependent on mitochondrial superoxide, it is likely that electrophilic Keap1 inhibitors are interfering with mitochondrial redox pathways concealing Nrf2's effects (Georgakopoulos et al., 2017). Most importantly, the PINK1-Parkin pathway was not required for mitophagy induced by PMI (Georgakopoulos et al., 2017). This is particularly exciting as PMI can be used to rescue mitochondrial turnover without relying on the PINK1-Parkin pathway which is often defective in PD.

1.5 PGAM5 in Mitophagy

Loss of the ΔΨm causes PARL to cleave PGAM5 (Sekine et al., 2012). Interestingly, PINK1 which is usually cleaved by PARL in homeostasis is actually stabilised under these conditions. Western blot analysis of a CCCP-dependent depolarisation time course showed that over 120 minutes, PINK1 stability coincided with PGAM5 cleavage (Sekine et al., 2012). This advocates that PARL can cleave different substrates leading to activation of different pathways depending on the health status of mitochondria and that PGAM5 may have significant role in mitophagy.

To further support this reciprocal PARL-mediated regulation of PINK1 and PGAM5, Lu et al. (2014) showed that PGAM5 regulated PINK1 by protecting it from PARL-mediated cleavage in CCCP-mediated depolarisation. Reported PINK1 mutations found in PD were resistant to this PGAM5 mediated stability. It is thought that this stability may partly be due to the binding of PGAM5 and PINK1. Investigations attempting to understand the potential binding of PINK1 to Parkin found PGAM5 to be a PINK1-binding protein (Imai et al., 2010). This was further confirmed, where highly conserved residues 98-110 of PGAM5 were required to bind to PINK1 (Lu et al., 2014).

Considering the significant amount of data showing the importance of PGAM5 in PINK1 stability, it is highly probable that PGAM5 can also affect PINK1-Parkin mitophagy. Swollen bulbous mitochondria lacking cristae were found in higher numbers in PGAM5 knockout mouse embryonic fibroblasts (MEFs) in comparison to the wild type (Lu et al., 2014). High levels of intracellular ROS and a small loss of mitochondrial potential were also observed in the PGAM5 knockout MEFs, suggesting that the presence of PGAM5 is important in the removal of unhealthy or damaged mitochondria (Lu et al., 2014). Further investigation using CCCP showed aggravated mitochondrial stress in wild-type MEFs leading to increased numbers of autophagosomes with some mitochondria enclosed and an overall decrease in mitochondria. Contrary to wild type, PGAM5 knockout MEFs only showed higher numbers of damaged mitochondria with no mitochondria

containing autophagosomes, suggesting the CCCP treatment failed to induce mitophagy in PGAM5 knockout cells (Lu et al., 2014). Biochemical analyses of mitochondrial clearance using the markers LC3I/II, the inner mitochondrial membrane protein COX IV and Tomm20, showed that PGAM5 knockout MEFs had reduced mitophagy (Lu et al., 2014). This was also confirmed using a lysosomal resistant, inner mitochondrial membrane targeted fluorescent protein, mt-Keima (Lu et al., 2014).

The fate of cleaved PGAM5 isn't fully understood. One study showed that despite being cleaved in CCCP-induced depolarisation, PGAM5 was not released from the mitochondria in HeLa cells, a cell line with no endogenous Parkin expression (Yamaguchi et al., 2019). However, with stable expression of HA-tagged Parkin, PGAM5 was diffusely distributed in approximately 30% of the cells (Yamaguchi et al., 2019). This may allow us to postulate that the cleaved PGAM5 form is unconstrained to the mitochondria in a potentially Parkin-dependent manner. Due to its involvement in ubiquitination of outer mitochondrial membrane proteins, it was hypothesised that the ubiquitin-proteasome system was involved. Indeed, treatment with proteasome inhibitors MG132 or epoxomicin reduced PGAM5 release but not its cleavage (Yamaguchi et al., 2019). Collectively, this may be due to proteasome-mediated rupture in mitophagy (Yoshii et al., 2011) which causes cleaved PGAM5 release, however further investigation is essential. The significance of cleaved PGAM5 release hasn't been elucidated. However, a recent study showed that cleaved PGAM5 dephosphorylated beta catenin in the cytosol to mediate Wnt signalling and ultimately mitochondrial biogenesis (Bernkopf et al., 2018).

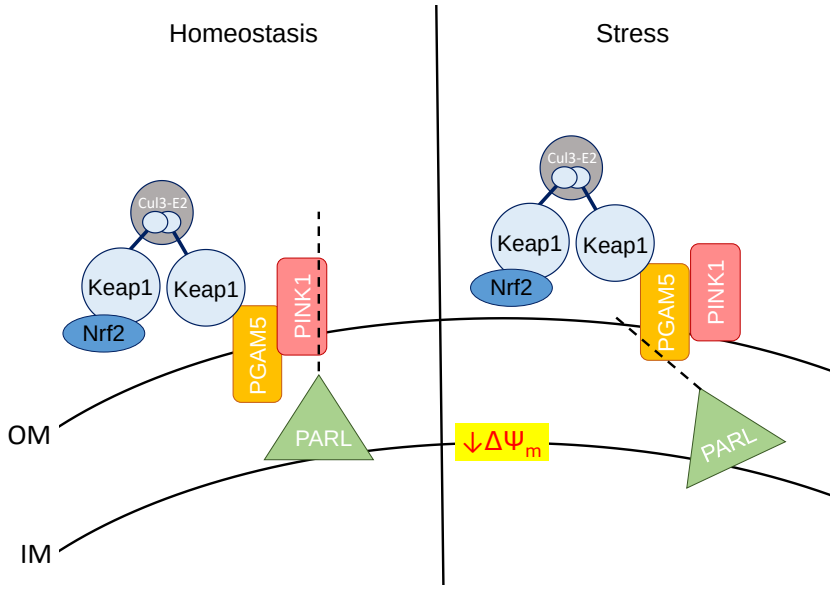

Figure 1.7. **PARL activity in homeostasis and conditions of mitochondrial depolarisation.** In homeostatic conditions, where the mitochondrial membrane potential ($\Delta\Psi_m$) is intact, presenilins-associated rhomboid-like (PARL) protease cleaves PINK1, causing it to be released into the cytoplasm where it is degraded by the proteasome. Under mitochondrial stress, where the $\Delta\Psi_m$ drops, PARL cleaves PGAM5 and allows PINK1 to be stabilised on the outer mitochondrial membrane. PGAM5 is essential for the stabilisation of PINK1 which is required for the induction of mitophagy.

Aside, from PINK1-Parkin mitophagy, PGAM5 has also been reported to regulate other forms of mitophagy. For example, as previously mentioned, FUNDC1 de-phosphorylation is required for mitophagy. This is carried out, in part, by PGAM5 which dephosphorylates the serine 13 residue in FUNDC1 under hypoxic conditions or after FCCP treatment (Chen et al., 2014). Such de-phosphorylation event enhanced FUNDC1's interaction with LC3 which was lost following knockdown of PGAM5 (Chen et al., 2014). Moreover, it was observed that CK2 phosphorylates at this same residue to reverse the effect of PGAM5 in initiating mitophagy (Chen et al., 2014). Collectively, this suggests that there is a potential 'on/off' switch for FUNDC1-mediated mitophagy via regulation of CK2 and PGAM5 activity.

1.6 Measuring Mitophagy

In the last few decades, several methodologies have been developed to measure mitophagy. For example, exposure to specific conditions or mitophagy inducers have been used to exaggerate the levels of mitophagy so that it is within a detectable range of these methodologies. Examples include pharmacological treatments with compounds like CCCP or DFP, or environments of hypoxia (Allen et al., 2013, Villa et al., 2017, Zhang et al., 2016). A major caveat of the available methodologies is that they provide indirect measurements of mitophagy. They tend to focus on one step of the process and assume that this will ultimately lead to mitochondrial turnover. For this reason, it is therefore important to use a couple of independent methodologies to obtain robust data.

Nonetheless, the use of mitophagy inducers coupled to fluorescence microscopy has provided substantial insight to what is currently understood in the field of mitophagy. Immunofluorescence microscopy with fixed cells has been used to detect a variety of mitochondrial proteins and proteins involved in selective autophagy. Co-localisation of these proteins often indicates whether the selective autophagy machinery is assembled to carry out mitophagy (Dolman et al., 2013). Examples include, co-localisation of mitochondria with mitophagy-related proteins like LC3 (Dolman et al., 2013). Such studies require mitochondrial labelling which is independent of its functional state. Examples include fluorescent dyes like the MitoTracker® dyes and fluorescent proteins targeted to the mitochondria (Dolman et al., 2013). These can be used to look at mitochondrial quantities, mass and morphology at different stages of mitophagy (Dolman et al., 2013)

Alternatively, fluorescent proteins can also be used to monitor mitophagy in live cells. For example, by labelling LC3 with green fluorescent protein (GFP) and a mitochondrial protein with mCherry, a combined yellow fluorescence will be emitted when the two co-localise in mitophagy. However, several issues need to be considered when transfecting these DNA plasmids into cells as contaminants or transfection reagents can cause autophagy responses to occur, confounding the outcomes of the study (Klionsky et al., 2012). Another issue is the likelihood

of a heterogeneous level of expression of the fluorescent protein in the cell which again can distort the outcomes of the study (Dolman et al., 2013). This could potentially be overcome with the production of a stable cell line. However, not only is this technically difficult and time consuming, the addition of this fluorescent protein-protein fusion can interfere or alter the function of the cell (Dolman et al., 2013)

Aside from measuring co-localisation of the autophagic machinery in cells, the delivery of mitochondria to the lysosomes can also be used to monitor mitophagy (Dolman et al., 2013). Similarly, antibodies and fluorescent proteins are employed to tag lysosomal resident proteins such as the lysosomal-associated membrane protein 1 (LAMP1) (Dolman et al., 2013). Additionally, lysosomal dyes, such as the LysoTracker® Deep Red, are available to label the lysosomes (Dolman et al., 2013). Using a combination of lysosomal protein markers and mitochondrial dyes or vice-versa, co-localisation of mitochondria and lysosomes can be used to measure mitophagy (Dolman et al., 2013).

A more sophisticated approach used to measure delivery of the mitochondria to the lysosomes was developed using a tandem fluorescent tag, coined as the MitoQC approach (Allen et al., 2013). Generally, a mitochondrial protein, Fis1, is tagged with two fluorescent proteins, GFP and mCherry. Under physiological conditions and the early stages of mitophagy, both mCherry and GFP fluoresce, producing a combined yellow fluorescence. However, when the dysfunctional mitochondria are delivered to the lysosome via autophagasomes, the fluorescent signal becomes predominately red. This is due to the acidic environment within the lysosome which quenches the green fluorescence emitted by GFP but not the red fluorescence emitted by mCherry (Figure 1.7). The number of red punta in the is then used to quantify the number of mitochondria undergoing mitophagy. Similar ratiometric fluorescence techniques have also been developed on similar principles. For example, mitochondrial matrix targeting pH-sensitive probe, the mt-Keima, which is often used to measure mitophagy in-vitro (Katayama et al., 2011, Sun et al., 2017).

Transmission electron microscopy (TEM) is a well-established tool to directly observe mitophagy. Using this technique key elements of mitophagy, such as the presence of the double-membraned autophagasomes capsuling the dysfunctional mitochondria, can be observed (Ding and Yin, 2012). Despite providing visual evidence of mitophagy occurring, TEM can be difficult to quantify due to large variations, limited cell numbers and sections (Ding and Yin, 2012). Moreover, it is time consuming and requires expertise in identification of cell types in tissues (McWilliams et al., 2016).

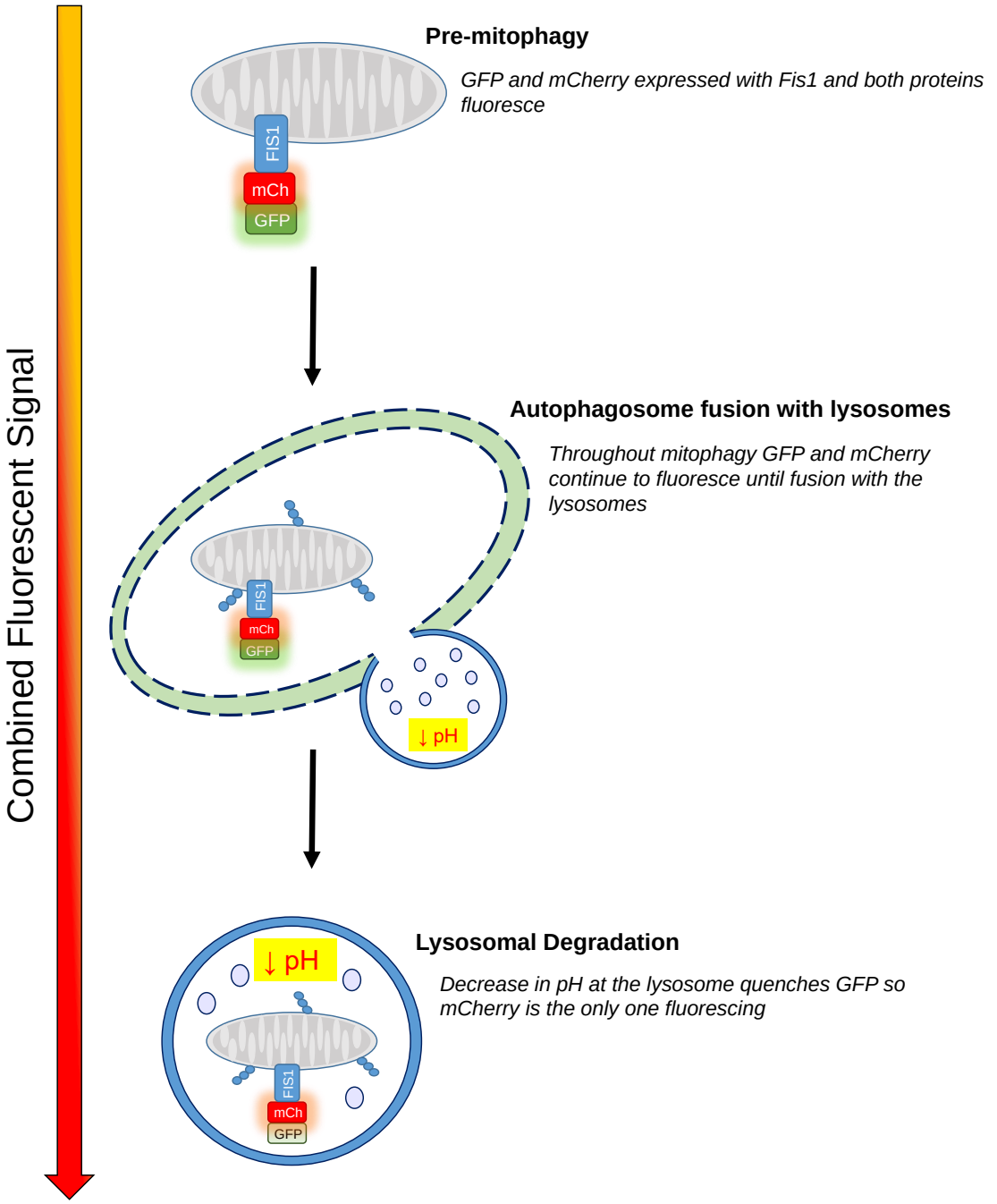

Figure 1.8. **The mitoQC-assay used to measure mitophagy.** Fis1, a mitochondrially localised protein, is tagged with two fluorescent proteins, mCherry and GFP (mCherry-GFP-Fis1). In environments of ~pH7, like the cytoplasm, a yellow fluorescent signal is observed at the mitochondria. This is due to both mCherry and GFP emitting red and green fluorescence respectively. In environments where the pH decreases, for example those of the lysosome, the GFP signal is quenched, leaving mCherry to fluoresce red alone. This occurs in mitophagy where

mitochondria containing autophagasomes are delivered to the lysosomes for degradation. The ratio between the GFP and mCherry signal is then used to quantitatively measure mitophagy.

In addition to microscopy techniques a variety of other biochemical approaches also provide indirect measurements of mitophagy. For example, using a fluorescence-activated cell sorting (FACS) technique with a mitochondrial stain like the Mitotracker® dyes, mitochondrial mass can be quantitatively measured (Ding and Yin, 2012). Similarly, an alternative to using mitochondrial retaining dyes, immunostaining of a mitochondrial markers like TOM20 or TIM23 can be used with FACS for measurements of mitochondrial mass (Ding and Yin, 2012). A consequence of such technique, if using the MitoTracker® dyes, is the reliance on an intact $\Delta\Psi_m$ (Ding and Yin, 2012). This means that damaged or unhealthy mitochondria may not be included in the total mass. Moreover, care must be taken when selecting the mitochondrial marker for FACS. A recent study showed that some mitochondrial outer membrane proteins were degraded via the proteasome instead of mitophagy and therefore incorrect selection of the marker can confound results obtained (Ding and Yin, 2012, Yoshii et al., 2011).

Western blot analysis is another method often used to indirectly measure mitophagy. Such analysis requires a selection of mitochondrial markers spanning the various compartments of the mitochondria, including proteins from the outer and inner membranes, intermembrane space and mitochondrial matrix (Ding and Yin, 2012). Although outer mitochondrial membrane proteins like TOM20 and VDAC are used, it is important to consider that these may be turned over by other mechanisms like proteasomal degradation (Ding and Yin, 2012). Proteins like heat-shock protein 60 (HSP60), a mitochondrial matrix protein and TIM23, a translocase of the inner mitochondrial membrane, should also be considered for the panel of mitophagy markers due to their differing mitochondrial localisations (Ding and Yin, 2012). To determine whether decreases in the mitochondrial protein marker panel are in fact due to mitophagy, autophagy inhibitors are often used. Treatment of cells with bafilomycin A1 after triggering mitophagy will

provide further evidence of whether the decrease in protein levels are due to an autophagic mechanism.

Lastly, measuring the activity of several enzymes involved in mitochondrial-mediated metabolism can also be used to indirectly monitor mitophagy. The lower the mitochondrial mass, the less activity detected from these enzymes. For example, monitoring citrate synthase, an enzyme involved in the citric acid cycle, is used to measure mitochondrial mass (Ding and Yin, 2012). Despite the acknowledgement that citrate synthase activity is not affected by factors that affect mitochondrial function, for example disruption of the electron transport chain, it must be considered that other factors may influence its activity (Ding and Yin, 2012).

1.7 Clinical relevance of mitophagy

Healthy mitochondria are fundamental for cell homeostasis and survival. Physiological quality control mechanisms, like mitophagy, are present in cells in order to keep the mitochondrial network functioning optimally. These mechanisms are of particular importance in post-mitotic cells, such as cardiomyocytes (Kubli and Gustafsson, 2012) and neurones (Granatiero and Manfredi, 2019), which cannot rely on being replenished after cell death or on cell division to dilute the damaged mitochondria. Moreover, these cells require optimal mitochondrial function to meet their high metabolic needs. High metabolic activity often leads to mitochondrial ROS production when unmanaged could cause damage to various cellular components such as proteins and lipids, making them ineffective and vulnerable to mitochondrial dysfunction and ultimately cell death.

One clinical disorder which may be associated to dysfunctional or inefficient mitophagy is Parkinson’s disease (PD). As previously explained, PINK1 and Parkin are two reported genes that are mutated in Parkinsonian-like disorders (Gao et al., 2017). Many investigations into the effects of Parkin and PINK1 on mitophagy have been carried out in *Drosophila*. For example, deficiency in either

gene led to damaged mitophagy and elongated mitochondria (Ziviani et al., 2010). Furthermore, Parkin mutants also had significant locomotor issues due to significant defects in flight muscle (Greene et al., 2003). Parkin and PINK1 mutant flies were also more susceptible to oxidative stress (Pesah et al., 2004, Clark et al., 2006) and had swollen mitochondria in indirect flight muscles and in dopaminergic neurones (Clark et al., 2006, Park et al., 2006). In drosophila brains, a subset of dopaminergic neurones degenerated and the levels of dopamine were lower in mutant-Parkin models (Cha et al., 2005, Whitworth et al., 2005). In aged mice, PINK1 knockouts had lower levels of dopamine and reduced motor function. More surprisingly, there was no significant neuron degeneration but instead, there was progressive mitochondrial dysfunction (Gispert et al., 2009). Mitochondria isolated from the brain of PINK1 knockout mice also showed defects in calcium ion regulation and increased the vulnerability of neurones to oxidative stress (Gandhi et al., 2009, Heeman et al., 2011). Contrary to these studies, PINK1-knockout mice with MitoQC reporters for the detection of mitophagy did not show decreased levels of mitochondrial clearance in PD related tissues (McWilliams et al., 2018). Further investigations using more extreme factors like aging may provide better understanding of how mitophagy defects become more apparent with stress.

Interestingly, aged PGAM5-knockout mice also displayed Parkinson-like movement difficulties with overall less locomotor activity, development of Parkinsonian gait, bradykinesia and defective balance (Lu et al., 2014). This phenotype was not directly associated with mitophagy due to lack of evidence for reduced mitochondrial clearance or PINK1 instability *in vivo*. However, biochemical analyses using isolated cells from these mice strongly suggest a significant role of PGAM5 in mitophagy, particularly in PD (Lu et al., 2014).

Several neurodegenerative disease models aside from PD are also reported to have dysfunctional mitophagy. For example, Huntington's disease (HD) and Alzheimer's disease (AD) are also reported to have mitochondrial dysfunction and excessive ROS (Mao et al., 2012). In HD fly models, mitochondria in the

photoreceptor neurones were abnormally ring-shaped and mitophagy was impaired in the striatal neurones. When PINK1 was overexpressed, improvements in ATP levels, neuronal integrity and survival were observed. In addition, mitophagy was also partially restored. This suggests that in HD, increasing the activity of the PINK1/Parkin pathway may offer neuroprotection and partially restore mitochondrial integrity (Khalil et al., 2015). With regards to AD, using AD animal models, impaired mitochondrial function has been reported prior to the amyloid-beta accumulation in the brain (Yao et al., 2009, Du et al., 2017). PINK1 deficiency was shown to accelerate amyloid-β accumulation by and exaggerates abnormalities in LTP, learning and memory, and mitochondrial function in mAPP mice (Du et al., 2017). When PINK1 was restored in these mice, decreases were observed in amyloid-beta levels, amyloid-associated pathology, oxidative stress, as well as mitochondrial and synaptic dysfunction (Du et al., 2017). Overexpression of PINK1 via gene therapy was also shown to stimulate removal of damaged mitochondria via autophagy receptors, OPTN and NDP52, reducing cognitive decline and amyloid-beta dependent synapse loss in AD mice (Du et al., 2017).

BNIP3 and NIX, in addition to PINK1 and Parkin, have also been implicated in a range of other diseases. For example, in mammary tumour cells, BNIP3 knockdown led to accumulation of dysfunctional mitochondrial and elevated ROS levels (Chourasia et al., 2015). This promoted HIF-1α stabilisation and expression of its downstream target genes involved in angiogenesis and glycolysis; two key hallmarks of cancer (Chourasia et al., 2015). Moreover, deficiency in BNIP3 was shown to be a prognostic marker of metastasis in triple-negative breast cancer (Chourasia et al., 2015).

With mitophagy being such a crucial physiological process in the cell, it would be of interest to manipulate the pathway for clinical use in a range of diseases. Indeed, a variety of *in-vivo* and *in-vitro* models using molecular techniques such as over-expressions, mutations and knockdowns of mitophagy-related proteins have provided promise for therapeutic targeting. Unfortunately, these techniques

cannot be mirrored in humans and therefore alternative ways of regulating mitophagy in cells must be explored. In order to target these alternative pathways, initial understanding of how mitophagy fits into the greater paradigm of cellular stress responses needs to be investigated. For example, the evidence explored here suggests a potential association between redox and mitophagy signalling pathways. Indeed, it has been shown that high levels of ROS can trigger autophagy (Scherz-Shouval and Elazar, 2011) and that dysfunctional mitochondria producing excessive ROS are targeted for mitophagy. Therefore, targeting the Nrf2-Keap1 complex, a “druggable” target, or PGAM5, may be exploited to potentially induce mitophagy, providing a desired treatment for defective-mitophagy related diseases such as PD.

1.8 Aims of the thesis

Based on the evidence discussed here, a potential regulatory pathway of mitophagy is the Nrf2/Keap1 pathway. Previous work suggests that Nrf2 and Keap1 have important functions in mitochondrial activity and autophagy. More importantly, accumulating studies suggest that the Nrf2/Keap1 complex may play a significant role in mitophagy but the underlying mechanisms remain to be elucidated.

To further explore the potential of Nrf2/Keap1 in mitophagy, my aims were:

1. To investigate whether PINK1 deficiency affects the half-life, sub-cellular localization, inducibility and transcriptional activity of Nrf2.
2. To investigate the effect of Keap1 knockdown on mitophagy.
3. To investigate the effect of pharmacological Nrf2 activators on mitophagy.

CHAPTER 2: MATERIALS AND METHODS

Chapter 2: Materials and Methods

2.1 Materials

2.1.1 Chemicals

All chemicals were purchased of analytical grade from Sigma-Aldrich or Merck Millipore (now merged into Merck) and stored in DMSO stocks at -20^{o}C unless otherwise specified.

2.1.2 Cells

S-HeLa wild-type and CRISPR-Cas9 S-HeLa PINK1-knockout cells were a generous gift from Professor Miratul Muqit (University of Dundee, UK). The ARPE-19 MitoQC reporter cell line (expressing mCherry-GFP-FIS1; hydromycin resistant, 800ug/mL) and the SH-SY5Y MitoQC reporter cell line were a kind gift from Dr Ian Ganley (University of Dundee, UK).

2.1.3 Buffers

The buffers used for the work in this thesis are listed in Table 2.1. When necessary, DTT and complete protease inhibitor cocktail tablets were added prior to use.

Table 2.1. **Composition of buffer and stock solutions used in this project.**

Buffer and Solutions	Composition
Blocking buffer	5% (w/v) milk powder, 0.1% (v/v) Tween 20, 1X PBS
Formaldehyde Fixing Solution	3.7% formaldehyde (w/v) 200mM HEPES, pH 7
PBS-Tween (PBST)	0.1% (v/v) Tween 20, 1X PBS
Ponceau	5% (w/v) acetic acid, 0.1% (w/v) Ponceau S
Running Buffer (1X)	25mM Tris, 192mM glycine, 0.1% (w/v) SDS
Transfer Buffer (1X)	25mM Tris, 192mM glycine, 20% (v/v) methanol

SDS-lysis Buffer (2X)	4% SDS (w/v), 125mM Tris (pH6.8), 20% (w/v) glycerol (1% (v/v) bromophenol blue added to produce 'blue 2X SDS lysis buffer'
Subcellular Fractionation Buffer	20mM HEPES ph7.4, 10mM KCL, 2mM $MgCl_2$, 1mM EDTA, 1mM EGTA
Reagent B for BCA assay	4% $CuSO_4$

2.1.4 Antibodies

The antibodies (primary and secondary) used for Western blot are listed in Table 2.2.

Table 2.2. **Antibodies used in this project.**

Target	Host Species	Supplier and Catalogue	Antibody Details	Western Blot Concentration
B-Actin	Mouse	Sigma, A5441	Monoclonal	1:15000 (milk)
AKR1B10*	Rabbit	Home-made		1:1000 (milk)
Anti-Mouse	Goat	LI-COR, 925-68070	IRDye® 680RD Secondary IgG	1:15000 (milk)
Anti-Rabbit	Goat	LI-COR, 925-32211	IRDye® 800CW Secondary IgG	1:15000 (milk)
Anti-Rat	Goat	LI-COR, 925-32219	IRDye® 800CW Secondary IgG	1:15000 (milk)
KEAP1	Rat	Merck, MABS514	Monoclonal Clone 144	1:16000 (milk)
HSP60	Rabbit	Cell Signalling Technology, 4870	Polyclonal D307	1:1000 (milk)
Lamin B2	Rabbit	Thermo Fisher, PA5-22066	Polyclonal	1:1000 (milk)
LC3	Rabbit	Cell Signalling Technology, 3868	Monoclonal (D11) XP®	1:1000 (milk)
NQO1*	Rabbit	Home-made		1:1000 (milk)

Nrf2	Rabbit	Cell Signalling Technology, 2721	Monoclonal (D1Z9C) XP®	1:1000 (milk)
p62	Mouse	Abcam, ab56416	Monoclonal	1:1000 (milk)
PGAM5	Rabbit	Merck, ABC517	Polyclonal	1:1000 (milk)
PINK1	Rabbit	Cell Signalling Technology, 6946	Monoclonal (D8G3)	1:1000 (milk)
TIM23	Rabbit	Abcam, ab230253	Polyclonal	1:1000 (milk)
VDAC1	Rabbit	Abcam, ab154856	Monoclonal	1:1000 (milk)

***** Both NQO1 and AKR1B10 antibodies were a kind gift from John Hayes lab.

2.1.5 TaqMan™ Probes

For qPCR, all TaqMan™ probes were purchased from Thermo Fisher Scientific and are listed in Table 2.3.

Table 2.3. **TaqMan™ probes used in this project.**

Target	Species	Catalogue	Probe Details
HMOX1	Human	Hs01110250_m1	Exon spanning, FAM-MGB dye
GCLC	Human	Hs00155249_m1	Exon spanning, FAM-MGB dye
GAPDH	Human	Hs02786624_g1	Single exon probe, FAM-MGB dye
KEAP1	Human	Hs00202227_m1	Exon spanning, FAM-MGB dye
NFE2L2	Human	Hs00975961_g1	Exon spanning, FAM-MGB dye
NQO1	Human	Hs01045993_g1	Exon spanning, FAM-MGB dye
SQSTM1/P62	Human	Hs01061917_g1	Exon spanning, FAM-MGB dye
PGAM5	Human	Hs00540846_g1	Exon spanning, FAM-MGB dye
PINK1	Human	Hs00260868_m1	Exon spanning, FAM-MGB dye

2.1.6 SiRNA Reagents

All small interfering RNAs (siRNAs) purchased are from the ON-TARGET *plus* SMART pool range supplied by Dharmacon and are listed on Table 2.4.

Table 2.4. **Small interfering (siRNA) used in this project.**

Target	Species	Catalogue
PINK1	Human	L-004030-00-0005
NRF2	Human	L-003755-00-0005
KEAP1	Human	L-012453-00-0005
Scrambled Negative	Human	D-001810-10-50

2.2 Methods

2.2.1 Cell Culture

2.2.1.1 Culturing Conditions

All cells were maintained and grown in sterile conditions at 37^{o}C with 5% CO_2. To passage, cells were washed twice with PBS and detached using trypsin-EDTA (0.25%) (Gibco) at 37^{o}C. CRISPR generated PINK1-knockout and wild-type HeLa cells were cultured in DMEM media (Gibco) supplemented with 10% (v/v) heat-inactivated FBS (Invitrogen). SH-SY5Y MitoQC cells were cultured with a 1:1 mix of DMEM and Ham's 12 nutrient mix (Gibco) containing 15% (v/v) heat-inactivated FBS (Invitrogen). The ARPE-19 MitoQC cells were cultured in a 1:1 mix of DMEM and Ham's F12 media (Gibco) supplemented with 10% (v/v) heat and charcoal-inactivated FBS (Invitrogen).

2.2.1.2 Freezing and Thawing of Cells

Cells cultured in 175cm^2 flasks at low passage and at 80% confluency were frozen down for long-term storage stocks. Once cells were detached using trypsin-EDTA (0.25%), 10 ml of complete medium was added to inactivate the trypsin. The cells were collected by centrifugation at 1000 rpm for 5 minutes. The trypsin/EDTA

containing medium was removed from the above the cell pellet, and the cells were resuspended in fresh mediaum. Next, the pelleted cells were resuspended in 3 ml of FBS containing 10% (w/v) DMSO. Approximately 1 ml of cell suspension was added per 1.5 ml cryogenic vial (Corning incorporated) and placed in a Mr.Frosty^{TM} Freezing Container (Thermo Scientific) for a minimum of 48 hours at -80^{o}C. The vials were then transferred into liquid nitrogen for long-term storage.

To thaw the cells, the cryogenic vials were placed in a 37^{o}C water bath and then transferred into a 75cm^{2} flask (Thermo Scientific) with 12 ml of pre-warmed media.

2.2.2 RNA Interference (RNAi)

Reverse transfections were carried out for all knockdown experiments. For 6-well dishes, 2.5 µL of 20 µM siRNA stock was added to 500 µL of Opti-MEM (Gibco). This solution was then added to the designated well and 5 µL of RNAiMax (Invitrogen) was added to the siRNA/Opti-MEM solution in the well. After mixing the RNAiMax thoroughly in the solution, the dish was left to incubate for 10-15 minutes at room temperature. Cells were then added to each well at a density of 2.5x10^{5} for ARPE-19 MitoQC and 3.5x10^{5} for SHSY5Y mitoQC cells in a 2 mL volume of culture media, producing a total volume of 2.5 mL and a final concentration of 20 nM siRNA.

For knockdowns in 15-cm dishes, 3x10^{6} SHSY5Y cells and 2x10^{6} ARPE-19 cells were seeded. A concentration of 20 nM siRNA was achieved by mixing 20 µL of 20 µM siRNA and 4 mL of Opti-MEM per dish. Next, 40 µL of RNAiMax was mixed into the 4 mL in the dish and this was left for 10-15 minutes at room temperature. The cell suspension was then added to the dish in a volume of 16 mL to make a total media volume of 20 mL.

The same protocols were simultaneously carried out with the scrambled siRNA and the Opti-MEM controls. All knockdown reactions were incubated for 48 hours in sterile conditions at 37^{o}C with 5% CO_2 before cells were harvested.

2.2.3 Drug Treatments

Carbonyl cyanide 4-(trifluoromethoxy)phenylhydrazone (FCCP) was dissolved in DMSO to produce 100 mM stocks which were sequentially diluted in PBS to make 100 µM working stocks. All DMSO stocks were stored at -20^{o}C and were ultimately diluted in medium to make a final concentration of 10 µM (unless otherwise stated). To induce FCCP-dependent stress, cells were treated with a final concentration of 10 µM (for SH-SY5Y and S-HeLa) or 20 µM (for ARPE-19 MitoQC) of FCCP in growth media. All treatments lasted for 3 hours unless otherwise stated.

Analysis of mitophagic flux by immunoblotting required bafilomycin (dissolved in DMSO, 200 µM or 50 µM stocks) to be added to the cell media for a final concentration of 50 nM (for ARPE-19 MitoQC) or 20 nM (for SH-SY5Y). Bafilomycin A1 was added 6 or 8 hours before cells were harvested.

Deferiprone (DFP) was used as a positive control for mitophagy activation. DFP powder was stored at room temperature and was made fresh for each experiment by adding sterile water to make a 0.125M solution, which was then dissolved at 95^{o}C for five minutes. Finally, a 1mM solution was made in growth medium and added to the cells for 24 hours when necessary.

TBE-31 was dissolved in acetonitrile to obtain a stock concentration of 5mM and was stored at -20^{o}C. A 500-µM intermediate stock was made in acetonitrile before it was further diluted in cell culture medium to 50 nM or 100 nM, and added to cells for 24 hours.

PMI was stored at -20^{o}C as a 50 mM stock dissolved in DMSO. A 50 µM stock was produced in DMSO before it was further diluted in cell culture medium to make 10 µM or 20 µM and added to cells for 24 hours.

2.2.4 Protein Extraction and Quantification

Cells were lysed in 2X SDS-lysis buffer (50% 2X SDS-lysis Buffer, 45% water supplemented with a complete protease inhibitor cocktail, 5%) after being washed twice with PBS. Cell lysates were then boiled for 2 minutes and sonicated using the following settings: 25% amplitude, total of 20 seconds with 4 seconds on and 1 second off. Protein concentrations were determined using the BCA assay (Pierce ™ BCA Protein Assay Reagent A and lab-made reagent B, see Table 2.1) according to the manufacturer's protocol. All samples were measured in triplicate and concentrations were determined by absorbance of 552nm using a plate reader spectrophotometer SpectraMax M2 (Molecular Devices) with the SoftMax Pro 5.4 software program. Bovine serum albumin (BSA) (Thermo Scientific) was used to produce a standard curve between 1-32 µg.

2.2.5 Cycloheximide Experiment

Cells were seeded between 0.3-1x10^6 cells per well into either 6-well plates or 6-cm dishes. At each time point, 10 uL of 2mg/ml cycloheximide was added to each designated well. At time point 0, all cells were washed with PBS twice and lysed with 1X SDS lysis buffer (50% 2X SDS-lysis Buffer, 45% water supplemented with a complete protease inhibitor cocktail, 5%). Cell lysates were then processed for protein extraction and quantification as described above. Proteins were resolved by SDS/PAGE and transferred to nitrocellulose membranes using wet transfer. Membranes were immunoblotted for Nrf2 and the loading control □-actin. The intensity of each band was then quantified using the Li-Cor Image Studio. The Nrf2 band density for each time point was normalised to the corresponding □-actin band for the same sample. The density of the band was then plotted against time and an exponential equation was fitted to the data. The Nrf2 half-life was then calculated using the following equation:

$$t_{\frac{1}{2}} = \frac{t}{log_{\frac{1}{2}}\left(\frac{N_{(t)}}{N_0}\right)}$$

$N_{(t}$ = final quantity; N_0 = initial quantity; t = time

2.2.6 RNA Extraction, cDNA and Quantitative Real-time PCR

Cells were seeded at a density of 2.5-4x10^5 cells per well in 6-well dishes. Depending on the experiment, cells were lysed 24 or 48 hours after seeding, and RNA extraction was carried using the RNeasy Kit (Qiagen Ltd.). RNA concentrations were measured using the Nanodrop Spectrophotometer ND-1000 (NanoDrop Technologies).

Using the Omniscript Reverse Transcription Kit (Qiagen Ltd.), either 500 ng or 1000 ng of cDNA was produced from the extracted RNA. Each cDNA sample was either diluted 1:10 (for 500 ng) or 1:20 (for 1000ng) with sterile water before quantitative real-time PCR was performed.

All quantitative real-time PCR experiments were performed using the QuantStudio® 5 Real Time PCR System with a 96-well 0.2 mL block (Thermo Fisher Scientific). For each studied gene a master-mix was produced with the following constituents per sample: 0.75 µl of the correct TaqMan probe (listed in Table 2.3), 4.75 µl of sterile water and 4.50 µl of the TaqMan Universal Master Mix II (Applied Biosystems by Life Technologies). Of this master-mix, 10 µl were pipetted into a MicroAmp® optical 96-well reaction plate (Applied Biosystems by Life Technologies) in addition to 5 µl of diluted cDNA, providing a final reaction volume of 15 µl. All data were normalised to GAPDH as an internal control and presented as a fold-change of the specified control sample.

2.2.7 Subcellular Fractionation

For subcellular fractions, cells were seeded in 15-cm dishes and pooled together when necessary. The cells were washed twice with ice-cold PBS before scraping in 1 ml of subcellular fractionation buffer into Eppendorf tubes. Cells were lysed using a 25G needle by syringing approximately 20 times before being left on ice

for 20 minutes. Lysis was confirmed using a light microscope. Next, cell lysates were subjected to centrifugation at 720 x *g* for five minutes to produce a pellet containing nuclei, cell debris and un-lysed cells. The supernatant was then spun at 10,000 x *g* for five minutes to obtain a mitochondrial pellet. Lastly, the remaining supernatant was centrifuged at 10,000 x *g* for 15 minutes to acquire a cytoplasmic fraction. Each fraction, with the exception of the cytoplasmic fraction, was lysed with SDS lysis buffer, boiled and sonicated at 15% amplitude for 15 seconds. All centrifugation steps were carried out at 4^{o}C and multiple washes and centrifugations were carried out using the subcellular fractionation buffer before lysing each pellet.

2.2.8 Protein Resolution by SDS/PAGE and Wet Transfer

Denatured proteins were diluted in blue SDS-lysis buffer (50% 2X SDS-Lysis Buffer with 0.5% bromophenol blue, 10% DTT and 40% water) and were loaded onto either 10% or 13% 10-well polyacrylamide (30% Bio-Rad) gels with a pre-stained standard protein marker (Pageruler, Invitrogen) flanking the samples Equal amounts of total protein (20-40 µg), at a concentration of 1µg/µl, were used for separation by sodium dodecyl sulphate-polyacrylamide gel electrophoresis (SDS-PAGE). Proteins were resolved using 75V for 15 minutes and 120V for 1 hour in running buffer (1X).

Resolved proteins in the gel were then transferred onto a 0.45 µm nitrocellulose membrane (Amersham Biosciences) at 75V for 1 hour 45 minutes surrounded by transfer buffer (1X). Once transfer was complete, membranes were blocked in 5% (w/v) milk (Marvel) prepared in PBS containing 0.1% Tween 20 (PBST) for an hour under constant agitation at 50-80 rpm on a shaker (SSM1, Stuart).

2.2.9 Immunoblotting

All primary antibodies (listed in Table 2.1.4) were prepared in 5% (w/v) milk (Marvel) dissolved in PBST and stored at -20ºC in 50 ml Falcon tubes (Corning). After blocking, membranes (except membranes used for detection of Nrf2) were added to 50 mL Falcon tubes containing 10 mL solutions of milk with the primary antibody of choice (see Table 2.2 for dilutions). The tubes were then placed on a rotator (SRT6, Stuart) at 4ºC overnight or at room temperature for 3-4 hours. Due to low abundance and weak antibody signal, Nrf2 membranes were placed in trimmed plastic pockets with excess primary antibody and were left at 4ºC overnight under constant agitation (Stuart, SSL4).

After incubation with the primary antibodies, membranes were washed thrice with PBST for a minimum time period of 10 minutes per wash. Appropriate LI-COR secondary antibodies were prepared in 5% (w/v) milk (Marvel) dissolved in PBST and membranes were left to incubate under agitation for 1 hour at room temperature. Excess secondary antibodies were washed three times with PBST for a minimum time period of 10 minutes per wash. Proteins were then revealed using the Odyssey® CLx Imaging System (Li-Cor).

2.2.10 Mitophagy Assay

To determine the effect of TBE-31 on mitophagy, ARPE-19 MitoQC cells were seeded onto glass coverslips (22x22mm, 1.5mm thickness; VWR) in 6-well dishes at a density of 2.0 x 10^5/2.5 x 10^5 cells per well for 48 hours. Each well was then washed twice with PBS before fixation with 3.7% formaldehyde solution for 10 minutes at room temperature. Next, cells were washed twice with phenol red free-DMEM/10mM HEPES (pH 7). DAPI (1:1000 in phenol red free-DMEM/10mM HEPES, pH 7), used to stain cell nuclei, was incubated for 15 minutes at room temperature in the absence of light. Cells were washed again in phenol red free-DMEM/10mM HEPES (pH 7) and incubated with the solution for 10 minutes before a final PBS wash. Coverslips were gently mounted onto super premium

microscope slides (VWR) using 20 µl of ProLong Gold Antifade Mountant (Invitrogen). Slides were left to cure overnight at room temperature in the absence of light.

Images of each sample were acquired using with the Deltavision Elite (GE Healthcare) microscope. Acquisition settings including intensity, objective and exposure were fixed for each channel across all samples. Images were visualised using ImageJ. For the microscopy experiment with ARPE-19 cells (Figure 5.5), 30–40 cells per treatment were selected at random for quantitative analysis in Image J. Cells were drawn around and within the selected area, fluorescence intensity of the GFP channel and mCherry channel were measured using a macro. This ultimately provided the number of red puncta that as present within the cell.

In parallel, cells were also seeded for western blot analysis and subjected to bafilomycin A1 (50nM) treatment 8 hours before harvest. The levels of mitochondrial markers TIM23 (inner mitochondrial membrane) and HSP60 (intramitochondrial chaperone), and the autophagy marker LC3 I/II were determined by immunoblotting as an independent measure of mitophagy and mitophagic flux. For experiments measuring mitophagy in cells after Keap1 knockdown, a similar western blot analysis was carried out.

2.2.12 Statistical Analysis

Data are presented as the mean ± standard deviation (SD) unless otherwise stated. Differences between groups were determined by a Student’s t-test or an analysis of variance (ANOVA). Post-hoc tests were also carried out where appropriate. All data analyses were performed using Excel (Microsoft Corp.) or GraphPad Prism 7.

CHAPTER 3: RESULTS

Chapter 3: Results

3.1 Investigating the effect of PINK1 deficiency on the half-life, sub-cellular localization, inducibility and transcriptional activity of Nrf2

To understand whether Nrf2 half-life, sub-cellular localisation, inducibility and transcriptional activity are associated with PINK1 status, CRISPR knockout (KO) PINK1 S-HeLa cells and the parental control cell line (WT) were used.

3.1.1 Basal protein and mRNA levels of Nrf2 and its downstream targets do not alter in PINK1-KO S-HeLa cells

Both protein and mRNA levels of Nrf2 and its downstream target genes were measured in basal conditions. Protein levels of Nrf2's negative modulator, Keap1, were also measured to investigate whether any changes in Nrf2 are due to effects on Keap1.

Nrf2 protein levels and its downstream targets NQO1 and p62 were all shown to have similar levels in both PINK1-WT and KO cells. AKR1B10 was the only downstream target of Nrf2 that showed a slight decrease at the protein level in PINK1-KO cells. Keap1 was also slightly lower in the PINK1-KO however this did not seem to affect Nrf2 and its downstream targets (Figure 3.1, A).

At the transcript level, PINK1-KO showed no effect on transcript levels of *NFE2L2*, *NQO1*, *SQSTM1* (gene encoding p62), *GCLC* or *HMOX1* under basal conditions.

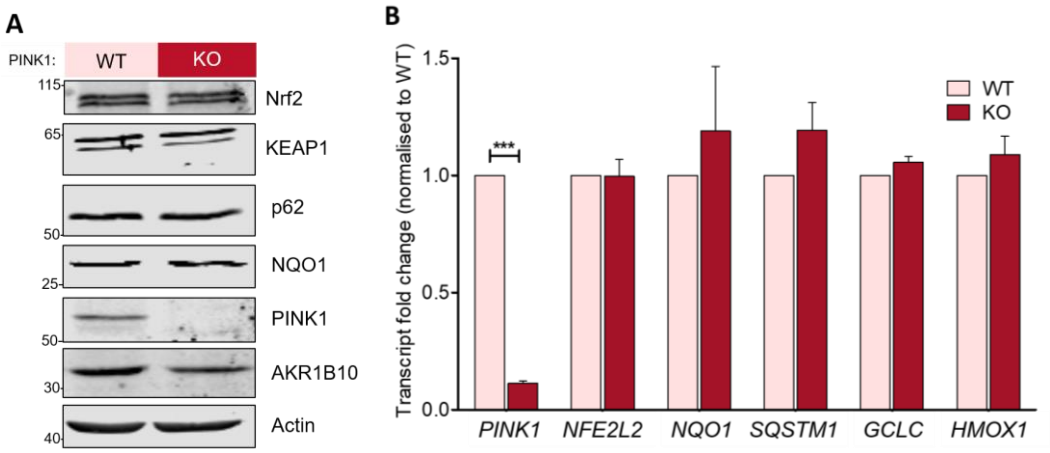

Figure 3.1. **Nrf2 and downstream targets protein and mRNA levels under basal conditions in PINK1 wild-type (WT) and knockout (KO) S-HeLa cells.** (A) Each cell line was seeded and lysed on the following day for protein analysis. Nrf2, KEAP1, p62, NQO1, PINK1, AKR1B10 and Actin were detected in cell lysates by Western blot analyses. Equal amounts of protein were loaded, and Actin was used as the loading control. Experiments were conducted three times, independently. (B) Each cell line was seeded and lysed on the following day for quantitative real-time PCR. *PINK1, NFE2L2, NQO1, SQSTM1, GCLC, HMOX1* and GAPDH mRNA transcripts were all detected using individual TaqMan™ probes. Data were normalised to *GAPDH*, the housekeeping gene, using the ΔΔCt method and the fold change was then calculated relative to WT samples using the $2^{-\Delta\Delta Ct}$ method. Data are from three independent experiments. *** $p<0.001$ (Two-way ANOVA with Bonferroni post-hoc test).

3.1.2 Nrf2 and downstream targets are induced with FCCP-induced stress in both PINK1-WT and KO S-HeLa cells

PINK1, similar to Nrf2, is continuously degraded under homeostatic conditions in the cell. It was therefore hypothesised that in order to investigate PINK1's effects on Nrf2 and its downstream targets, PINK1 would need to be stabilised on the mitochondria. In these experiments, PINK1 was stabilised using FCCP, a potent uncoupling agent of the mitochondrial electron transport chain. Both PINK1-WT and KO cells were treated with 10 µM of FCCP (or the vehicle, 0.001% DMSO) for 3 hours and were either lysed then (0 hours after treatment, 0h) or 24 hours later (treatment media was changed at time point 0 hours after FCCP treatment with fresh growth media) for protein or mRNA analysis (Figure 3.2.).

After 3 hours of 10 µM FCCP treatment, PINK1 protein was clearly stabilised in PINK1-WT cells with no significant effect on PINK1 transcript levels. Within 24 hours, PINK1 protein levels returned to their basal levels, and were even lower than in vehicle-treated cells, whilst transcript levels remained unaffected (Figure 3.3, Figure 3.4). Nrf2 protein levels increased to a similar extent in PINK1-WT and KO cells after the 3-hour treatment, suggesting the stabilisation of Nrf2 was PINK1 independent (Figure 3.3). After 24 hours, Nrf2 protein levels decreased. In agreement with the western blots, Nrf2 transcript levels increased approximately 2-fold in both PINK1-WT and KO cells after the 3-hour treatment (Figure 3.4 A) but returned to basal levels 24 hours later (Figure 3.4 B). On the protein level p62 was higher in FCCP treated PINK1-WT and KO cells at the 24-hour time point in comparison to the 0-hour time point (Figure 3.3). However, transcript levels remained similar at the 0 hour and 24-hour time point (Figure 3.4). NQO1 levels were slightly higher in the PINK1-KO cells with both the DMSO and the FCCP treatment in comparison to the PINK1-WT cells (Figure 3.3). However, after 24 hours, a slight increase in NQO1 protein levels in both cell lines occurred and was clearly observed with an over 2-fold increase in transcript levels (Figure 3.4 B). Alike NQO1 and p62, small increases in AKR1B10 occurred 24 hours after FCCP treatment. AKR1B10 transcript levels were detectable outside the linear range and therefore were not measured in this experiment. Interestingly, Keap1 protein levels decrease 24 hours after the FCCP treatment in both PINK1-WT and KO. Collectively, these results suggest that independently of PINK1, FCCP stabilises Nrf2. Initially, this stabilisation of Nrf2 is independent of the levels of KEAP1, which remain unchanged 3 hours post-exposure to FCCP, and may be due to increased transcription of *NFE2L2*. However, the stabilization of Nrf2 at the 24-hour time point could potentially be due to increased Keap1 protein degradation, in turn allowing Nrf2-dependent gene transcription to occur.

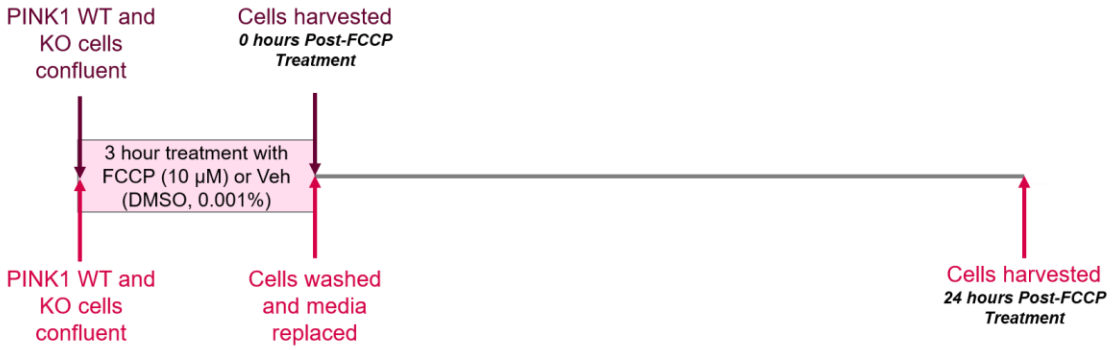

Figure 3.2. **Experimental set-up to measure protein and transcript levels of Nrf2 and Nrf2 targets at 0 hours and 24 hours after FCCP (10 µM) or DMSO (0.001%, Veh) treatment.** PINK1 WT and PINK1 KO S-HeLa cells were seeded 6-well dishes. Once 75% confluent cells were either treated with FCCP or the vehicle DMSO for 3 hours. Half of these cells were harvested after 3 hours for protein and transcript analyses. The remaining cells were washed with fresh media and were incubated for 24 hours in fresh media. After 24 hours, these cells were also harvested for protein and transcript analyses.

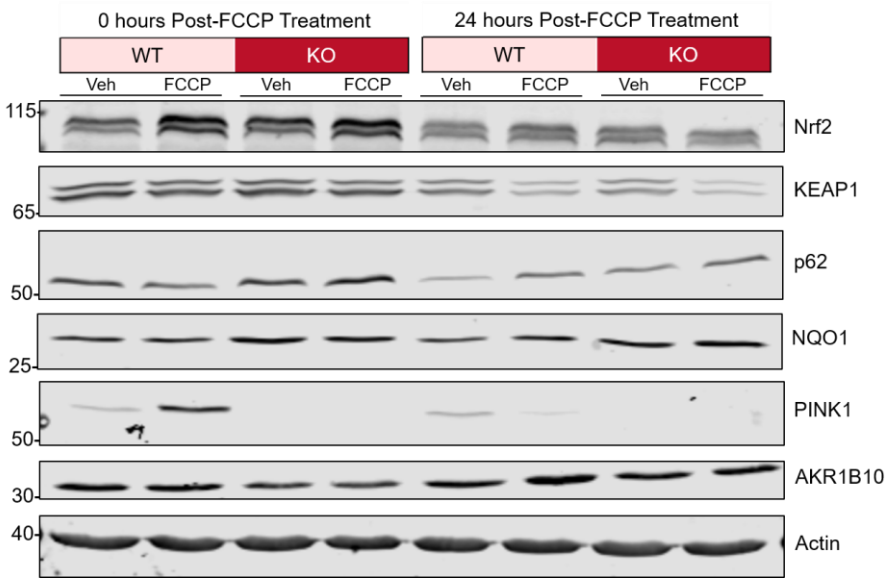

Figure 3.3. **Protein levels of Nrf2 and Nrf2 targets at 0 and 24 hours after FCCP treatment (10 µM, 3 hours).** Cells were seeded and the following day treated with 10 µM of FCCP or 0.001% DMSO (vehicle, Veh) for 3 hours. Cells were either harvested after the treatment or growth media were changed. Cells with media changed were harvested 24 hours later. Cell lysates were subject to protein analysis via Western blot where equal amounts of protein were loaded. Membranes were blotted for Nrf2, Keap1, p62, NQO1, PINK1, AKR1B10 and the loading control, Actin. Data shown are representative of three independent experiments.

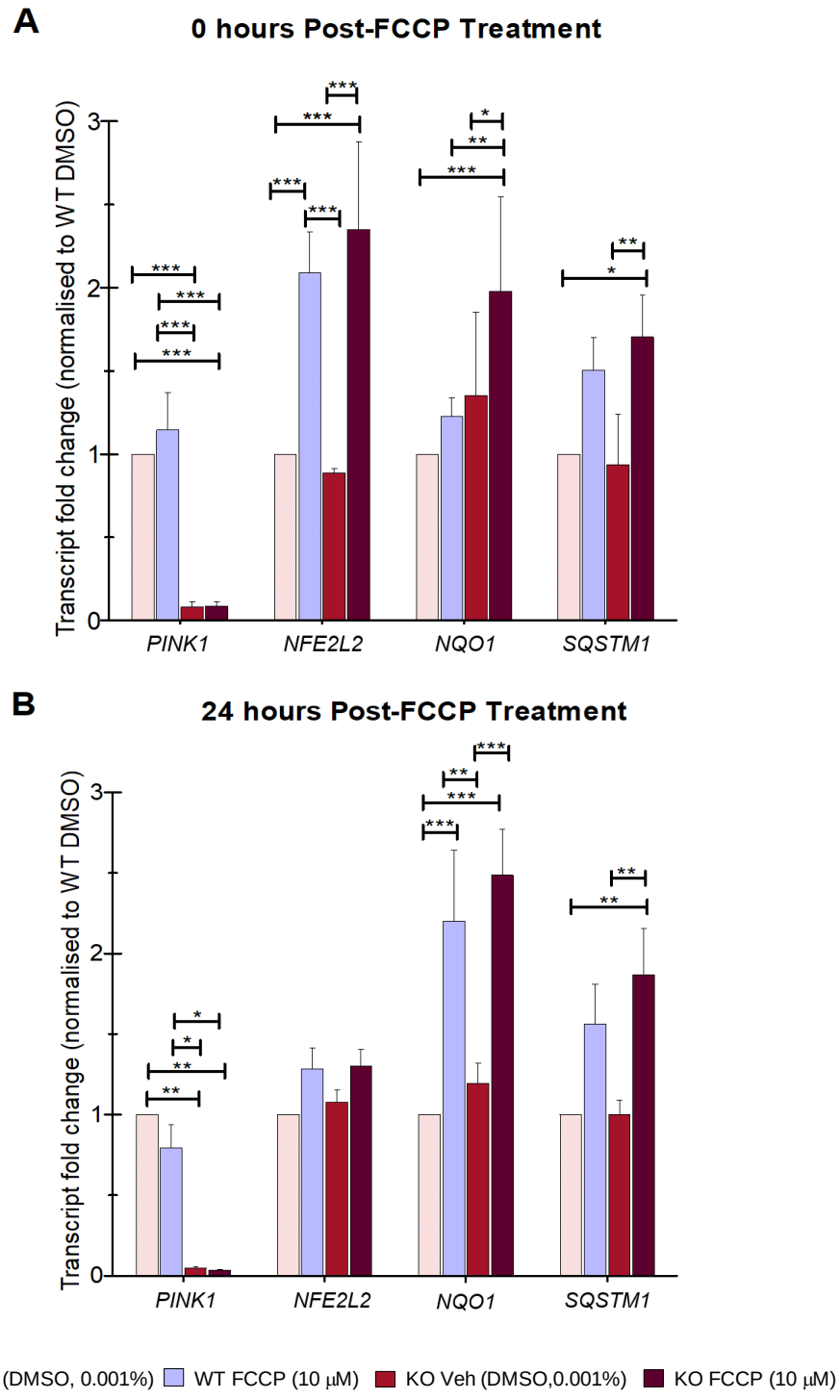

Figure 3.4. **Transcript levels of Nrf2 and Nrf2 targets at 0 and 24 hours after FCCP treatment (10 μM, 3 hours).** Cells were seeded and on the following day treated with 10 μM FCCP or 0.001% DMSO (vehicle, Veh) for 3 hours. Cells were harvested after the treatment (A) or had their media changed and were harvested 24 hours later (B) for quantitative real-time PCR. *PINK, NFE2L2, NQO1, GAPDH* and *SQSTM1* mRNA transcripts were all detected using individual TaqMan™

probes. Data were normalised to *GAPDH*, the housekeeping gene, using the ΔΔCt method and the fold change was then calculated relative to WT Veh samples using the $2^{-\Delta\Delta Ct}$ method. Data are from three independent experiments. * p<0.05, ** p<0.01, *** p<0.001 (Two-way ANOVA with Bonferroni post-hoc test).

3.1.3 Nrf2 turnover does not change in PINK1-WT and KO S-HeLa cells under basal conditions

To determine whether Nrf2 turnover changes in the absence of PINK1, cycloheximide was added to wells containing either S-HeLa KO and WT cells as shown in Figure 3.5. Under basal conditions, the half-life for Nrf2 was 13.6 and 13.03 minutes for PINK-WT and KO, respectively (Figure 3.6). Such values suggest that Nrf2 turnover is not altered in the absence of PINK1.

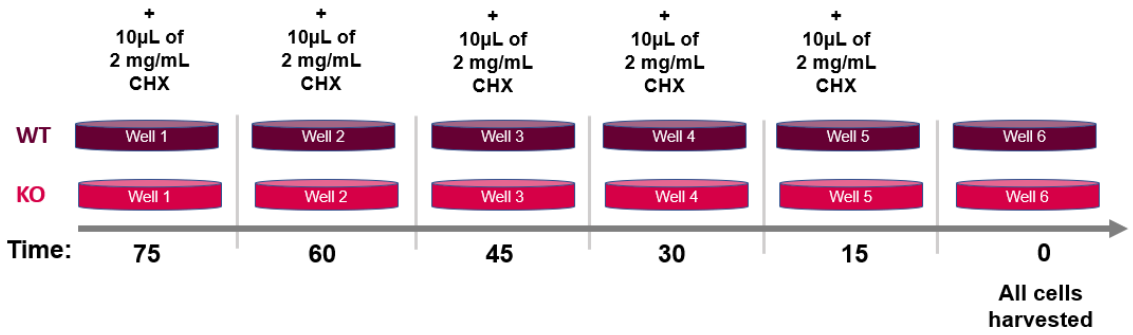

Figure 3.5. **Cycloheximide experiment to measure Nrf2 turnover in S-HeLa PINK1 WT and KO cells**. Each cell line was seeded onto six 6-cm dishes. Each dish was designated a specific time point of either 75, 60, 45, 30, 15 and 0 minutes in which the cells were subjected to 10µL of 2 mg/mL cycloheximide to inhibit protein synthesis. At 0 minutes, all cells were harvested for protein analysis.

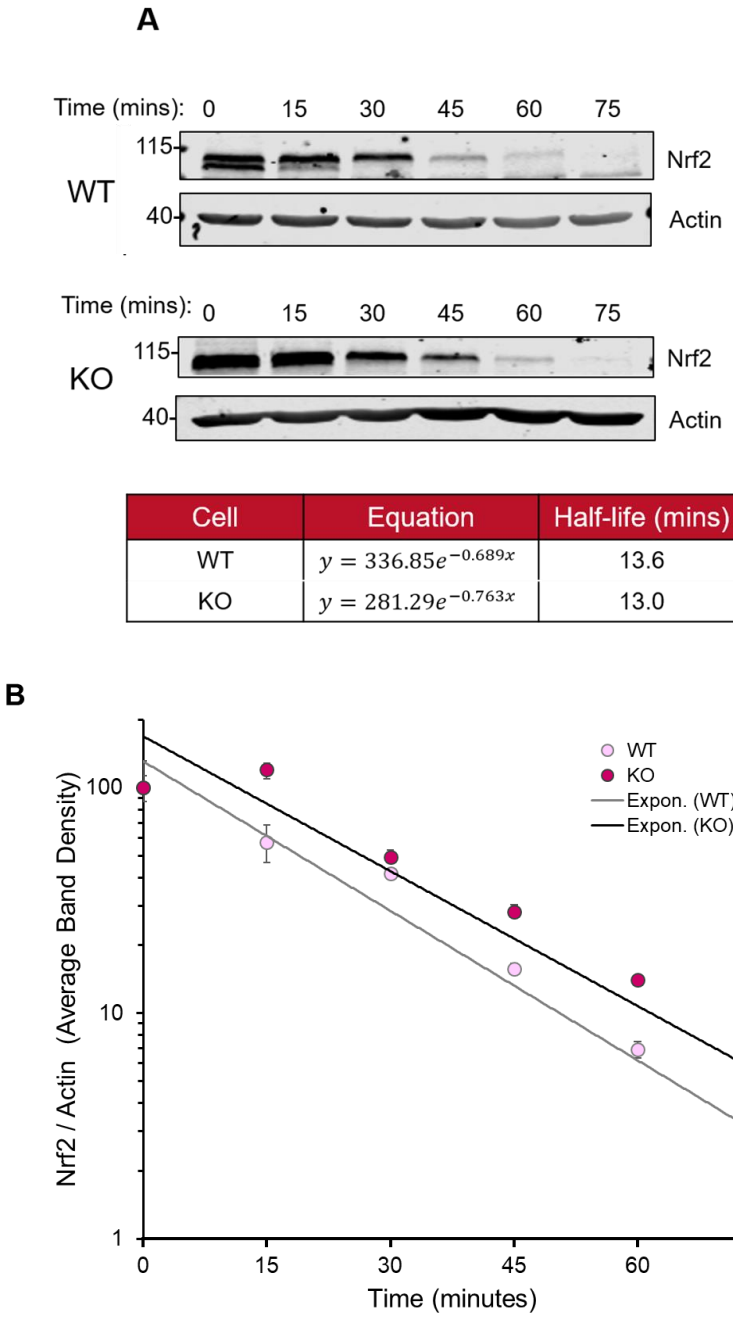

Cell	Equation	Half-life (mins)
WT	$y = 336.85e^{-0.689x}$	13.6
KO	$y = 281.29e^{-0.763x}$	13.0

Figure 3.6. **Nrf2 protein turnover in PINK1-WT and KO S-HeLa cells under basal conditions.** Each cell line was seeded onto six 6-cm dishes. Each dish was designated a specific time point of either 75, 60, 45, 30, 15 and 0 minutes in which the cells were subjected to 10µL of 2 mg/mL cycloheximide. At 0 minutes, all cells were lysed and equally loaded for Western blot analysis. Membranes were blotted for Nrf2 and the loading control ACTIN. Band intensities were quantified using Image Studio Ver 5.2 (Li-Cor). Nrf2 band intensities were normalised to Actin band intensities and are expressed as a percentage of the band at 0 minutes. Exponential equations

were fitted to the data and half-lives were calculated. Data are from three independent experiments.

3.1.4 Nrf2 turnover does not change in PINK1-WT and KO S-HeLa cells under FCCP-induced stress conditions

Previously, FCCP was used to depolarise the mitochondrial membrane and stabilise PINK1 (Deas et al., 2011). We wanted to determine whether its presence on the mitochondria is important for Nrf2 regulation and function. In a preliminary experiment, we also looked at whether PINK1 stabilisation would affect Nrf2 turnover. Cells were treated with 10μM FCCP for 3 hours before carrying out the experiment described in Figure 3.5. The half-life of Nrf2 was approximately 17 minutes under all experimental conditions and cell types except for KO S-HeLa cells treated with FCCP in which Nrf2 had a half-life of approximately 15 minutes (Figure 3.7).

A

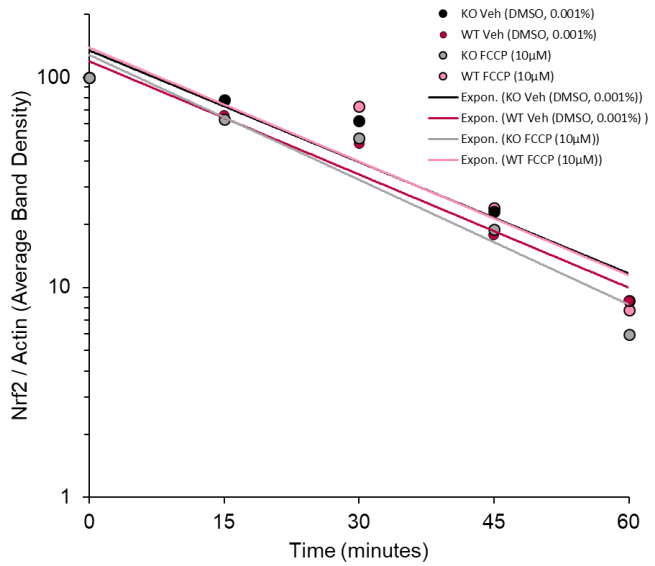

Cell/ Treatment	Equation	Half-life (mins)
KO Veh (DMSO, 0.001%)	$y = 247.79e^{-0.611x}$	16.9
WT Veh (DMSO, 0.001%)	$y = 222.23e^{-0.621x}$	16.9
KO FCCP (10µM)	$y = 253.88e^{-0.684x}$	15.1
WT FCCP (10µM)	$y = 259.01e^{-0.624x}$	17.3

B

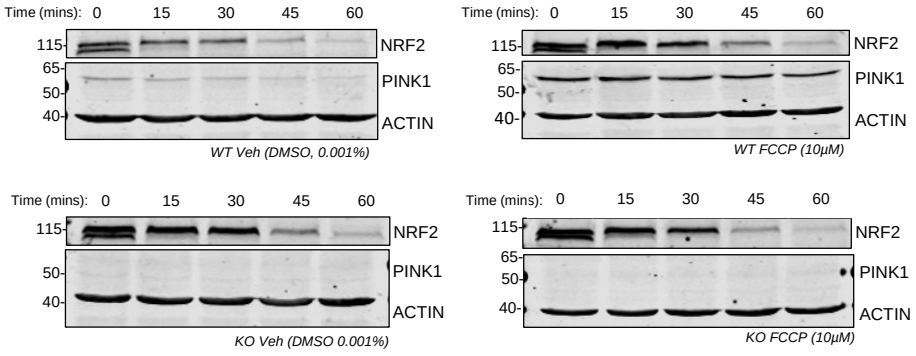

Figure 3.7 **Nrf2 protein turnover in PINK1-WT and KO S-HeLa cells under FCCP induced conditions.** Cells were seeded onto 6-cm dishes and were treated with either 10µM of FCCP or 0.001% DMSO (Vehicle) for 3 hours the following day. Each dish was designated a specific time point of either 60, 45, 30, 15 and 0 minutes in which the cells were subjected to 10µL of 2 mg/mL cycloheximide At 0 minutes, all cells were lysed and equally loaded for Western blot analysis. Membranes were blotted for Nrf2 and the loading control Actin. Band intensities were quantified using Image Studio Version 5.2 (Li-Cor). Nrf2 band intensities were normalised to Actin band

intensities and are expressed as a percentage of time point 0 minute (0). Exponential equations were fitted to the data and half-lives were calculated. Data is from one experiment. (n=1).

3.1.5 Nrf2 localisation does not differ in basal or FCCP-induced stress conditions between PINK1 WT and KO cells

To understand if PINK1 could affect the subcellular localisation of Nrf2, subcellular fractionation was carried out in both PINK1-KO and -WT cells in the presence and absence of FCCP (10 μM). Nrf2 and Keap1 were found in all three fractions and no difference was observed in Nrf2 localisation between PINK1-WT and -KO under basal or FCCP-induced stress conditions. This experiment further revealed that Nrf2 stabilisation upon FCCP treatment occurred primarily in the mitochondria, and possibly the nucleus (Figure 3.8). The latter is difficult to assess as the nuclear fraction contained a significant amount of mitochondria, based on the readily-detectable levels of VDAC1 in the nuclear fraction

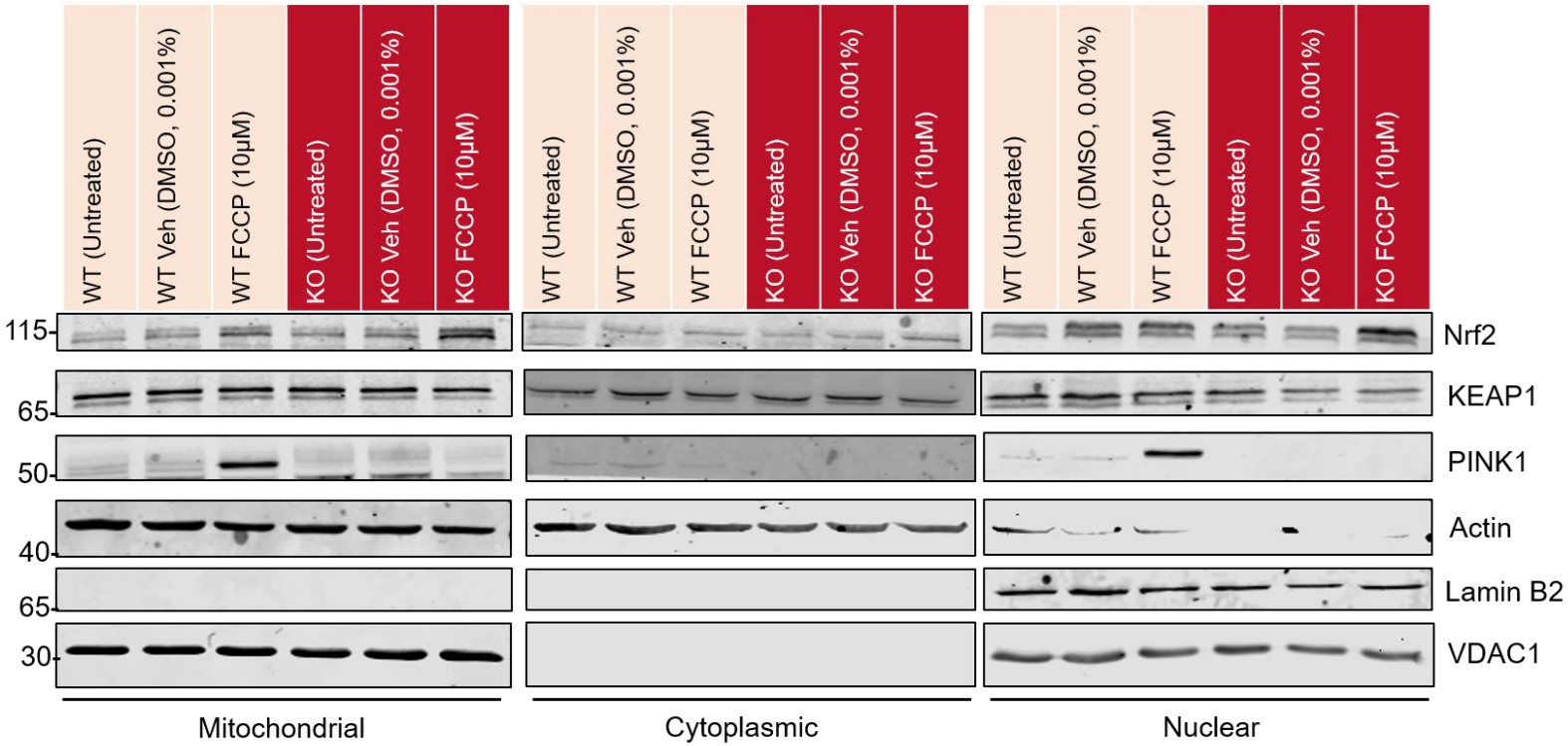

Figure 3.8. **Nrf2 localisation in subcellular fractions in S-HeLa PINK1 WT and KO cells.** Cells were subjected to treatment with 10µM FCCP or 0.001% DMSO (Vehicle) for 3 hours. They were then harvested for subcellular fractionation using ice-cold PBS and subcellular fractionation buffer. Several rounds of centrifugation were carried out to obtain a nuclear, mitochondrial and cytoplasmic pellet. Each fraction (except the cytoplasmic) was lysed with SDS buffer and quantified for Western blot analysis. Membranes were blotted for PINK1, KEAP1 and Nrf2. VDAC1, Actin and Lamin B2 were used as loading controls for the mitochondrial, cytoplasmic and nuclear fractions respectively. Data are representative of three experiments (n=3).

3.1.6 Nrf2 knockdown in WT PINK1 S-HeLa does not alter PINK1 protein and transcript levels

The data so far suggest that the PINK1 status does not alter Nrf2 function, subcellular localisation or expression in S-HeLa cells. It was next investigated whether Nrf2 status could alternatively influence PINK1 at the protein and mRNA level. siRNA-mediated Nrf2 knockdown was successful at the protein level as no band was detected in the siNRF2 samples. Moreover, *NQO1*, a downstream target gene of NRF2 also decreased in these cells. As expected, PINK1 protein was stabilised with FCCP treatment (3 hours). However, in Nrf2 knockdown cells treated with FCCP, PINK1 protein levels were slightly lower (Figure 3.9). When cells were treated with FCCP for 6 hours, a similar trend was observed (Appendix Fig 5.1). At the RNA level, Nrf2 knockdown had no effect on PINK1 transcripts in the presence of FCCP or DMSO (3 hours) (Figure 3.10).

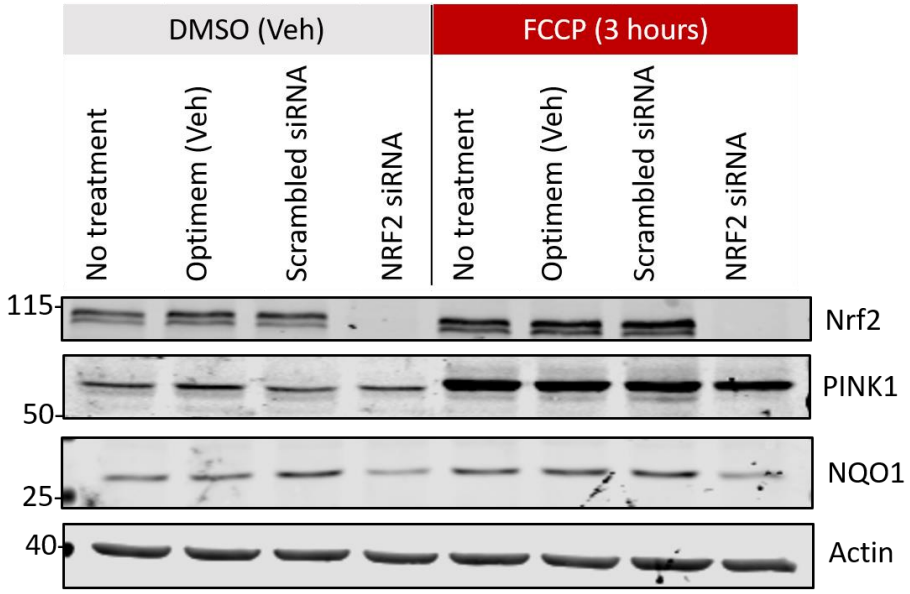

Figure 3.9. **Protein levels after Nrf2 knockdown in WT PINK1 S-HeLa cells in the presence and absence of FCCP.** Nrf2 was knocked down using RNAiMax reverse transfection for 48 hours. Three hours before harvest, cells were treated 0.001% DMSO or 10μM of FCCP. After lysis with SDS buffer, all samples were equally loaded for Western blot analysis. Membranes were blotted for Nrf2, NQO1, PINK1 and the loading control Actin. These blots represent one experiment (n=1).

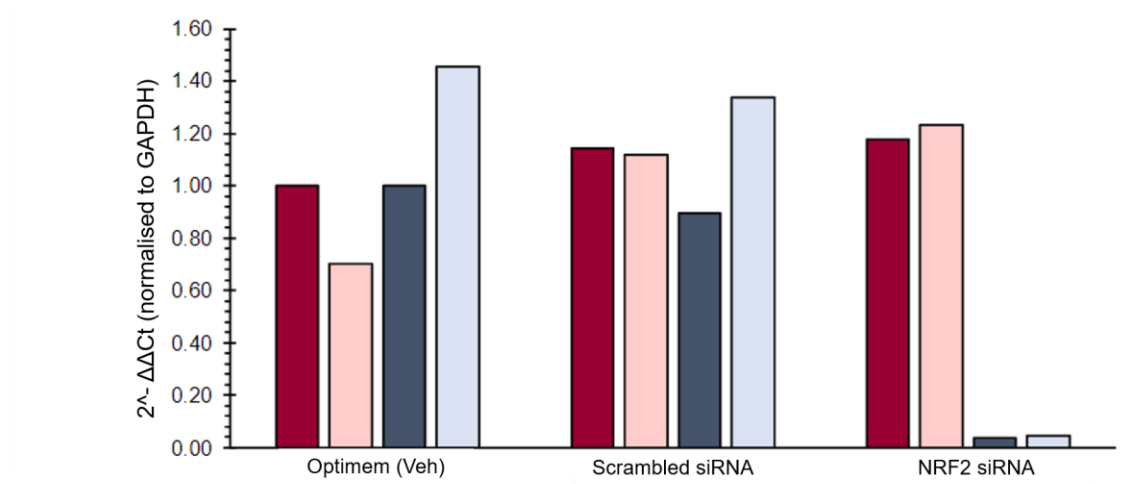

		Optimem (Veh)	Scrambled siRNA	NRF2 siRNA
PINK1	DMSO	1.00	1.15	1.18
	FCCP	0.70	1.12	1.23
NFE2L2	DMSO	1.00	0.90	0.04
	FCCP	1.45	1.34	0.05

Figure 3.10. **Transcript levels after Nrf2 knockdown in WT PINK1 S-HeLa cells in the presence and absence of FCCP.** Nrf2 was knocked down using RNAiMax reverse transfection for 48 hours. Six hours before harvest for quantitative PCR, cells were treated 0.001% DMSO or 10 µM of FCCP. *PINK*, *NFE2L2* and *GAPDH* mRNA transcripts were all detected using individual TaqMan™ probes. Data were normalised to *GAPDH*, the housekeeping gene, using the ΔΔCt method and the fold change was then calculated relative to Optimem DMSO using the 2-ΔΔCt method.

3.2 Investigating the effect of Keap1 knockdown on mitophagy

Studies show that Keap1 (and indirectly Nrf2) are tethered to the mitochondria via PGAM5 which has an important role in the stability of PINK1 and PINK1-induced mitophagy (Park et al., 2018). It was therefore hypothesised that Keap1 and Nrf2 may serve a function in the process of mitophagy through the regulation of PGAM5.

Co-expression of Keap1 with the long isoform of PGAM5 increased ubiquitin conjugation on PGAM5 and Keap1-dependent ubiquitination of PGAM5 by a Cul3-Rbx1-dependent E3 ubiquitin ligase complex. Additionally, Keap1

expression was shown to decrease steady-state levels of co-expressed PGAM5. However, PGAM5 levels were recovered with the inhibition of the 26S proteasome suggesting that Keap1 promotes ubiquitination and proteasomal degradation of PGAM5. Further supporting this, treatment with *tert*-butylhydroquinone (tBHQ) or sulforaphane, both of which inactivate Keap1, also caused elevated levels of PGAM5 (Lo and Hannink, 2008).

To determine if PGAM5 regulation mediated by Keap1 influences mitophagy Keap1 knockdown was carried out in Mito-QC SHSY5Y cells. The hypothesis was that Keap1 knockdown would increase mitophagy due to increased stability of PGAM5 and therefore increased stability of PINK1 on the mitochondria.

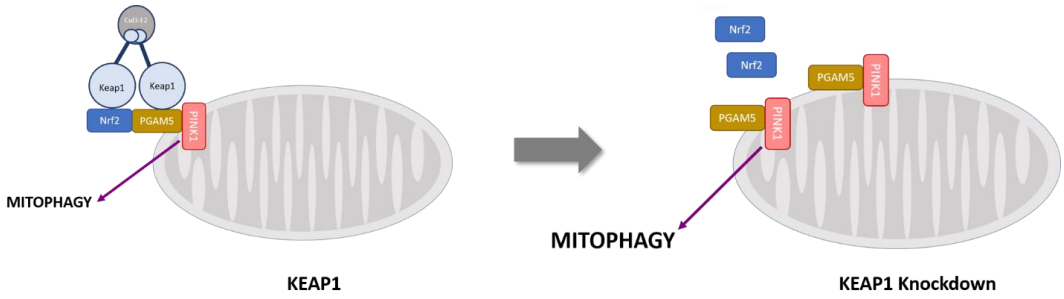

Figure 3.11. **Hypothesis: Keap1 influences PINK1-induced mitophagy through the regulation of PGAM5.** In situations of oxidative stress, Keap1's cysteines are modified leading to a conformational alteration. Like Nrf2, this may stop it from ubiquitinating PGAM5, preventing proteasomal-mediated degradation. Instead PGAM5 is stabilised, allowing for increased stability of PINK1 on the mitochondrial membrane for PINK1-mediated mitophagy.

3.2.1 Keap1 knockdown increases PINK1 transcript levels

Keap1 was effectively knocked down in SHSY5Y cells at the transcript level (Figure 3.12). In addition to Keap1, transcript levels of Nrf2, PGAM5 and PINK1 were also measured (Figure 3.12). Keap1 knockdown slightly, but statistically significantly increased Nrf2 transcript ($p<0.05$) but decreased PGAM5 transcript levels ($p<0.01$). However, Keap1 knockdown had the greatest impact on PINK1 transcript levels, increasing them by 2-fold ($p<0.001$).

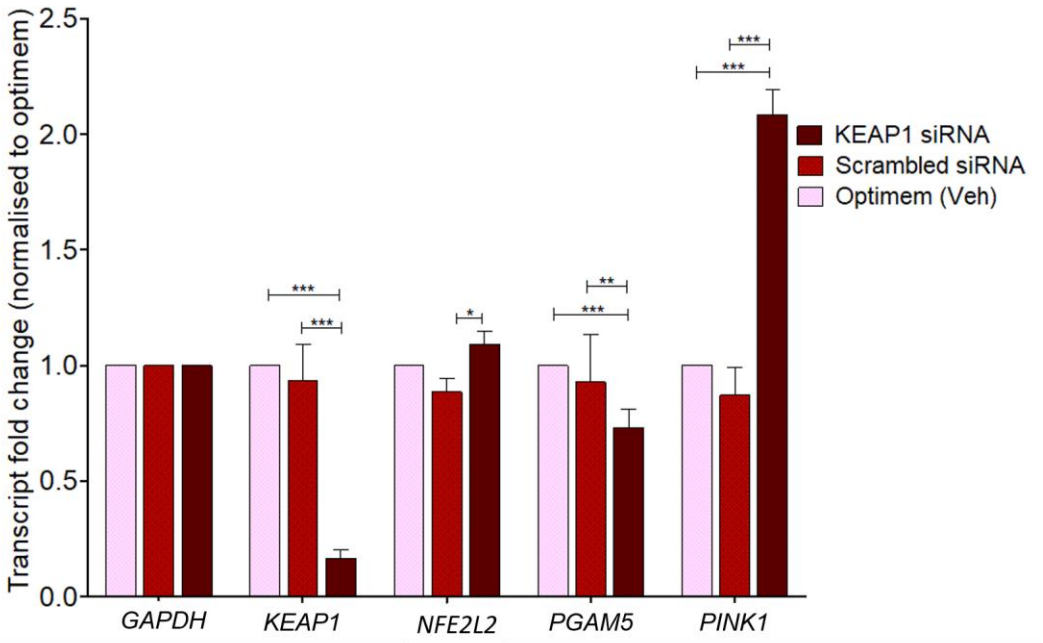

Figure 3.12 **Transcript levels of *KEAP1, NFE2L2, PGAM5* and *PINK1* after Keap1 knockdown in SHSY5Y cells**. Keap1 was knocked down using RNAiMax reverse transfection for 48 hours. *KEAP1, NFE2L2, PGAM5, PINK1* and *GAPDH* mRNA transcripts were all detected using individual TaqMan™ probes. Data were normalised to GAPDH, the housekeeping gene, using the ΔΔCt method and the fold change was then calculated relative to Optimem (Vehicle) using the $2^{-\Delta\Delta Ct}$ method. Data are from three independent experiments (n=3). * p<0.05, ** p<0.01, *** p<0.001 (Two-way ANOVA with Bonferroni post-hoc test).

3.2.2 Keap1 knockdown increases PINK1 protein

Protein analysis was carried out to determine if Keap1 knockdown had an effect on PGAM5 and PINK1 stability. FCCP (10 μM) treatment was also given to cells 3 hours before harvest to better visualise PINK1. Forty-eight-hour knockdown of Keap1 using RNAiMax reverse transfection successfully knocked down Keap1 on the protein level (Figure 3.13). Consequently, this led Nrf2 protein to stabilise. Either in the presence of DMSO or FCCP, PGAM5 protein levels did not differ between scrambled siRNA treated cells and Keap1 siRNA treated cells, suggesting that Keap1 knockdown had no effect on PGAM5 stability. However,

FCCP treatment clearly showed a distribution change in band density in the PGAM5 blot with the bottom band becoming denser than the top.

In DMSO treated cells, Keap1 knockdown did not appear to influence PINK1, perhaps due to the very low levels of this protein at basal conditions. In SHSY5Y cells treated with FCCP, PINK1 protein levels decreased with Keap1 knockdown. Although this trend was inconsistent across replicate experiments (data not shown), it is noteworthy that the reduced levels of PINK1 upon Keap1 knockdown in cells treated with FCCP correlate with the lower levels of PINK1 and Keap1 24h after FCCP treatment in HeLa cells (Figure 3.3). Consistently, in ARPE-19 cells, PINK1 protein levels decreased with Keap1 siRNA (Appendix, Figure 5.2) under both basal and FCCP-treatment conditions. ARPE-19 cells appear to have higher PINK1 protein levels than SHSY5Y cells, making it easier to observe changes in PINK1. Together, these experiments suggest that the levels of Keap1 and PINK1 are related, where the levels of PINK1 might be determined in part by the levels of Keap1. Furthermore, the increase in the mRNA for PINK1 under conditions of Keap1 knockdown (Figure 3.12) could represent a compensatory mechanism for the reduction in PINK1 protein.

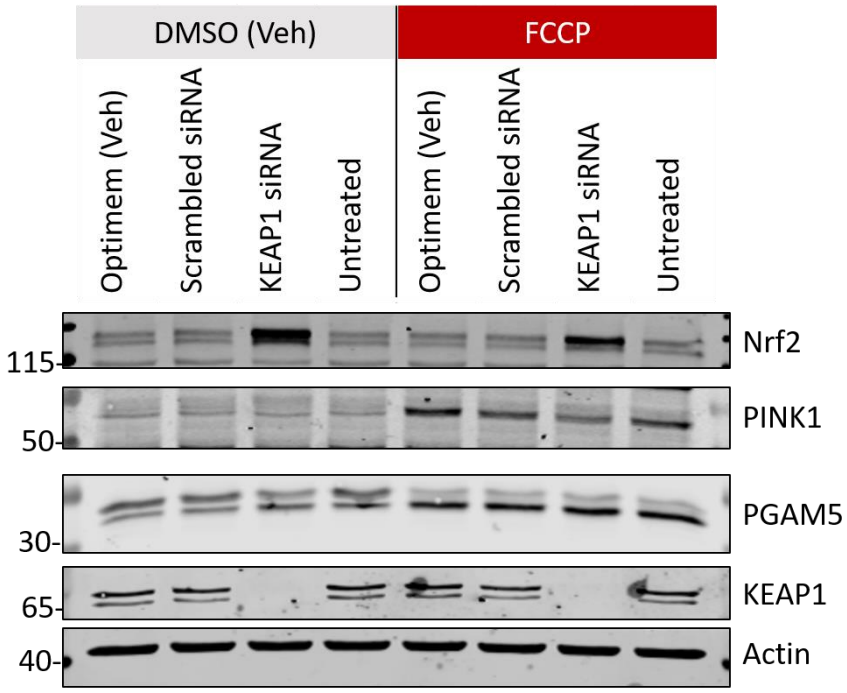

Figure 3.13. **Protein levels after Keap1 knockdown in SHSY5Y cells in the presence and absence of FCCP.** Keap1 was knocked down using RNAiMax reverse transfection for 48 hours. Three hours before harvest, cells were treated 0.001% DMSO or 10µM of FCCP. After lysis with SDS buffer, all samples were equally loaded for Western blot analysis. Membranes were blotted for Nrf2, PINK1, PGAM5, Keap1 and the loading control Actin. This is a representative blot of three independent experiments (n=3).

3.2.3 Keap1 knockdown does not affect basal mitophagy

To determine if Keap1 knockdown could influence PINK1-mediated mitophagy, protein analysis via western blot was carried out using ARPE-19 cells (see Appendix) and SHSY5Y cells. Protein analysis involved blotting for the autophagy marker LC3 and the mitochondrial markers HSP60 and TIM23 in the absence and presence of bafilomycin, an inhibitor of autophagy.

As observed previously, Keap1 knockdown led to Nrf2 stabilisation at the protein level. Contrary to before, PINK1 marginally increased with Keap1 knockdown but PGAM5 did not change. The mitochondrial markers TIM23 and HSP60 were not

affected by Keap1 knockdown in comparison the scrambled control suggesting basal mitophagy was not affected. This was further confirmed with LC3 protein levels remaining the same across all treatments (Figure 3.14).

In ARPE-19 cells, Keap1 knockdown had no effect on the mitochondrial markers HSP60 and TIM23 (Appendix, Figure 5.3), confirming that there was no effect on basal mitophagy. The distribution between the two LC3 bands (LC3 I/II) altered across the different treatments. Of note, in this experiment too, there appeared to be a correlation between the levels of Keap1 and PINK1.

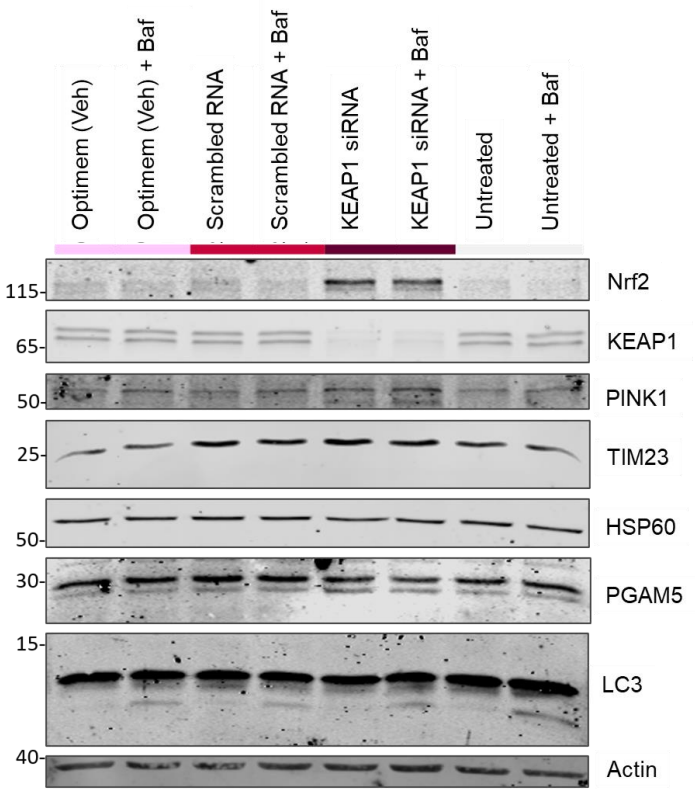

Figure 3.14. **Protein levels of autophagy and mitochondrial markers in the presence and absence of bafilomycin after Keap1 knockdown in SHSY5Y cells.** Keap1 was knocked down using RNAiMax reverse transfection for 48 hours. Six hours before harvest, cells were treated with 20 nM bafilomycin. After lysis with SDS buffer, all samples were equally loaded for Western blot analysis. Membranes were blotted for Nrf2, Keap1, PINK1, TIM23, HSP60, PGAM5, LC3 and the loading control Actin. This is a representative blot of three independent experiments (n=3).

3.3 Investigating the effect of Nrf2 activators with different mechanisms of action on mitophagy

Traditionally, most drugs which stabilise Nrf2 are electrophilic activators that modify cysteine residues on Keap1 (Cuadrado et al., 2019).This leads to a conformational change in Keap1, preventing Nrf2 ubiquitination and degradation by the 26S proteasome. However, more recently new molecules have been designed to specifically disrupt the Nrf2 protein and Keap1 protein interaction (Cuadrado et al., 2019). Studies have shown that unlike the electrophilic activators, these protein-protein disrupters can induce mitophagy (East et al., 2014). This led to further investigation as to how Nrf2 stabilising drugs with different mechanisms of action could trigger different cellular responses. In these experiments SHSY5Y MitoQC cells were treated with either TBE-31, an electrophilic activator or PMI, a protein-protein interaction inhibitor, and mitophagy was measured using both mitochondrial protein analysis and fluorescence microscopy.

Deferiprone (DFP), an iron chelator shown to induce mitophagy, was included in this set of experiments. This was to determine whether these cells were capable of inducing mitophagy as reported in (Allen et al., 2013).

3.3.1 The effect of DFP treatment on mitophagy in SHSY5Y cells

The effect of DFP treatment on Nrf2 was difficult to elucidate due to the quality of the Nrf2 blots (Figure 3.15). However, Keap1 protein levels decreased with DFP treatment and bafilomycin was partially rescued this, suggesting that a fraction of Keap1 might be degraded during mitophagy. PINK1 protein levels increased with DFP treatment and further increased with bafilomycin treatment. p62 protein levels were highest in cells treated with bafilomycin and DFP. Mitochondrial marker TIM23 decreased with DFP treatment and this was partially rescued with bafilomycin. However, protein levels of the other mitochondrial marker HSP60 in cells treated with DFP remained the same as the vehicle DMSO.

The same levels were observed in cells with DFP and bafilomycin treatment. The autophagy marker LC3 suggests that autophagy or mitophagy may have occurred in cells with DFP treatment as a faint band (LC3-II) was observed. LC3-II increased with DFP and bafilomycin treatment.

In ARPE-19 cells, DFP also appeared to induce autophagy or mitophagy as the LC3-II band appeared (Appendix, Figure 5.3). Microscopy data of these cells showed an increase in the number of red puncta with DFP treatment in comparison to the untreated control. This further supports that DFP induced mitophagy in ARPE-19 cells.

3.3.2 The effect of TBE-31 treatment on mitophagy in SHSY5Y cells

Twenty-four-hour treatment with TBE-31 at a concentration of 50 nM or 100 nM clearly stabilised Nrf2 (Figure 3.15). A similar trend was observed in p62 levels. Co-treatment with TBE-31 and bafilomycin further increased p62 protein levels but did not increase Nrf2 protein levels further. 100 nM of TBE-31 reduced PINK1 protein levels but this was rescued with bafilomycin treatment. A similar effect was observed on the levels of Keap1. Mitochondrial protein HSP60 was not affected by TBE-31 treatments but TIM23 protein levels decreased with 100 nM TBE-31. This was not rescued with bafilomycin treatment. LC3II (bottom band on the blot) did not appear in cells treated with TBE-31 alone. Overall, these data suggest that TBE-31 does not induce mitophagy in SHSY5Y cells.

Similarly, to SHSY5Y cells, TBE-31 did not appear to induce mitophagy or autophagy in ARPE-19 cells (Appendix, Figure 5.3). Microscopy data showed that cells treated with TBE-31 had a similar number of red spots to cells treated with the vehicle control, acetonitrile, and untreated cells.

3.3.3 The effect of PMI treatment on mitophagy in SHSY5Y cells

PMI treatment (24 hours) at 10 μM or 20 μM stabilised Nrf2 but in the presence of bafilomycin Nrf2 protein levels decreased (Figure 3.15). Keap1 protein levels remained stable with PMI treatment in presence and absence of bafilomycin. PINK1 and p62 protein levels were also weakly stabilised with 20 μM PMI treatment. The mitochondrial markers HSP60 and TIM23 did not decrease in protein levels with PMI treatment and these did not increase when the cells were treated with bafilomycin, suggesting no mitophagy was induced with PMI treatment. Further supporting this, LC3II (bottom band of the blot) did not appear in cells treated with PMI alone.

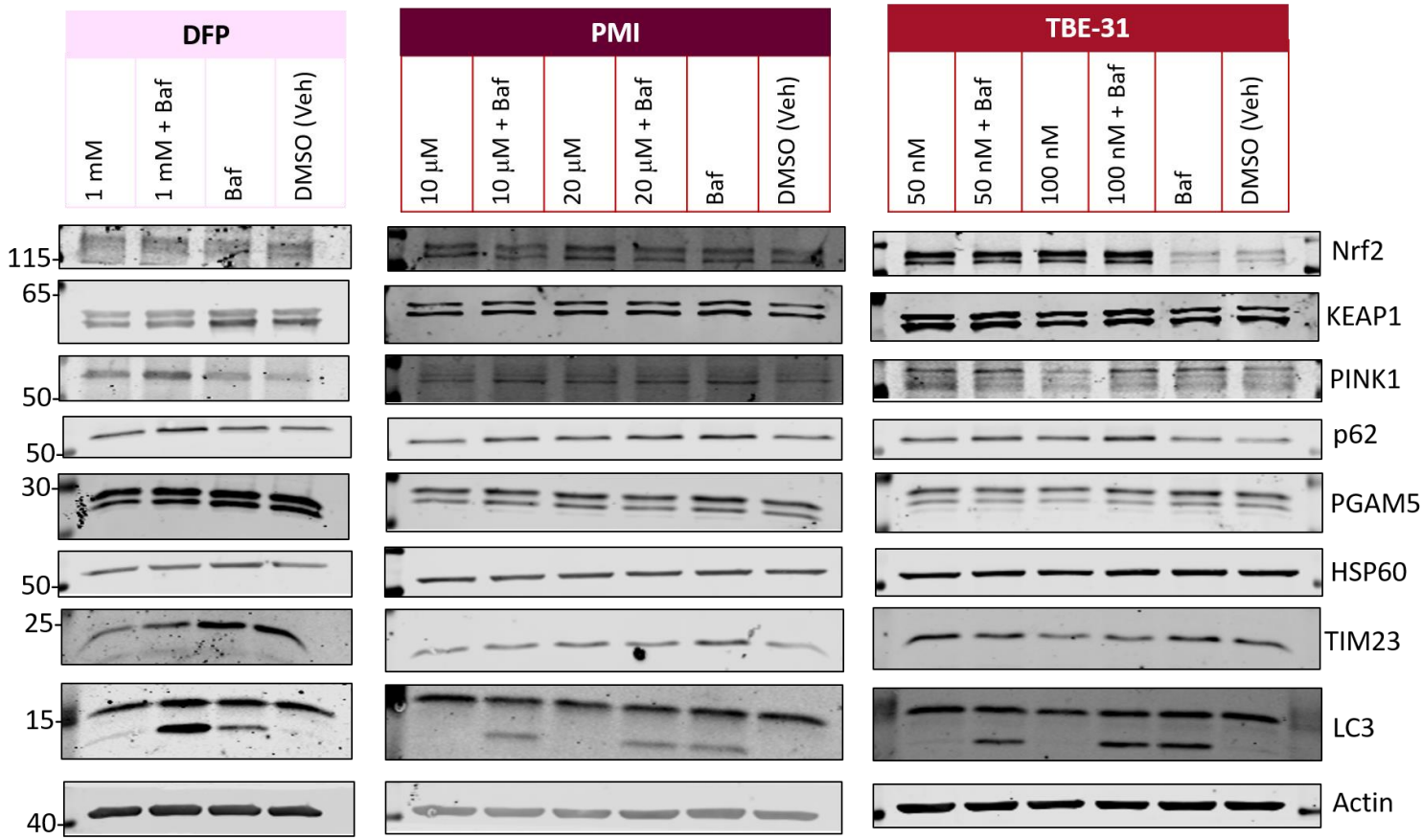

Figure 3.15. **Protein levels of autophagy and mitochondrial marker in the presence and absence of bafilomycin after PMI, TBE-31 and DFP in SHSY5Y cells**. Cells were treated with PMI, DFP and TBE-31 for 24 hours. Six hours before harvest, cells were treated with 20 nM bafilomycin. After lysis with SDS buffer, all samples were equally loaded for Western blot analysis. Membranes were blotted for Nrf2, Keap1, PINK1, TIM23, HSP60, PGAM5, LC3 and the loading control Actin. This is a representative blot of two independent experiments (n=2).

CHAPTER 4: DISCUSSION

Chapter 4: Discussion

Nrf2 and PINK1 play significant protective roles in response to stress within the cell. Limited studies have begun exploring the potential relationship between these two proteins and what this provides cells in conditions of stress. To investigate the potential relationship between PINK1 and Nrf2 further, Nrf2 and Nrf2 downstream targets protein and transcript levels were measured in PINK1 knockout and wild-type S-HeLa cells under basal and stressed conditions. The absence of PINK1 had no effect on basal Nrf2 transcript and protein levels (Figure 3.1). Similarly, after three hours of FCCP treatment, stabilisation of Nrf2 and its downstream targets did not differ between the PINK1 wildtype and knockout cells (Figure 3.3, Figure 3.4)). Together, this suggests that PINK1 does not influence Nrf2 protein or transcript levels. Measuring Nrf2 downstream targets at 0 hours and 24 hours showed that PINK1 does not influence Nrf2 transcriptional activity either. As Nrf2 is a short-lived protein under basal conditions due to its continuous degradation by the 26S proteasome, it was hypothesised that PINK1 could influence Nrf2's half-life. Under both basal (Figure 3.6) and FCCP-mediated stress conditions (Figure 3.7), Nrf2's half-life was similar in PINK1 wild-type and knockout S-HeLa cells. Sub-cellular localisation of Nrf2 was also not influenced by the absence of PINK1 (Figure 3.8). Generally, it can be concluded that the absence of PINK1 does not affect Nrf2 protein and transcript levels, it's half-life, subcellular localisation and transcriptional activity in S-HeLa cells.

These findings do not support published studies, which have shown that PINK1 can influence Nrf2. For example, loss of function mutant PINK1 (G309S) has been shown to antagonise Nrf2 translocation to the nucleus and inhibit heme-oxygenase 1 (HO-1) expression, an Nrf2 target gene. The reasons for these differences could be the use of different cell lines and/or the use of MG132 treatment to model ubiquitin proteasome system dysfunction, which also prevents the degradation of Nrf2 (Sheng et al., 2017). It should also be noted that the gene expression of HO-1 has a complex regulation and Nrf2 is not the only transcription factor involved.

We also assessed whether the absence of Nrf2 would affect PINK1. The protein levels of PINK1 were slightly lower in siNrf2-transfected cells than in cells transfected with scrambled siRNA after 3 and 6 hours of FCCP treatment (Figure 3.9 and Figure 5.1) without affecting its mRNA levels (Figure 3.10). This very modest effect is surprising as Murata et al (2015), showed that Nrf2 regulated *PINK1* expression under oxidative stress conditions, as well as following treatment with the Nrf2 activator *tert*-butylhydroquinone (tBHQ). FCCP uncouples the mitochondrial respiratory chain, which leads to increase in ROS that in turn, can activate Nrf2. Therefore, we expected to see a significant decrease in PINK1 protein and transcript levels in siNrf2 cells treated with FCCP. However, the highlighted differences may be attributable to the different mechanisms of action of FCCP and tBHQ. FCCP targets the mitochondria (Reily et al., 2013) whereas tBHQ targets Keap1, activating Nrf2 (Li et al., 2005). Nrf2 is largely found in the cytoplasm and therefore tBHQ may have a greater effect on Nrf2 than FCCP. Although Nrf2 can be found tethered to the mitochondria, the concentrations of FCCP used may not have been enough to elicit such an effect on *PINK1* expression. However, this is not to say that these compounds do not have off-target effects, which could also explain the differences observed. Future experiments could involve ROS measurements before and after treatment with FCCP and tBHQ to see whether the level of ROS is the reason for the different results.

We found that Nrf2 is stabilised by FCCP at the protein level (Figure 3.3). Several hypotheses explain why this may occur. For example, FCCP is electrophilic and may directly modify Keap1's thiols, inducing a conformational change and preventing Keap1 from correctly binding or degrading Nrf2 (Kane et al., 2018). Alternatively, the effect on Keap1 may occur indirectly, via FCCP-mediated ROS production. Another observation was the reduced Keap1 protein levels and the increased p62 protein levels 24-hours after the 3-hour FCCP treatment (Figure 3.3). Supporting our experimental data, Kane et al. also suggest that FCCP may increase p62-Keap1 complexes which facilitates autophagy and hence

degradation of Keap1 due to p62-dependendent recruitment of autophagosomes (Kane et al., 2018). Additionally, FCCP treatment increased Nrf2 transcript levels within 3 hours. Mirroring this, NQO1 transcript levels also increased after 24 hours suggesting that FCCP increases Nrf2 transcriptional activity (Figure 3.4). Interestingly, p62s transcript levels increased with FCCP treatment (3 hours) in comparison to the vehicle, earlier than NQO1 (Figure 3.4). Thus far, there has been limited experimental data on the relationship between FCCP treatment and the Nrf2-Keap1 pathway. In this set of experiments, we have clearly demonstrated that FCCP leads to Nrf2 activation.

Lo and Hannick (2008) have shown that Keap1 tethers Nrf2 to the mitochondria in a quaternary complex with PGAM5. The importance or role of this complex is not entirely understood. However, it has been shown that in SHSY5Y cells, PGAM5 is involved in stabilising PINK1 which is essential for PINK1-induced mitophagy (Park et al. 2018). Loss of PGAM5 inhibited mitochondrial recruitment of PINK1 and Parkin and inhibited CCCP-mediated mitophagy (Park et al. 2018). PGAM5 is ubiquitinated by Keap1 (Lo and Hannick, 2008), therefore it was hypothesised that through the regulation of PGAM5, Keap-Nrf2 may have a role in PINK1-mediated mitophagy.

Keap1 knockdown led to an increase in PINK1 transcript levels by two-fold (Figure 3.12). At first glance, this agrees with results from Murata et al's study, where Nrf2 activation led to increased *PINK1* expression. However, in our study, despite the increase in mRNA, the protein levels of PINK1 were not correspondingly increased, and even showed a tendency to be slightly decreased, both basally as well as after FCCP treatment (Figure 3.13 and Figure 5.2). This is also consistent with results from experiments where we measured mitophagy in Keap1 knockdown cells and found that basal mitophagy was unaffected by the lack of Keap1. Overall, we propose that the increase in PINK1 mRNA mediated by Keap1 knockdown may be a compensatory mechanism for the decrease in PINK1 protein. Therefore, PINK1 levels may be determined, in part, by Keap1 levels. However, this effect is subtle, does not appear to influence mitophagy, and might

be counteracted by the fact that Nrf2 activation, one of the consequences of Keap1 knockdown, promotes macroautophagy (Pajares et al., 2016). Further investigation is required with a more robust and sensitive measure of PINK1 protein levels. This may include additional cell lines or microscopy with a fluorescent PINK1 protein in which fluorescence could be measured in cells with and without Keap1 knockdown.

The third aim of this project was to determine if pharmacological Nrf2 activators with two different mechanisms of action affect mitophagy. PMI, a small-molecule protein-protein interaction inhibitor, was shown by East et al. (2014) to stabilise Nrf2, increase NQO1 protein levels and induce PINK1/Parkin-independent mitophagy when SHSY5Y cells were exposed to the compound at a concentration of 10 μM for 24 hours. We also used TBE-31, an electrophilic Nrf2 activator, which modifies cysteines in Keap1. A 24-hour treatment with either PMI (10 μM or 20 μM) or TBE-31 (50 nM or 100 nM) did not induce mitophagy in our SHSY5Y cells, although both types of compounds stabilised Nrf2 and increased p62 protein levels (Figure 3.15). This is in contrast with the positive control, DFP, which decreased the levels of Nrf2 and induced mitophagy. Interestingly, PINK1 protein levels increased with all treatments except for the high dose of TBE-31. This is consistent with the slightly decreased levels of PINK1 that were observed upon Nrf2 knockdown (Figure 3.9 and Figure 5.1).

CHAPTER 5: CONCLUSION

Chapter 5: Conclusion

Overall, it has been demonstrated that FCCP activates Nrf2, although the underlying mechanism was not investigated and remains unclear. In addition, we found a subtle, but consistent correlation between the Keap1 protein levels and the PINK1 protein levels, whereby reduction in the Keap1 levels (consequent to FCCP treatment, Keap1 knockdown or high dose TBE-31) correlated with reduction in the levels of PINK1.

CHAPTER 6: APPENDIX

Chapter 6: Appendix

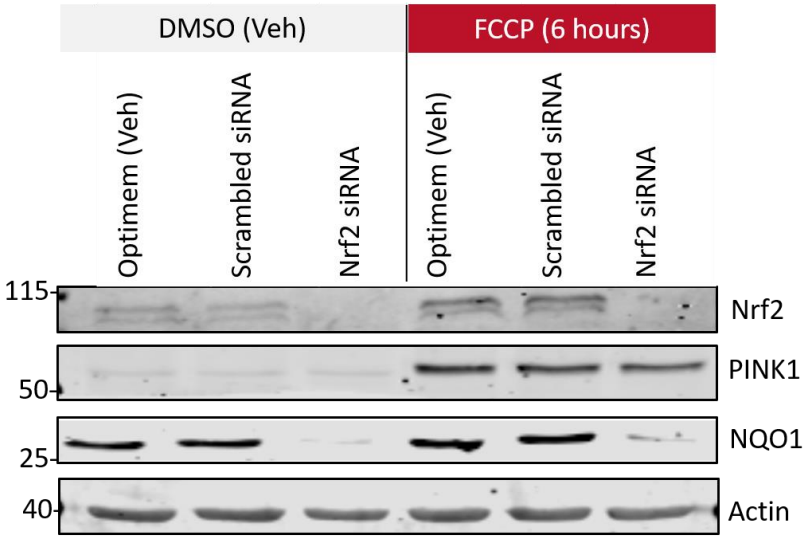

Figure 5.1**. Protein levels after Nrf2 knockdown in WT PINK1 S-HeLa cells in the presence and absence of FCCP.** Nrf2 was knocked down using RNAiMax reverse transfection for 48 hours. Six hours before harvest, cells were treated 0.001% DMSO or 10µM of FCCP. After lysis with SDS buffer, all samples were equally loaded for Western blot analysis. Membranes were blotted for Nrf2, NQO1, PINK1 and the loading control Actin. These blots represent one experiment (n=1).

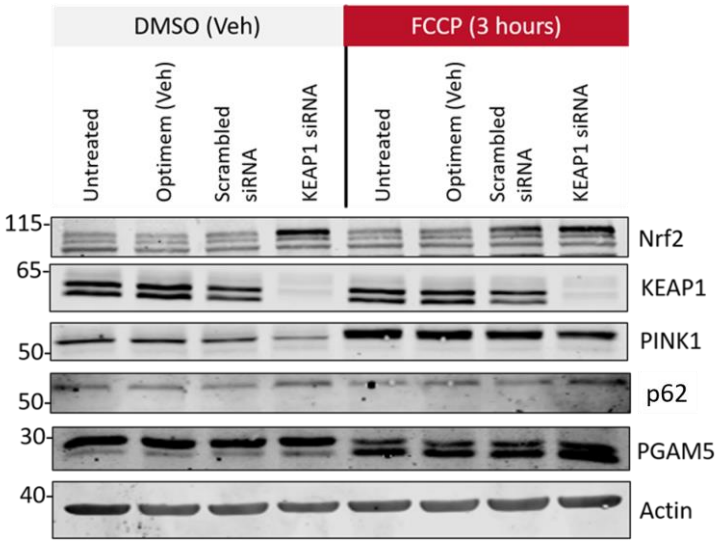

Figure 5.2**. Protein levels after Keap1 knockdown in ARPE-19 cells in the presence and absence of FCCP.** Keap1 was knocked down using RNAiMax reverse transfection for 48 hours. Three hours before harvest, cells were treated 0.002% DMSO or 20 µM of FCCP. After lysis with

SDS buffer, all samples were equally loaded for Western blot analysis. Membranes were blotted for Nrf2, Keap1, PINK1, p62, PGAM5 and the loading control Actin. These blots are representative of three independent experiment (n=3).

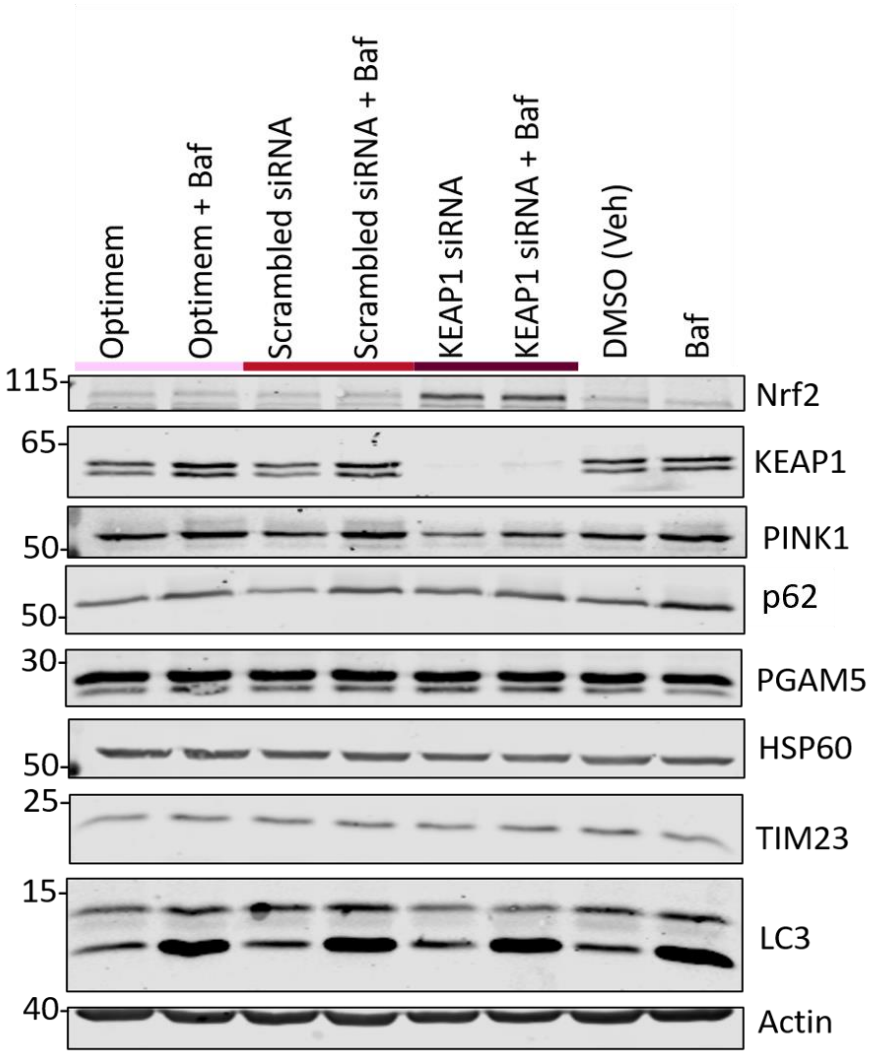

Figure 5.3**. Protein levels of autophagy and mitochondrial markers in the presence and absence of bafilomycin after Keap1 knockdown in ARPE-19 cells.** Keap1 was knocked down using RNAiMax reverse transfection for 48 hours. Six hours before harvest, cells were treated 50 nM with bafilomycin. After lysis with SDS buffer, all samples were equally loaded for Western blot analysis. Membranes were blotted for Nrf2, Keap1, PINK1, TIM23, HSP60, PGAM5, LC3 and the loading control Actin. This is a representative blot of three independent experiments (n=2).

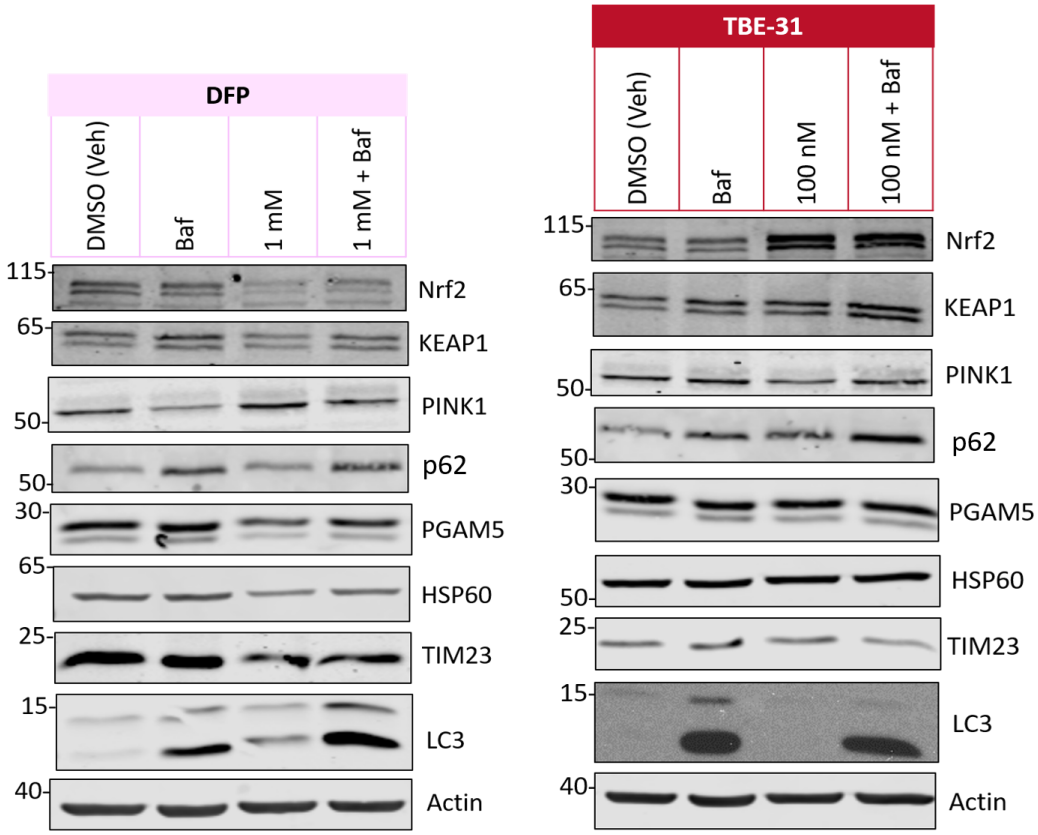

Figure 5.3 **Protein levels of autophagy and mitochondrial markers in the presence and absence of bafilomycin after TBE-31 and DFP in ARPE-19 cells.** Cells were treated with DFP (1 mM) and TBE-31 (100 nM) for 24 hours. Six hours before harvest, cells were treated 20 nM with bafilomycin. After lysis with SDS buffer, all samples were equally loaded for Western blot analysis. Membranes were blotted for Nrf2, Keap1, PINK1, TIM23, HSP60, PGAM5, LC3 and the loading control Actin. This is a representative blot of two independent experiments (n=3)

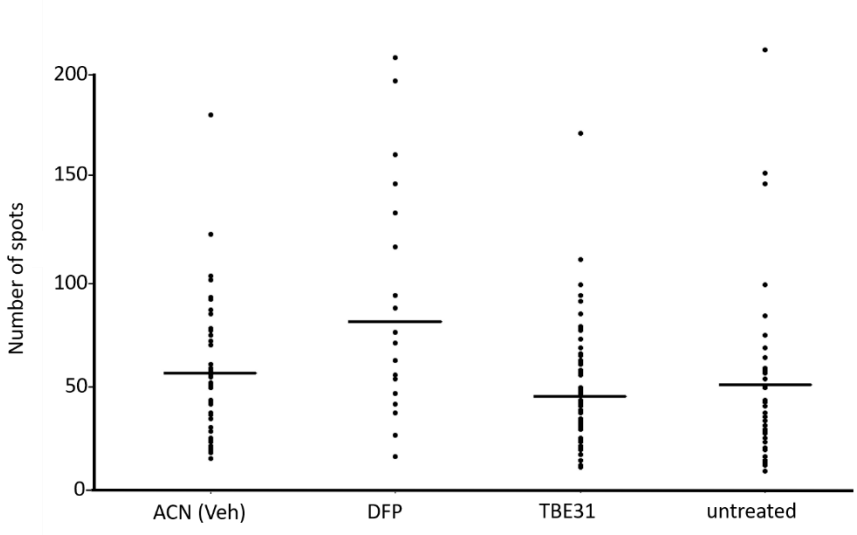

Figure 5.4 **Using fluorescence microscopy to measure mitophagy in ARPE-19 cells.** These are ARPE-19 cells have two fluorophores, mCherry and GFP, attached to the mitochondrial protein FIS1. When mitophagy occurs, GFP fluorescence is quenched and red puncta (mCherry fluorescence) can be detected. The number of red puncta were measured after 24-hour treatment with acetonitrile (ACN), DFP (1mM) and TBE-31 (100 nM).

REFERENCES

ALLEN, G. F., TOTH, R., JAMES, J. & GANLEY, I. G. 2013. Loss of iron triggers PINK1/Parkin-independent mitophagy. *EMBO Rep,* 14**,** 1127-1135.

ASHFORD, T. P. & PORTER, K. R. 1962. Cytoplasmic components in hepatic cell lysosomes. *J Cell Biol,* 12**,** 198-202.

BEAL, M. F. 2003. Mitochondria, oxidative damage, and inflammation in Parkinson's disease. *Ann N Y Acad Sci,* 991**,** 120-31.

BELL, K. F., AL-MUBARAK, B., MARTEL, M. A., MCKAY, S., WHEELAN, N., HASEL, P., MÁRKUS, N. M., BAXTER, P., DEIGHTON, R. F., SERIO, A., BILICAN, B., CHOWDHRY, S., MEAKIN, P. J., ASHFORD, M. L., WYLLIE, D. J., SCANNEVIN, R. H., CHANDRAN, S., HAYES, J. D. & HARDINGHAM, G. E. 2015. Neuronal development is promoted by weakened intrinsic antioxidant defences due to epigenetic repression of Nrf2. *Nat Commun,* 13**,** 7066.

BERGMAN, O. & BEN-SHACHAR, D. 2016. Mitochondrial Oxidative Phosphorylation System (OXPHOS) Deficits in Schizophrenia: Possible Interactions with Cellular Processes. *Can J Psychiatry.,* 61**,** 457-469.

BERNKOPF, D. B., JALAL, K., BRÜCKNER, M., KNAUP, K. X., GENTZEL, M., SCHAMBONY, A. & BEHRENS, J. 2018. Pgam5 released from damaged mitochondria induces mitochondrial biogenesis via Wnt signaling. *J Cell Biol.,* 217**,** 1383-1394.

BRAAK, H., DEL TREDICI, K., RUB, U., DE VOS, R. A., JANSEN STEUR, E. N. & BRAAK, E. 2003. Staging of brain pathology related to sporadic Parkinson's disease. *Neurobiol Aging,* 24**,** 197-211.

CAMP, N. D., JAMES, R. G., DAWSON, D. W., YAN, F., DAVISON, J. M., HOUCK, S. A., TANG, X., ZHENG, N., MAJOR, M. B. & MOON, R. T. 2012. Wilms tumor gene on X chromosome (WTX) inhibits degradation of NRF2 protein through competitive binding to KEAP1 protein. *J Biol Chem,* 287**,** 6539-50.

CHA, G. H., KIM, S., PARK, J., LEE, E., KIM, M., LEE, S. B., KIM, J. M., CHUNG, J. & CHO, K. S. 2005. Parkin negatively regulates JNK pathway in the dopaminergic neurons of Drosophila. *Proc Natl Acad Sci U S A. ,* 102**,** 10345-10350.

CHAIKUAD, A., FILIPPAKOPOULOS, P., MARCSISIN, S. R., PICAUD, S., SCHRODER, M., SEKINE, S., ICHIJO, H., ENGEN, J. R., TAKEDA, K. & KNAPP, S. 2017. Structures of PGAM5 Provide Insight into Active Site Plasticity and Multimeric Assembly. *Structure,* 25**,** 1089-1099 e3.

CHAN, N. C., SALAZAR, A. M., PHAM, A. H., SWEREDOSKI, M. J., KOLAWA, N. J., GRAHAM, R. L., HESS, S. & CHAN, D. C. 2011. Broad activation of the ubiquitin-proteasome system by Parkin is critical for mitophagy. *Hum Mol Genet,* 20**,** 1726-37.

CHAUHAN, N., CHAUNSALI, L., DESHMUKH, P. & PADMANABHAN, B. 2013. Analysis of dimerization of BTB-IVR domains of Keap1 and its interaction with Cul3, by molecular modeling. *Bioinformation,* 9**,** 450-5.

CHEN, G., HAN, Z., FENG, D., CHEN, Y., CHEN, L., WU, H., HUANG, L., ZHOU, C., CAI, X., FU, C., DUAN, L., WANG, X., LIU, L., LIU, X., SHEN, Y., ZHU, Y. & CHEN, Q. 2014. A regulatory signaling loop comprising the PGAM5 phosphatase and CK2 controls receptor-mediated mitophagy. *Mol Cell,* 54**,** 362-77.

CHEN, M., CHEN, Z., WANG, Y., TAN, Z., ZHU, C., LI, Y., HAN, Z., CHEN, L., GAO, R., LIU, L. & CHEN, Q. 2016. Mitophagy receptor FUNDC1 regulates mitochondrial dynamics and mitophagy. *Autophagy,* 12**,** 689-702.

CHOURASIA, A. H., TRACY, K., FRANKENBERGER, C., BOLAND, M. L., SHARIFI, M. N., DRAKE, L. E., SACHLEBEN, J. R., ASARA, J. M., LOCASALE, J. W., KARCZMAR, G. S. & MACLEOD, K. F. 2015. Mitophagy defects arising from BNip3 loss promote mammary tumor progression to metastasis. *EMBO Rep,* 16**,** 1145-1163.

CHOWDHRY, S., ZHANG, Y., MCMAHON, M., SUTHERLAND, C., CUADRADO, A. & HAYES, J. D. 2013. Nrf2 is controlled by two distinct beta-TrCP recognition motifs in its Neh6 domain, one of which can be modulated by GSK-3 activity. *Oncogene,* 32**,** 3765-81.

CLARK, I. E., DODSON, M. W., JIANG, C., CAO, J. H., HUH, J. R., SEOL, J. H., YOO, S. J., HAY, B. A. & GUO, M. 2006. Drosophila pink1 is required for mitochondrial function and interacts genetically with parkin. *Nature,* 441**,** 1162-6.

CUADRADO, A., ROJO, A. I., WELLS, G., HAYES, J. D., COUSIN, S. P., RUMSEY, W. L., ATTUCKS, O. C., FRANKLIN, S., LEVONEN, A. L., KENSLER, T. W. & DINKOVA-KOSTOVA, A. T. 2019. Therapeutic targeting of the NRF2 and KEAP1 partnership in chronic diseases. *Nat Rev Drug Discov,* 18**,** 295-317.

DAYALAN NAIDU, S., MURAMATSU, A., SAITO, R., ASAMI, S., HONDA, T., HOSOYA, T., ITOH, K., YAMAMOTO, M., SUZUKI, T. & DINKOVA-KOSTOVA, A. T. 2018. C151 in KEAP1 is the main cysteine sensor for the cyanoenone class of NRF2 activators, irrespective of molecular size or shape. *Sci Rep,* 8**,** 8037.

DEAS, E., WOOD, N. W. & PLUN-FAVREAU, H. 2011. Mitophagy and Parkinson's disease: the PINK1-parkin link. *Biochim Biophys Acta,* 1813**,** 623-633.

DEY, R. & MORAES, C. T. 2000. Lack of oxidative phosphorylation and low mitochondrial membrane potential decrease susceptibility to apoptosis and do not modulate the protective effect of Bcl-x(L) in osteosarcoma cells. *J Biol Chem,* 275**,** 7087-94.

DING, W. & YIN, X. 2012. Mitophagy: mechanisms, pathophysiological roles, and analysis. *Biol Chem. ,* 393**,** 547–564.

DINKOVA-KOSTOVA, A., HOLTZCLAW, D., COLE, R., ITOH, K., WAKABAYASHI, N., KATOH, Y., YAMAMOTO, M. & TALALAY, P. 2002. Direct evidence that sulfhydryl groups of Keap1 are the sensors regulating induction of phase 2 enzymes that protect against carcinogens and oxidants. *Proc Natl Acad Sci U S A. ,* 99**,** 11908-11913

DINKOVA-KOSTOVA, A. T. & ABRAMOV, A. Y. 2015. The emerging role of Nrf2 in mitochondrial function. *Free Radic Biol Med,* 88**,** 179-188.

DINKOVA-KOSTOVA, A. T., KOSTOV, R. V. & CANNING, P. 2017. Keap1, the cysteine-based mammalian intracellular sensor for electrophiles and oxidants. *Arch Biochem Biophys,* 617**,** 84-93.

DINKOVA-KOSTOVA, A. T. & TALALAY, P. 2000. Persuasive evidence that quinone reductase type 1 (DT diaphorase) protects cells against the toxicity of electrophiles and reactive forms of oxygen. *Free Radic Biol Med,* 29**,** 231-40.

DINKOVA-KOSTOVA, A. T., TALALAY, P., SHARKEY, J., ZHANG, Y., HOLTZCLAW, W. D., WANG, X. J., DAVID, E., SCHIAVONI, K. H., FINLAYSON, S., MIERKE, D. F. & HONDA, T. 2010. An exceptionally potent inducer of cytoprotective enzymes: elucidation of the structural features that determine inducer potency and reactivity with Keap1. *J Biol Chem,* 285**,** 33747-55.

DODSON, M. & ZHANG, D. D. 2017. Non-canonical activation of NRF2: New insights and its relevance to disease. *Curr Pathobiol Rep,* 5**,** 171-176.

DOLMAN, N. J., CHAMBERS, K. M., MANDAVILLI, B., BATCHELOR, R. H. & JANES, M. S. 2013. Tools and techniques to measure mitophagy using fluorescence microscopy. *Autophagy.,* 9**,** 1653-1662.

DU, F., YU, Q., YAN, S., HU, G., LUE, L. F., WALKER, D. G., WU, L., YAN, S. F., TIEU, K. & YAN, S. S. 2017. PINK1 signalling rescues amyloid pathology and mitochondrial dysfunction in Alzheimer's disease. *Brain,* 140**,** 3233-3251

DUCHEN, M. R. 2004. Roles of mitochondria in health and disease. *Diabetes,* 53 Suppl 1**,** S96-102.

EAST, D. A., FAGIANI, F., CROSBY, J., GEORGAKOPOULOS, N. D., BERTRAND, H., SCHAAP, M., FOWKES, A., WELLS, G. & CAMPANELLA, M. 2014. PMI: an independent pharmacological regulator of mitophagy. *Chem Biol,* 21**,** 1585-96.

EGGLER, A. L., LUO, Y., VAN BREEMEN, R. B. & MESECAR, A. D. 2007. Identification of the highly reactive cysteine 151 in the chemopreventive agent-sensor Keap1 protein is method-dependent. *Chem Res Toxicol,* 20**,** 1878-84.

ERICKSON, A. M., NEVAREA, Z., GIPP, J. J. & MULCAHY, R. T. 2002. Identification of a variant antioxidant response element in the promoter of the human glutamate-cysteine ligase modifier subunit gene. Revision of the ARE consensus sequence. *J Biol Chem,* 277**,** 30730-7.

FANG, E. F., WALTZ, T. B., KASSAHUN, H., LU, Q., KERR, J. S., MOREVATI, M., FIVENSON, E. M., WOLLMAN, B. N., MAROSI, K., WILSON, M. A., ISER, W. B., ECKLEY, D. M., ZHANG, Y., LEHRMANN, E., GOLDBERG, I. G., SCHEIBYE-KNUDSEN, M., MATTSON, M. P., NILSEN, H., BOHR, V. A. & BECKER, K. G. 2017. Tomatidine enhances lifespan and healthspan in C. elegans through mitophagy induction via the SKN-1/Nrf2 pathway. *Sci Rep. ,* 7**,** 46208.

FRILING, R. S., BENSIMON, A., TICHAUER, Y. & DANIEL, V. 1990. Xenobiotic-inducible expression of murine glutathione S-transferase Ya subunit gene is controlled by an electrophile-responsive element. *Proc Natl Acad Sci U S A,* 87**,** 6258-62.

GANDHI, S., MUQIT, M. M., STANYER, L., HEALY, D. G., ABOU-SLEIMAN, P. M., HARGREAVES, I., HEALES, S., GANGULY, M., PARSONS, L., LEES, A. J., LATCHMAN, D. S., HOLTON, J. L., WOOD, N. W. & REVESZ, T. 2006. PINK1 protein in normal human brain and Parkinson's disease. *Brain,* 129**,** 1720-31.

GANDHI, S., WOOD-KACZMAR, A., YAO, Z., PLUN-FAVREAU, H., DEAS, E., KLUPSCH, K., DOWNWARD, J., LATCHMAN, D. S., TABRIZI, S. J., WOOD, N. W. W., DUCHEN, M. R. & ABRAMOV, A. Y. 2009. PINK1-Associated Parkinson's Disease Is Caused by Neuronal Vulnerability to Calcium-Induced Cell Death. *Mol Cell.,* 33**,** 627–638.

GAO, F., YANG, J., WANG, D., LI, C., FU, Y., WANG, H., HE, W. & ZHANG, J. 2017. Mitophagy in Parkinson’s Disease: Pathogenic and Therapeutic Implications. *Front Neurol,* 8.

GEISLER, S., HOLMSTRÖM, K. M., SKUJAT, D., FIESEL, F. C., ROTHFUSS, O. C., KAHLE, P. J. & SPRINGER, W. 2010. PINK1/Parkin-mediated mitophagy is dependent on VDAC1 and p62/SQSTM1. *Nat Cell Biol* 12**,** 119-131.

GEORGAKOPOULOS, N. D., FRISON, M., ALVAREZ, M. S., BERTRAND, H., WELLS, G. & CAMPANELLA, M. 2017. Reversible Keap1 inhibitors are preferential pharmacological tools to modulate cellular mitophagy. *Sci Rep,* 7**,** 10303.

GISPERT, S., RICCIARDI, F., KURZ, A., AZIZOV, M., HOEPKEN, H. H., BECKER, D., VOOS, W., LEUNER, K., MÜLLER, W. E., KUDIN, A. P., KUNZ, W. S., ZIMMERMANN, A., ROEPER, J., WENZEL, D., JENDRACH, M., GARCÍA-ARENCÍBIA, M., FERNÁNDEZ-RUIZ, J., HUBER, L., ROHRER, H., BARRERA, M., REICHERT, A. S., RÜB, U., CHEN, A., NUSSBAUM, R. L. & AUBURGER, G. 2009. Parkinson phenotype in aged PINK1-deficient mice is accompanied by progressive mitochondrial dysfunction in absence of neurodegeneration. *PLoS One,* 4**,** e5777.

GRANATIERO, V. & MANFREDI, G. 2019. Mitochondrial Transport and Turnover in the Pathogenesis of Amyotrophic Lateral Sclerosis. *Biology (Basel) ;8(2),* 8**,** pii: E36.

GREENE, J. C., WHITWORTH, A. J., KUO, I., ANDREWS, L. A., FEANY, M. B. & PALLANCK, L. J. 2003. Mitochondrial pathology and apoptotic muscle degeneration in Drosophila parkin mutants. *Proc Natl Acad Sci U S A,* 100**,** 4078-83.

GUO, C., SUN, L., CHEN, X. & ZHANG, D. 2013. Oxidative stress, mitochondrial damage and neurodegenerative diseases. *Neural Regen Res,* 8**,** 2003-14.

HA, S., JEONG, S. H., YI, K., CHUNG, K. M., HONG, C. J., KIM, S. W., KIM, E. K. & YU, S. W. 2017. Phosphorylation of p62 by AMP-activated protein kinase mediates autophagic cell death in adult hippocampal neural stem cells. *J Biol Chem,* 292**,** 13795-13808.

HAMMOND, P. W., ALPIN, J., RISE, C. E., WRIGHT, M. & KREIDER, B. L. 2001. In vitro selection and characterization of Bcl-X(L)-binding proteins from a mix of tissue-specific mRNA display libraries. *J Biol Chem,* 276**,** 20898-906.

HARVEY, C. J., THIMMULAPPA, R. K., SINGH, A., BLAKE, D. J., LING, G., WAKABAYASHI, N., FUJII, J., MYERS, A. & BISWAL, S. 2009. Nrf2-regulated glutathione recycling independent of biosynthesis is critical for cell survival during oxidative stress. *Free Radic Biol Med,* 46**,** 443-53.

HAST, B. E., GOLDFARB, D., MULVANEY, K. M., HAST, M. A., SIESSER, P. F., YAN, F., HAYES, D. N. & MAJOR, M. B. 2013. Proteomic analysis of ubiquitin ligase KEAP1 reveals associated proteins that inhibit NRF2 ubiquitination. *Cancer Res,* 73**,** 2199-210.

HAYES, J. D. & DINKOVA-KOSTOVA, A. T. 2014. The Nrf2 regulatory network provides an interface between redox and intermediary metabolism. *Trends Biochem Sci,* 39**,** 199-218.

HE, X. & MA, Q. 2009. NRF2 cysteine residues are critical for oxidant/electrophile-sensing, Kelch-like ECH-associated protein-1-dependent ubiquitination-proteasomal degradation, and transcription activation. *Mol Pharmacol,* 76**,** 1265-78.

HEEMAN, B., VAN DEN HAUTE, C., AELVOET, S. A., VALSECCHI, F., RODENBURG, R. J., REUMERS, V., DEBYSER, Z., CALLEWAERT, G., KOOPMAN, W. J., WILLEMS, P. H. & BAEKELANDT, V. 2011. Depletion of PINK1 affects mitochondrial metabolism, calcium homeostasis and energy maintenance. *J Cell Sci,* 124.

HOLLAND, R., HAWKINS, A. E., EGGLER, A. L., MESECAR, A. D., FABRIS, D. & FISHBEIN, J. C. 2008. Prospective type 1 and type 2 disulfides of Keap1 protein. *Chem Res Toxicol,* 21**,** 2051-60.

HU, C., EGGLER, A. L., MESECAR, A. D. & VAN BREEMEN, R. B. 2011. Modification of keap1 cysteine residues by sulforaphane. *Chem Res Toxicol,* 24**,** 515-21.

ICHIMURA, Y., WAGURI, S., SOU, Y. S., KAGEYAMA, S., HASEGAWA, J., ISHIMURA, R., SAITO, T., YANG, Y., KOUNO, T., FUKUTOMI, T., HOSHII, T., HIRAO, A., TAKAGI, K., MIZUSHIMA, T., MOTOHASHI, H., LEE, M. S., YOSHIMORI, T., TANAKA, K., YAMAMOTO, M. & KOMATSU, M. 2013. Phosphorylation of p62 activates the Keap1-Nrf2 pathway during selective autophagy. *Mol Cell,* 51**,** 618-31.

IMAI, Y., KANAO, T., SAWADA, T., KOBAYASHI, Y., MORIWAKI, Y., ISHIDA, Y., TAKEDA, K., ICHIJO, H., LU, B. & TAKAHASHI, R. 2010. The loss of PGAM5 suppresses the mitochondrial degeneration caused by inactivation of PINK1 in Drosophila. *PLOS Genet.,* 6**,** e1001229.

ISHIMURA, R., TANAKA, K. & KOMATSU, M. 2014. Dissection of the role of p62/Sqstm1 in activation of Nrf2 during xenophagy. *FEBS Lett,* 588**,** 822-8.

ITOH, K., CHIBA, T., TAKAHASHI, S., ISHII, T., IGARASHI, K., KATOH, Y., OYAKE, T., HAYASHI, N., SATOH, K., HATAYAMA, I., YAMAMOTO, M. & NABESHIMA, Y. 1997. An Nrf2/small Maf heterodimer mediates the induction of phase II detoxifying enzyme genes through antioxidant response elements. *Biochem Biophys Res Commun,* 236**,** 313-22.

ITOH, K., WAKABAYASHI, N., KATOH, Y., ISHII, T., IGARASHI, K., ENGEL, J. D. & YAMAMOTO, M. 1999. Keap1 represses nuclear activation of antioxidant responsive elements by Nrf2 through binding to the amino-terminal Neh2 domain. *Genes Dev,* 13**,** 76-86.

JAIN, A., LAMARK, T., SJOTTEM, E., LARSEN, K. B., AWUH, J. A., OVERVATN, A., MCMAHON, M., HAYES, J. D. & JOHANSEN, T. 2010. p62/SQSTM1 is a target gene for transcription factor NRF2 and creates a positive feedback loop by inducing antioxidant response element-driven gene transcription. *J Biol Chem,* 285**,** 22576-91.

JEONG, S. Y. & SEOL, D. W. 2008. The role of mitochondria in apoptosis. *BMB Rep,* 41**,** 11-22.

JIN, S. M., LAZAROU, M., WANG, C., KANE, L. A., NARENDRA, D. P. & YOULE, R. J. 2010. Mitochondrial membrane potential regulates PINK1 import and proteolytic destabilization by PARL. *J Cell Biol,* 191**,** 933-42.

KANE, M. S., PARIS, A., CODRON, P., CASSEREAU, J., PROCACCIO, V., LENAERS, G., REYNIER, P. & CHEVROLLIER, A. 2018. Current mechanistic insights into the CCCP-induced cell survival response. *Biochem Pharmacol,* 148**,** 100-110.

KANKI, T. & KLIONSKY, D. J. 2008. Mitophagy in yeast occurs through a selective mechanism. *J Biol Chem,* 283**,** 32386-93.

KATAOKA, T., HOLLER, N., MICHEAU, O., MARTINON, F., TINEL, A., HOFMANN, K. & TSCHOPP, J. 2001. Bcl-rambo, a novel Bcl-2 homologue that induces apoptosis via its unique C-terminal extension. *J Biol Chem,* 276**,** 19548-19554.

KATAYAMA, H., KOGURE, T., MIZUSHIMA, N., YOSHIMORI, T. & MIYAWAKI, A. 2011. A sensitive and quantitative technique for detecting autophagic events based on lysosomal delivery. *Chem Biol,* 18**,** 1042-1052

KATOH, Y., ITOH, K., YOSHIDA, E., MIYAGISHI, M., FUKAMIZU, A. & YAMAMOTO, M. 2001. Two domains of Nrf2 cooperatively bind CBP, a CREB binding protein, and synergistically activate transcription. *Genes Cells,* 6**,** 857-68.

KAZLAUSKAITE, A., KONDAPALLI, C., GOURLAY, R., CAMPBELL, D. G., RITORTO, M. S., HOFMANN, K., ALESSI, D. R., KNEBEL, A., TROST, M. & MUQIT, M. M. 2014. Parkin is activated by PINK1-dependent phosphorylation of ubiquitin at Ser65. *Biochem J,* 460**,** 127-39.

KHALIL, B., EL FISSI, N., AOUANE, A., CABIROL-POL, M.-J., RIVAL, T. & LIÉVENS, J.-C. 2015. PINK1-induced mitophagy promotes neuroprotection in Huntington's disease. *Cell Death Dis.,* 6**,** e1617.

KIRKIN, V., MCEWAN, D. G., NOVAK, I. & DIKIC, I. 2009. A role for ubiquitin in selective autophagy. *Mol Cell,* 34**,** 259-69.

KITADA, T., ASAKAWA, S., HATTORI, N., MATSUMINE, H., YAMAMURA, Y., MINOSHIMA, S., YOKOCHI, M., MIZUNO, Y. & SHIMIZU, N. 1998. Mutations in the parkin gene cause autosomal recessive juvenile parkinsonism. *Nature,* 392**,** 605-8.

KLIONSKY, D. J., ABDALLA, F. C., ABELIOVICH, H., ABRAHAM, R. T., ACEVEDO-AROZENA, A., ADELI, K., AGHOLME, L., AGNELLO, M., AGOSTINIS, P., AGUIRRE-GHISO, J. A., JUN AHN, H. & AIT-MOHAMED, O. 2012. Guidelines for the use and interpretation of assays for monitoring autophagy. *Autophagy,* 8**,** 445–544.

KOBAYASHI, M. & YAMAMOTO, M. 2006. Nrf2-Keap1 regulation of cellular defense mechanisms against electrophiles and reactive oxygen species. *Adv Enzyme Regul,* 46**,** 113-40.

KOMATSU, M., KUROKAWA, H., WAGURI, S., TAGUCHI, K., KOBAYASHI, A., ICHIMURA, Y., SOU, Y. S., UENO, I., SAKAMOTO, A., TONG, K. I., KIM, M., NISHITO, Y., IEMURA, S., NATSUME, T., UENO, T., KOMINAMI, E., MOTOHASHI, H., TANAKA, K. & YAMAMOTO, M. 2010. The selective autophagy substrate p62 activates the stress responsive transcription factor Nrf2 through inactivation of Keap1. *Nat Cell Biol,* 12**,** 213-23.

KOYANO, F., OKATSU, K., KOSAKO, H., TAMURA, Y., GO, E., KIMURA, M., KIMURA, Y., TSUCHIYA, H., YOSHIHARA, H., HIROKAWA, T., ENDO, T., FON, E. A., TREMPE, J. F., SAEKI, Y., TANAKA, K. & MATSUDA, N. 2014. Ubiquitin is phosphorylated by PINK1 to activate parkin. *Nature,* 510**,** 162-6.

KUANG, Y., MA, K., ZHOU, C., DING, P., ZHU, Y., CHEN, Q. & XIA, B. 2016. Structural basis for the phosphorylation of FUNDC1 LIR as a molecular switch of mitophagy. *Autophagy,* 12**,** 2363-2373.

KUBLI, A. D. & GUSTAFSSON, Å. B. 2012. Mitochondria and Mitophagy: The Yin and Yang of Cell Death Control. *Circ Res,* 111**,** 1208-1221.

KUSSMAUL, L. & HIRST, J. 2006. The mechanism of superoxide production by NADH:ubiquinone oxidoreductase (complex I) from bovine heart mitochondria. *Proc Natl Acad Sci U S A,* 103**,** 7607-12.

KWAK, M. K., WAKABAYASHI, N., GREENLAW, J. L., YAMAMOTO, M. & KENSLER, T. W. 2003. Antioxidants enhance mammalian proteasome expression through the Keap1-Nrf2 signaling pathway. *Mol Cell Biol,* 23**,** 8786-94.

LAU, A., WANG, X. J., ZHAO, F., VILLENEUVE, N. F., WU, T., JIANG, T., SUN, Z., WHITE, E. & ZHANG, D. D. 2010. A noncanonical mechanism of Nrf2 activation by autophagy deficiency: direct interaction between Keap1 and p62. *Mol Cell Biol,* 30**,** 3275-85.

LAZAROU, M., JIN, S. M., KANE, L. A. & YOULE, R. J. 2012. Role of PINK1 binding to the TOM complex and alternate intracellular membranes in recruitment and activation of the E3 ligase Parkin. *Dev Cell,* 22**,** 320-33.

LEE, J. Y., NAGANO, Y., TAYLOR, J. P., LIM, K. L. & YAO, T. P. 2010. Disease-causing mutations in parkin impair mitochondrial ubiquitination, aggregation, and HDAC6-dependent mitophagy. *J Cell Biol,* 189**,** 671-679.

LEMASTERS, J. J. 2005. Selective mitochondrial autophagy, or mitophagy, as a targeted defense against oxidative stress, mitochondrial dysfunction, and aging. *Rejuvenation Res,* 8**,** 3-5.

LI, J., JOHNSON, D., CALKINS, M., WRIGHT, L., SVENDSEN, C. & JOHNSON, J. 2005. Stabilization of Nrf2 by tBHQ confers protection against oxidative stress-induced cell death in human neural stem cells. *Toxicol Sci,* 83**,** 313-328.

LI, W., YU, S., LIU, T., KIM, J. H., BLANK, V., LI, H. & KONG, A. N. 2008. Heterodimerization with small Maf proteins enhances nuclear retention of Nrf2 via masking the NESzip motif. *Biochim Biophys Acta,* 1783**,** 1847-56.

LI, W., YU, S. W. & KONG, A. N. 2006. Nrf2 possesses a redox-sensitive nuclear exporting signal in the Neh5 transactivation domain. *J Biol Chem,* 281**,** 27251-63.

LI, Y., PAONESSA, J. D. & ZHANG, Y. 2012. Mechanism of chemical activation of Nrf2. *PLoS One,* 7**,** e35122.

LIN, W. & KANG, U. J. 2008. Characterization of PINK1 processing, stability, and subcellular localization. *J Neurochem,* 106**,** 464-74.

LIOU, G. Y. & STORZ, P. 2010. Reactive oxygen species in cancer. *Free Radic Res,* 44**,** 479-96.

LIU, L., FENG, D., CHEN, G., CHEN, M., ZHENG, Q., SONG, P., MA, Q., ZHU, C., WANG, R., QI, W., HUANG, L., XUE, P., LI, B., WANG, X., JIN, H., WANG, J., YANG, F., LIU, P., ZHU, Y., SUI, S.

& CHEN, Q. 2012. Mitochondrial outer-membrane protein FUNDC1 mediates hypoxia-induced mitophagy in mammalian cells. *Nat Cell Biol,* 14**,** 177-85.

LO, S. C. & HANNINK, M. 2006. PGAM5, a Bcl-XL-interacting protein, is a novel substrate for the redox-regulated Keap1-dependent ubiquitin ligase complex. *J Biol Chem,* 281**,** 37893-903.

LO, S. C. & HANNINK, M. 2008. PGAM5 tethers a ternary complex containing Keap1 and Nrf2 to mitochondria. *Exp Cell Res,* 314**,** 1789-803.

LO, S. C., LI, X., HENZL, M. T., BEAMER, L. J. & HANNINK, M. 2006. Structure of the Keap1:Nrf2 interface provides mechanistic insight into Nrf2 signaling. *EMBO J,* 25**,** 3605-17.

LOU, H., DU, S., JI, Q. & STOLZ, A. 2006. Induction of AKR1C2 by phase II inducers: identification of a distal consensus antioxidant response element regulated by NRF2. *Mol Pharmacol,* 69**,** 1662-72.

LU, W., KARUPPAGOUNDER, S. S., SPRINGER, D. A., ALLEN, M. D., ZHENG, L., CHAO, B., ZHANG, Y., DAWSON, V. L., DAWSON, T. M. & LENARDO, M. 2014. Genetic deficiency of the mitochondrial protein PGAM5 causes a Parkinson's-like movement disorder. *Nat Commun,* 5**,** 4930.

LU, W., SUN, J., YOON, J. S., ZHANG, Y., ZHENG, L., MURPHY, E., MATTSON, M. P. & LENARDO, M. J. 2016. Mitochondrial Protein PGAM5 Regulates Mitophagic Protection against Cell Necroptosis. *PLoS One,* 11**,** e0147792.

LYAKHOVICH, V. V., VAVILIN, V. A., ZENKOV, N. K. & MENSHCHIKOVA, E. B. 2006. Active defense under oxidative stress. The antioxidant responsive element. *Biochemistry (Mosc),* 71**,** 962-74.

MA, J., CAI, H., WU, T., SOBHIAN, B., HUO, Y., ALCIVAR, A., MEHTA, M., CHEUNG, K. L., GANESAN, S., KONG, A. N., ZHANG, D. D. & XIA, B. 2012. PALB2 interacts with KEAP1 to promote NRF2 nuclear accumulation and function. *Mol Cell Biol,* 32**,** 1506-17.

MAHER, J. & YAMAMOTO, M. 2010. The rise of antioxidant signaling--the evolution and hormetic actions of Nrf2. *Toxicol Appl Pharmacol,* 244**,** 4-15.

MAO, P., MANCZAK, M., CALKINS, M. J., TRUONG, Q., REDDY, T. P., REDDY, A. P., SHIRENDEB, U., LO, H. H., RABINOVITCH, P. S. & REDDY, P. H. 2012. Mitochondria-targeted catalase reduces abnormal APP processing, amyloid β production and BACE1 in a mouse model of Alzheimer's disease: implications for neuroprotection and lifespan extension. *Hum Mol Genet* 21**,** 2973-2990

MATAK, P., MATAK, A., MOUSTAFA, S., ARYAL, D. K., BENNER, E. J., WETSEL, W. & ANDREWS, N. C. 2016. Disrupted iron homeostasis causes dopaminergic neurodegeneration in mice. *Proc Natl Acad Sci U S A. ,* 113**,** 3428-3435.

MATSUMOTO, G., SHIMOGORI, T., HATTORI, N. & NUKINA, N. 2015. TBK1 controls autophagosomal engulfment of polyubiquitinated mitochondria through p62/SQSTM1 phosphorylation. *Hum Mol Genet,* 24**,** 4429-42.

MCMAHON, M., LAMONT, D. J., BEATTIE, K. A. & HAYES, J. D. 2010. Keap1 perceives stress via three sensors for the endogenous signaling molecules nitric oxide, zinc, and alkenals. *Proc Natl Acad Sci U S A,* 107**,** 18838-43.

MCMAHON, M., THOMAS, N., ITOH, K., YAMAMOTO, M. & HAYES, J. D. 2004. Redox-regulated turnover of Nrf2 is determined by at least two separate protein domains, the redox-sensitive Neh2 degron and the redox-insensitive Neh6 degron. *J Biol Chem,* 279**,** 31556-67.

MCWILLIAMS, T. G., PRESCOTT, A. R., ALLEN, G. F. G., TAMJAR, J., MUNSON, M. J., THOMSON, C., MUQIT, M. M. K. & GANLEY, I. G. 2016. mito-QC illuminates mitophagy and mitochondrial architecture in vivo. 214**,** 333-345.

MCWILLIAMS, T. G., PRESCOTT, A. R., MONTAVA-GARRIGA, L., BALL, G., SINGH, F., BARINI, E., MUQIT, M. M. K., BROOKS, S. P. & GANLEY, I. G. 2018. Basal Mitophagy Occurs Independently of PINK1 in Mouse Tissues of High Metabolic Demand. *Cell Metab,* 27**,** 439-449 e5.

MI, L., DI PASQUA, A. J. & CHUNG, F. L. 2011. Proteins as binding targets of isothiocyanates in cancer prevention. *Carcinogenesis,* 32**,** 1405-13.

MITCHELL, P. 1966. Chemiosmotic coupling in oxidative and photosynthetic phosphorylation. *Biol Rev Camb Philos Soc,* 41**,** 445-502.

MIZUSHIMA, N. 2007. Autophagy: process and function. *Genes Dev,* 21**,** 2861-73.

MOI, P., CHAN, K., ASUNIS, I., CAO, A. & KAN, Y. W. 1994. Isolation of NF-E2-related factor 2 (Nrf2), a NF-E2-like basic leucine zipper transcriptional activator that binds to the tandem NF-E2/AP1 repeat of the beta-globin locus control region. *Proc Natl Acad Sci U S A,* 91**,** 9926-30.

MORIWAKI, K., FARIAS LUZ, N., BALAJI, S., DE ROSA, M. J., O'DONNELL, C. L., GOUGH, P. J., BERTIN, J., WELSH, R. M. & CHAN, F. K. 2016. The Mitochondrial Phosphatase PGAM5 Is Dispensable for Necroptosis but Promotes Inflammasome Activation in Macrophages. *J Immunol,* 196**,** 407-15.

MOTOHASHI, H. & YAMAMOTO, M. 2004. Nrf2-Keap1 defines a physiologically important stress response mechanism. *Trends Mol Med,* 10**,** 549-57.

MURAKAMI, S. & MOTOHASHI, H. 2015. Roles of Nrf2 in cell proliferation and differentiation. *Free Radic Biol Med,* 88**,** 168-178.

MURAKAWA, T., YAMAGUCHI, O., HASHIMOTO, A., HIKOSO, S., TAKEDA, T., OKA, T., YASUI, H., UEDA, H., AKAZAWA, Y., NAKAYAMA, H., TANEIKE, M., MISAKA, T., OMIYA, S., SHAH, A. M., YAMAMOTO, A., NISHIDA, K., OHSUMI, Y., OKAMOTO, K., SAKATA, Y. & OTSU, K. 2015. Bcl-2-like protein 13 is a mammalian Atg32 homologue that mediates mitophagy and mitochondrial fragmentation. *Nat Commun,* 6**,** 7527.

MURATA, H., TAKAMATSU, H., LIU, S., KATAOKA, K., HUH, N. H. & SAKAGUCHI, M. 2015. NRF2 Regulates PINK1 Expression under Oxidative Stress Conditions. *PLoS One,* 10**,** e0142438.

NARENDRA, D., KANE, L. A., HAUSER, D. N., FEARNLEY, I. M. & YOULE, R. J. 2010a. p62/SQSTM1 is required for Parkin-induced mitochondrial clustering but not mitophagy; VDAC1 is dispensable for both. *Autophagy,* 6**,** 1090-1106.

NARENDRA, D. P., JIN, S. M., TANAKA, A., SUEN, D. F., GAUTIER, C. A., SHEN, J., COOKSON, M. R. & YOULE, R. J. 2010b. PINK1 is selectively stabilized on impaired mitochondria to activate Parkin. *PLoS Biol,* 8**,** e1000298.

NEUPERT, W. & HERRMANN, J. M. 2007. Translocation of proteins into mitochondria. *Annu Rev Biochem,* 76**,** 723-49.

NEY, P. A. 2015. Mitochondrial autophagy: Origins, significance, and role of BNIP3 and NIX. *Biochim Biophys Acta,* 1853**,** 2775-83.

NGUYEN, T., NIOI, P. & PICKETT, C. B. 2009. The Nrf2-antioxidant response element signaling pathway and its activation by oxidative stress. *J Biol Chem,* 284**,** 13291-5.

NIOI, P., NGUYEN, T., SHERRATT, P. J. & PICKETT, C. B. 2005. The carboxy-terminal Neh3 domain of Nrf2 is required for transcriptional activation. *Mol Cell Biol,* 25**,** 10895-906.

NITURE, S. K. & JAISWAL, A. K. 2012. Nrf2 protein up-regulates antiapoptotic protein Bcl-2 and prevents cellular apoptosis. *J Biol Chem,* 287**,** 9873-86.

NODA, N. N., OHSUMI, Y. & INAGAKI, F. 2010. Atg8-family interacting motif crucial for selective autophagy. *FEBS Lett.,* 584**,** 1379-1385.

NOVAK, I., KIRKIN, V., MCEWAN, D. G., ZHANG, J., WILD, P., ROZENKNOP, A., ROGOV, V., LO, F., POPOVIC, D., OCCHIPINTI, A., REICHERT, A. S., TERZIC, J., DOTSCH, V., NEY, P. A. & DIKIC, I. 2010. Nix is a selective autophagy receptor for mitochondrial clearance. *EMBO Rep,* 11**,** 45-51.

NUNNARI, J. & SUOMALAINEN, A. 2012. Mitochondria: in sickness and in health. *Cell,* 148**,** 1145-59.

O'MEALEY, G. B., PLAFKER, K. S., BERRY, W. L., JANKNECHT, R., CHAN, J. Y. & PLAFKER, S. M. 2017. A PGAM5-KEAP1-Nrf2 complex is required for stress-induced mitochondrial retrograde trafficking. *J Cell Sci,* 130**,** 3467-3480.

OHNUMA, T., NAKAYAMA, S., ANAN, E., NISHIYAMA, T., OGURA, K. & HIRATSUKA, A. 2010. Activation of the Nrf2/ARE pathway via S-alkylation of cysteine 151 in the chemopreventive agent-sensor Keap1 protein by falcarindiol, a conjugated diacetylene compound. *Toxicol Appl Pharmacol,* 244**,** 27-36.

OKAMOTO, K., KONDO-OKAMOTO, N. & OHSUMI, Y. 2009. Mitochondria-anchored receptor Atg32 mediates degradation of mitochondria via selective autophagy. *Dev Cell,* 17**,** 87-97.

OKATSU, K., OKA, T., IGUCHI, M., IMAMURA, K., KOSAKO, H., TANI, N., KIMURA, M., GO, E., KOYANO, F., FUNAYAMA, M., SHIBA-FUKUSHIMA, K., SATO, S., SHIMIZU, H., FUKUNAGA, Y., TANIGUCHI, H., KOMATSU, M., HATTORI, N., MIHARA, K., TANAKA, K. & MATSUDA, N. 2012. PINK1 autophosphorylation upon membrane potential dissipation is essential for Parkin recruitment to damaged mitochondria. *Nat Commun,* 3**,** 1016.

PAJARES, M., JIMÉNEZ-MORENO, N., GARCÍA-YAGÜE, Á. J., ESCOLL, M., DE CEBALLOS, M. L., VAN LEUVEN, F., RÁBANO, A., YAMAMOTO, M., ROJO, A. I. & CUADRADO, A. 2016. Transcription factor NFE2L2/NRF2 is a regulator of macroautophagy genes. *Autophagy,* 12**,** 1902-1916.

PANDA, S., SRIVASTAVA, S., LI, Z., VAETH, M., FUHS, S. R., HUNTER, T. & SKOLNIK, E. Y. 2016. Identification of PGAM5 as a Mammalian Protein Histidine Phosphatase that Plays a Central Role to Negatively Regulate CD4(+) T Cells. *Mol Cell,* 63**,** 457-69.

PANKIV, S., CLAUSEN, T. H., LAMARK, T., BRECH, A., BRUUN, J. A., OUTZEN, H., OVERVATN, A., BJORKOY, G. & JOHANSEN, T. 2007. p62/SQSTM1 binds directly to Atg8/LC3 to facilitate degradation of ubiquitinated protein aggregates by autophagy. *J Biol Chem,* 282**,** 24131-45.

PARK, J., LEE, S. B., LEE, S., KIM, Y., SONG, S., KIM, S., BAE, E., KIM, J., SHONG, M., KIM, J. M. & CHUNG, J. 2006. Mitochondrial dysfunction in Drosophila PINK1 mutants is complemented by parkin. *Nature,* 441**,** 1157-61.

PARK, Y. S., CHOI, S. E. & KOH, H. C. 2018. PGAM5 regulates PINK1/Parkin-mediated mitophagy via DRP1 in CCCP-induced mitochondrial dysfunction. *Toxicol Lett.,* 284**,** 120-128.

PAUL, B. T., MANZ, D. H., TORTI, F. M. & TORTI, S. V. 2017. Mitochondria and Iron: current questions. *Expert Rev Hematol,* 10**,** 65-79.

PESAH, Y., PHAM, T., BURGESS, H., MIDDLEBROOKS, B., VERSTREKEN, P., ZHOU, Y., HARDING, M., BELLEN, H. & MARDON, G. 2004. Drosophila parkin mutants have decreased mass and cell size and increased sensitivity to oxygen radical stress. *Development. ,* 131**,** 2183-2194.

PRESTERA, T., HOLTZCLAW, W. D., ZHANG, Y. & TALALAY, P. 1993. Chemical and molecular regulation of enzymes that detoxify carcinogens. *Proc Natl Acad Sci U S A,* 90**,** 2965-9.

QUINLAN, C. L., ORR, A. L., PEREVOSHCHIKOVA, I. V., TREBERG, J. R., ACKRELL, B. A. & BRAND, M. D. 2012. Mitochondrial complex II can generate reactive oxygen species at high rates in both the forward and reverse reactions. *J Biol Chem,* 287**,** 27255-64.

RADA, P., ROJO, A. I., CHOWDHRY, S., MCMAHON, M., HAYES, J. D. & CUADRADO, A. 2011. SCF/{beta}-TrCP promotes glycogen synthase kinase 3-dependent degradation of the Nrf2 transcription factor in a Keap1-independent manner. *Mol Cell Biol,* 31**,** 1121-33.

RADA, P., ROJO, A. I., EVRARD-TODESCHI, N., INNAMORATO, N. G., COTTE, A., JAWORSKI, T., TOBON-VELASCO, J. C., DEVIJVER, H., GARCIA-MAYORAL, M. F., VAN LEUVEN, F., HAYES, J. D., BERTHO, G. & CUADRADO, A. 2012. Structural and functional characterization of Nrf2 degradation by the glycogen synthase kinase 3/beta-TrCP axis. *Mol Cell Biol,* 32**,** 3486-99.

RAGHUNATH, A., SUNDARRAJ, K., NAGARAJAN, R., ARFUSO, F., BIAN, J., KUMAR, A. P., SETHI, G. & PERUMAL, E. 2018. Antioxidant response elements: Discovery, classes, regulation and potential applications. *Redox Biol,* 17**,** 297-314.

RAMSEY, C. P., GLASS, C. A., MONTGOMERY, M. B., LINDL, K. A., RITSON, G. P., CHIA, L. A., HAMILTON, R. L., CHU, C. T. & JORDAN-SCIUTTO, K. L. 2007. Expression of Nrf2 in neurodegenerative diseases. *J Neuropathol Exp Neurol,* 66**,** 75-85.

REICHARD, J. F., MOTZ, G. T. & PUGA, A. 2007. Heme oxygenase-1 induction by NRF2 requires inactivation of the transcriptional repressor BACH1. *Nucleic Acids Res,* 35**,** 7074-86.

REILY, C., MITCHELL, T., CHACKO, B. K., BENAVIDES, G., MURPHY, M. P. & DARLEY-USMAR, V. 2013. Mitochondrially targeted compounds and their impact on cellular bioenergetics. *Redox Biol,* 1**,** 86-93.

SAITO, R., SUZUKI, T., HIRAMOTO, K., ASAMI, S., NAGANUMA, E., SUDA, H., ISO, T., YAMAMOTO, H., MORITA, M., BAIRD, L., FURUSAWA, Y., NEGISHI, T., ICHINOSE, M. & YAMAMOTO, M. 2016. Characterizations of Three Major Cysteine Sensors of Keap1 in Stress Response. *Mol Cell Biol,* 36**,** 271-84.

SAJADIMAJD, S. & KHAZAEI, M. 2018. Oxidative Stress and Cancer: The Role of Nrf2. *Curr Cancer Drug Targets,* 18**,** 538-557.

SCHERZ-SHOUVAL, R. & ELAZAR, Z. 2011. Regulation of autophagy by ROS: physiology and pathology. *Trends Biochem Sci,* 36**,** 30-38.

SCHWEERS, R. L., ZHANG, J., RANDALL, M. S., LOYD, M. R., LI, W., DORSEY, F. C., KUNDU, M., OPFERMAN, J. T., CLEVELAND, J. L., MILLER, J. L. & NEY, P. A. 2007. NIX is required for programmed mitochondrial clearance during reticulocyte maturation. *Proc Natl Acad Sci U S A,* 104**,** 19500-5.

SEKINE, S., KANAMARU, Y., KOIKE, M., NISHIHARA, A., OKADA, M., KINOSHITA, H., KAMIYAMA, M., MARUYAMA, J., UCHIYAMA, Y., ISHIHARA, N., TAKEDA, K. & ICHIJO, H. 2012. Rhomboid protease PARL mediates the mitochondrial membrane potential loss-induced cleavage of PGAM5. *J Biol Chem,* 287**,** 34635-45.

SHENG, X. J., TU, H. J., CHIEN, W. L., KANG, K. H., LU, D. H., LIOU, H. H., LEE, M. J. & FU, W. M. 2017. Antagonism of proteasome inhibitor-induced heme oxygenase-1 expression by PINK1 mutation. *PLoS One,* 14**,** e0183076.

STEWART, D., KILLEEN, E., NAQUIN, R., ALAM, S. & ALAM, J. 2003. Degradation of transcription factor Nrf2 via the ubiquitin-proteasome pathway and stabilization by cadmium. *J Biol Chem,* 278**,** 2396-402.

SUN, N., MALIDE, D., LIU, J., ROVIRA, I. I., COMBS, C. A. & FINKEL, T. 2017. A fluorescence-based imaging method to measure in vitro and in vivo mitophagy using mt-Keima. *Nat Protoc.,* 12**,** 1576-1587.

TAGUCHI, K., FUJIKAWA, N., KOMATSU, M., ISHII, T., UNNO, M., AKAIKE, T., MOTOHASHI, H. & YAMAMOTO, M. 2012. Keap1 degradation by autophagy for the maintenance of redox homeostasis. *Proc Natl Acad Sci U S A,* 109**,** 13561-6.

TAGUCHI, K., MOTOHASHI, H. & YAMAMOTO, M. 2011. Molecular mechanisms of the Keap1-Nrf2 pathway in stress response and cancer evolution. *Genes Cells,* 16**,** 123-40.

TAKEDA, K., KOMURO, Y., HAYAKAWA, T., OGUCHI, H., ISHIDA, Y., MURAKAMI, S., NOGUCHI, T., KINOSHITA, H., SEKINE, Y., IEMURA, S., NATSUME, T. & ICHIJO, H. 2009. Mitochondrial phosphoglycerate mutase 5 uses alternate catalytic activity as a protein serine/threonine phosphatase to activate ASK1. *Proc Natl Acad Sci U S A,* 106**,** 12301-5.

TAKEDA, K., NOGUCHI, T., NAGURO, I. & ICHIJO, H. 2008. Apoptosis signal-regulating kinase 1 in stress and immune response. *Annu Rev Pharmacol Toxicol,* 48**,** 199-225.

TANIDA, I., UENO, T. & KOMINAMI, E. 2004. LC3 conjugation system in mammalian autophagy. *Int J Biochem Cell Biol,* 36**,** 2503-18.

TASAKI, T., MULDER, L. C., IWAMATSU, A., LEE, M. J., DAVYDOV, I. V., VARSHAVSKY, A., MUESING, M. & KWON, Y. T. 2005. A family of mammalian E3 ubiquitin ligases that contain the UBR box motif and recognize N-degrons. *Mol Cell Biol,* 25**,** 7120-36.

TELAKOWSKI-HOPKINS, C. A., KING, R. G. & PICKETT, C. B. 1988. Glutathione S-transferase Ya subunit gene: identification of regulatory elements required for basal level and inducible expression. *Proc Natl Acad Sci U S A,* 85**,** 1000-4.

THIMMULAPPA, R. K., MAI, K. H., SRISUMA, S., KENSLER, T. W., YAMAMOTO, M. & BISWAL, S. 2002. Identification of Nrf2-regulated genes induced by the chemopreventive agent sulforaphane by oligonucleotide microarray. *Cancer Res,* 62**,** 5196-203.

TKACHEV, V. O., MENSHCHIKOVA, E. B. & ZENKOV, N. K. 2011. Mechanism of the Nrf2/Keap1/ARE signaling system. *Biochemistry (Mosc),* 76**,** 407-22.

TONG, K. I., KATOH, Y., KUSUNOKI, H., ITOH, K., TANAKA, T. & YAMAMOTO, M. 2006. Keap1 recruits Neh2 through binding to ETGE and DLG motifs: characterization of the two-site molecular recognition model. *Mol Cell Biol,* 26**,** 2887-900.

TONG, K. I., PADMANABHAN, B., KOBAYASHI, A., SHANG, C., HIROTSU, Y., YOKOYAMA, S. & YAMAMOTO, M. 2007. Different electrostatic potentials define ETGE and DLG motifs as hinge and latch in oxidative stress response. *Mol Cell Biol,* 27**,** 7511-21.

VALENTE, E. M., SALVI, S., IALONGO, T., MARONGIU, R., ELIA, A. E., CAPUTO, V., ROMITO, L., ALBANESE, A., DALLAPICCOLA, B. & BENTIVOGLIO, A. R. 2004. PINK1 mutations are associated with sporadic early-onset parkinsonism. *Ann Neurol,* 56**,** 336-41.

VAN HUMBEECK, C., CORNELISSEN, T. & VANDENBERGHE, W. 2011. Ambra1: a Parkin-binding protein involved in mitophagy. *Autophagy,* 7**,** 1555-6.

VENUGOPAL, R. & JAISWAL, A. K. 1996. Nrf1 and Nrf2 positively and c-Fos and Fra1 negatively regulate the human antioxidant response element-mediated expression of NAD(P)H:quinone oxidoreductase1 gene. *Proc Natl Acad Sci U S A,* 93**,** 14960-5.

VILLA, E., PROÏCS, E., RUBIO-PATIÑO, C., OBBA, S., ZUNINO, B., BOSSOWSKI, J. P., ROZIER, R. M., CHICHE, J., MONDRAGÓN, L., RILEY, J. S., MARCHETTI, S., VERHOEYEN, E., TAIT, S. W. G. & RICCI, J. E. 2017. Parkin-Independent Mitophagy Controls Chemotherapeutic Response in Cancer Cells. *Cell Rep.,* 20**,** 2846-2859.

WANG, H., LIU, K., GENG, M., GAO, P., WU, X., HAI, Y., LI, Y., LI, Y., LUO, L., HAYES, J. D., WANG, X. J. & TANG, X. 2013. RXRalpha inhibits the NRF2-ARE signaling pathway through a direct interaction with the Neh7 domain of NRF2. *Cancer Res,* 73**,** 3097-108.

WANG, Z., JIANG, H., CHEN, S., DU, F. & WANG, X. 2012. The mitochondrial phosphatase PGAM5 functions at the convergence point of multiple necrotic death pathways. *Cell,* 148**,** 228-43.

WATAI, Y., KOBAYASHI, A., NAGASE, H., MIZUKAMI, M., MCEVOY, J., SINGER, J. D., ITOH, K. & YAMAMOTO, M. 2007. Subcellular localization and cytoplasmic complex status of endogenous Keap1. *Genes Cells,* 12**,** 1163-78.

WHITWORTH, A. J., THEODORE, D. A., GREENE, J. C., BENES, H., WES, P. D. & PALLANCK, L. J. 2005. Increased glutathione S-transferase activity rescues dopaminergic neuron loss in a Drosophila model of Parkinson's disease. *Proc Natl Acad Sci U S A. ,* 102**,** 8024-8029.

WU, H., XUE, D., CHEN, G., HAN, Z., HUANG, L., ZHU, C., WANG, X., JIN, H., WANG, J., ZHU, Y., LIU, L. & CHEN, Q. 2014. The BCL2L1 and PGAM5 axis defines hypoxia-induced receptor-mediated mitophagy. *Autophagy,* 10**,** 1712–1725.

XIONG, L., XIE, J., SONG, C., LIU, J., ZHENG, J., LIU, C., ZHANG, X., LI, P. & WANG, F. 2015. The Activation of Nrf2 and Its Downstream Regulated Genes Mediates the Antioxidative Activities of Xueshuan Xinmaining Tablet in Human Umbilical Vein Endothelial Cells. *Evid Based Complement Alternat Med,* 2015**,** 187265.

YAMADA, T., DAWSON, T. M., YANAGAWA, T., IIJIMA, M. & SESAKI, H. 2019. SQSTM1/p62 promotes mitochondrial ubiquitination independently of PINK1 and PRKN/parkin in mitophagy. *Autophagy,* 15**,** 2012-2018.

YAMADA, T., MURATA, D., ADACHI, Y., ITOH, K., KAMEOKA, S., IGARASHI, A., KATO, T., ARAKI, Y., HUGANIR, R. L., DAWSON, T. M., YANAGAWA, T., OKAMOTO, K., IIJIMA, M. & SESAKI, H. 2018. Mitochondrial Stasis Reveals p62-Mediated Ubiquitination in Parkin-Independent Mitophagy and Mitigates Nonalcoholic Fatty Liver Disease. *Cell Metab,* 28**,** 588-604.

YAMAGUCHI, A., ISHIKAWA, H., FURUOKA, M., YOKOZEKI, M., MATSUDA, N., TANIMURA, S. & TAKEDA, K. 2019. Cleaved PGAM5 is released from mitochondria depending on proteasome-mediated rupture of the outer mitochondrial membrane during mitophagy. *J Biochem.,* 165**,** 19-25

YAMANO, K. & YOULE, R. J. 2013. PINK1 is degraded through the N-end rule pathway. *Autophagy,* 9**,** 1758-69.

YAO, J., IRWIN, R. W., ZHAO, L., NILSEN, J., HAMILTON, R. T. & BRINTON, R. D. 2009. Mitochondrial bioenergetic deficit precedes Alzheimer's pathology in female mouse model of Alzheimer's disease. *Proc Natl Acad Sci U S A.,* 106**,** 14670-14675

YOSHII, S. R., KISHI, C., ISHIHARA, N. & MIZUSHIMA, N. 2011. Parkin mediates proteasome-dependent protein degradation and rupture of the outer mitochondrial membrane. *J Biol Chem,* 286**,** 19630-40.

ZHANG, D. D. & HANNINK, M. 2003. Distinct cysteine residues in Keap1 are required for Keap1-dependent ubiquitination of Nrf2 and for stabilization of Nrf2 by chemopreventive agents and oxidative stress. *Mol Cell Biol,* 23**,** 8137-51.

ZHANG, D. D., LO, S. C., SUN, Z., HABIB, G. M., LIEBERMAN, M. W. & HANNINK, M. 2005. Ubiquitination of Keap1, a BTB-Kelch substrate adaptor protein for Cul3, targets Keap1 for degradation by a proteasome-independent pathway. *J Biol Chem,* 280**,** 30091-9.

ZHANG, H., BOSCH-MARCE, M., SHIMODA, L. A., TAN, Y. S., BAEK, J. H., WESLEY, J. B., GONZALEZ, F. J. & SEMENZA, G. L. 2008. Mitochondrial autophagy is an HIF-1-dependent adaptive metabolic response to hypoxia. *J Biol Chem,* 283**,** 10892-903.

ZHANG, J. & NEY, P. A. 2009. Role of BNIP3 and NIX in cell death, autophagy, and mitophagy. *Cell Death Differ,* 16**,** 939-46.

ZHANG, W., REN, H., XU, C., ZHU, C., WU, H., LIU, D., WANG, J., LIU, L., LI, W., MA, Q., DU, L., ZHENG, M., ZHANG, C., LIU, J. & CHEN, Q. 2016. Hypoxic mitophagy regulates mitochondrial quality and platelet activation and determines severity of I/R heart injury. *Elife,* 20**,** e21407

ZHANG, Y. 2012. The molecular basis that unifies the metabolism, cellular uptake and chemopreventive activities of dietary isothiocyanates. *Carcinogenesis,* 33**,** 2-9.

ZHANG, Y., TALALAY, P., CHO, C. G. & POSNER, G. H. 1992. A major inducer of anticarcinogenic protective enzymes from broccoli: isolation and elucidation of structure. *Proc Natl Acad Sci U S A,* 89**,** 2399-403.

ZHOU, C., HUANG, Y., SHAO, Y., MAY, J., PROU, D., PERIER, C., DAUER, W., SCHON, E. A. & PRZEDBORSKI, S. 2008. The kinase domain of mitochondrial PINK1 faces the cytoplasm. *Proc Natl Acad Sci U S A,* 105**,** 12022-7.

ZHUANG, C., WU, Z., XING, C. & MIAO, Z. 2017. Small molecules inhibiting Keap1-Nrf2 protein-protein interactions: a novel approach to activate Nrf2 function. *Medchemcomm,* 8**,** 286-294.

ZIPPER, L. M. & MULCAHY, R. T. 2002. The Keap1 BTB/POZ dimerization function is required to sequester Nrf2 in cytoplasm. *J Biol Chem,* 277**,** 36544-52.

ZIVIANI, E., TAO, R. N. & WHITWORTH, A. J. 2010. Drosophila parkin requires PINK1 for mitochondrial translocation and ubiquitinates mitofusin. *Proc Natl Acad Sci U S A,* 107**,** 5018-1023.